Sites U1302 and U1303[1]

Expedition 303 Scientists[2]

Chapter contents

[1]Expedition 303 Scientists, 2006. Sites U1302 and U1303. *In* Channell, J.E.T., Kanamatsu, T., Sato, T., Stein, R., Alvarez Zarikian, C.A., Malone, M.J., and the Expedition 303/306 Scientists, 2006. *Proc. IODP,* 303/306: College Station TX (Integrated Ocean Drilling Program Management International, Inc.). doi:10.2204/iodp.proc.303306.103.2006
[2]**Expedition 303 Scientists' addresses.**

Background and objectives

Orphan Knoll, located 650 km northeast of St. John's (Newfoundland, Canada), is a topographic high consisting of a fragment of continental crust that detached from North America during continental rifting (Keen and Beaumont, 1990; Chian et al., 2001). It rises 2 km above the Labrador Sea abyssal plain and coincides with the junction of oceanic and continental crust.

Integrated Ocean Drilling Program (IODP) Sites U1302 and U1303 are separated by 5.68 km in 3250–3500 m water depth ~35–45 km southeast of the crest of Orphan Knoll (1800 m water depth), the location of Deep Sea Drilling Project Site 111 drilled in 1970. The axis of the Northwest Atlantic Mid-Ocean Channel (NAMOC) (see Chough et al., 1987), at ~4000 m water depth, lies 200 km to the northeast (Fig. **F1**). Sites U1302 and U1303 are on the crest of a small ridge to the east of a fault scarp marking the eastern side of Orphan Knoll (Fig. **F2**). Surrounding canyons partially protect this location from debris flow wedges associated with advances of ice tongues to the edge of the shelf (Aksu and Hiscott, 1992).

The impetus for IODP sampling at Sites U1302 and U1303 stems from sedimentologic observations made in piston Core HU91-045-094P recovered close to Site U1303 (Fig. **F3**) by the *CCGS Hudson* (HU) in 1991. This 11 m piston core revealed the presence of numerous detrital layers deposited during the last glacial cycle (Hillaire-Marcel et al., 1994; Stoner et al., 1995, 1996), providing a proximal record of Laurentide Ice Sheet (LIS) instability, equivalent to the more distal Heinrich layers of the central Atlantic ice-rafted debris (IRD) belt (Heinrich, 1988; Broecker et al., 1992).

For Core HU91-045-094P, Stoner et al. (1995) introduced a labeling scheme for detrital carbonate (DC1–DC6) and low detrital carbonate (LDC 5–6) layers. The detrital layers can be detected by a range of proxies such as gamma ray attenuation (GRA) density, magnetic susceptibility (Fig. **F4**), color reflectance, and grain-size-sensitive magnetic parameters (see Stoner et al., 1996). Low planktonic $\delta^{18}O$ and $\delta^{13}C$ values coincide with detrital layers, indicating the presence of meltwater and low productivity in surface water (Hillaire-Marcel et al., 1994; Hillaire-Marcel and Bilodeau, 2000).

Following the important results from Core HU91-045-094P, the Site U1303 location was sampled during the 1995 and 1999 *Images* cruises of the *Marion-Dufresne* (MD; Cores MD95-2024 and MD99-2237). The stratigraphy in these MD cores can be corre-

doi:10.2204/iodp.proc.303306.103.2006

lated to the HU core (Fig. F4) and extends the environmental record into marine isotope Stage (MIS) 6, although the record is incomplete beyond MIS 5d (Turon et al., 1999; Stoner et al., 2000). The detrital layers have been shown to correlate to cold stadials in the Greenland Summit GRIP/GISP2 ice core on the basis of correlation of both marine/ice core $\delta^{18}O$ records and relative geomagnetic paleointensity data from Core MD95-2024 to cosmogenic isotope flux at GRIP/GISP2 (Stoner et al., 2000). An enigma in the correlation between Core HU91-045-094P and the two MD cores is the apparent contrast in accumulation rates among cores, whereby the MD cores have approximately twice the apparent accumulation rates of the HU core (Fig. F4). This may be explained partly by the stretching in the MD "calypso" cores.

Two piston cores were also collected in the Orphan Basin, 85.6 km (46.17 nmi) southwest of Sites U1302 and U1303. One of these piston cores (Core HU92-045-11P) is 11.7 m long and was described by Hiscott and Aksu (1996). The other (Core MD95-2025) was collected during the 1995 *Images* cruise of the *Marion-Dufresne* (Hiscott et al., 2001). These cores have mean sedimentation rates of 10 cm/k.y. and record both detrital carbonate and low detrital carbonate "Heinrich-like" events back to 340 ka. The identification of detrital events is based on the "Heinrich variable," the ratio of undifferentiated rock fragments and silicate minerals to foraminifers in the 180–3000 µm grain-size fraction.

Although it is generally believed that detrital layers at Sites U1302 and U1303 denote LIS instability and are a proximal analog to the central Atlantic Heinrich layers, the depositional origin of the layers remains open to speculation. The layers appear to have multiple components including IRD and sediments deposited from suspension possibly related to turbiditic flow along the NAMOC or spillover turbidites derived from the NAMOC (Hillaire-Marcel et al., 1994; Stoner et al., 1995, 1996). Fine-grained detrital carbonate (glacial flour) does not flocculate as readily as detrital clay and may be transported over 100 km in suspension (see Hesse et al., 1997), possibly supporting the NAMOC origin of the carbonate-rich suspended sediment component of these detrital layers.

The objectives at Sites U1302 and U1303 were to document the detrital layer stratigraphy at the sites, understand the structure and origin of individual detrital layers, and extend the sediment record beyond MIS 5d. We aim to place this important environmental record into a paleointensity-assisted chronology, building on the Labrador Sea chronostratigraphy developed by Stoner et al. (1998, 2000) for the last glacial cycle. Are detrital carbonate events present in glacial stages beyond the last glacial period? How did the occurrence and pacing of millennial-scale IRD events evolve during the late Pleistocene under changing orbital and glacial boundary conditions? In addition to these objectives, isotopic data from epipelagic, deeper dwelling, and benthic foraminifers, as well as dinocyst and microfossil abundance, will be used to document changes in hydrography and structure of water masses in the Labrador Sea (Hillaire-Marcel and Bilodeau, 2000; Hillaire-Marcel et al., 2001a, 2001b).

The rationale for drilling at Site U1302, located 5.68 km southeast of Site U1303 (Fig. F3), was that Site U1302 appeared to have a thicker sediment drape above the underlying mudwaves (Fig. F5). The Pollution Prevention and Safety Panel authorized penetration to 300 meters below seafloor (mbsf) at Site U1302 and 200 mbsf at Site U1303. These maximum penetration depths were not achieved because of a debris flow encountered at ~90 mbsf at both sites. Although the drilling did not achieve the proposed penetration, the record extends the existing piston core records at this site from MIS 5d to MIS 17. Site positioning successfully avoided debris flows associated with MIS 5 and MIS 7 (Fig. F6).

Operations

Expedition 303 officially began with the first line ashore at St. John's, Newfoundland, at 0628 h on 25 September 2004. The port call, which included an underwater hull inspection for the American Bureau of Shipping and extensive refueling, concluded when the last line was released at 1925 h on 30 September 2004. We completed the 276 nmi transit from St. John's to Site U1302 at an average speed of 8.8 kt, traveling into a 20–25 kt headwind for most of the transit.

Site U1302

Hole U1302A

We arrived at Site U1302 at 0330 h on 2 October 2004 and spudded Hole U1302A at 1530 h. The recovery in the first core (only 50 cm) suggested a seafloor depth at 3568.6 meters below sea level (mbsl) (3579.4 meters below rig floor [mbrf]) or 5 m deeper than the corrected precision depth recorder depth (see **"Hole U1302D"** and **"Hole U1302E"** for more realistic seafloor depth estimates). Piston coring utilizing nonmagnetic core barrels advanced to 107.1 mbsf (Cores 1H through 13H) (Table T1), where detrital gravel caused problems with penetration and hole stability. An attempt was made to clean out the hole and continue coring, but hole stability problems persisted. Hole U1302A was terminated when the bit cleared the seafloor at 1245 h on 3 October.

Additional operations included core orientation starting with Core 4H and two deployments of the advanced piston corer (APC) temperature tool at 76.1 mbsf (Core 9H) and 104.6 mbsf (Core 12H). The latter attempt was unsuccessful because the cutting shoe and associated electronics were damaged by hard debris. In Hole U1302A, we cored 107.1 m, recovering 91.7 m (85.6%); recovery may have been affected by heave as large as 3 m.

Hole U1302B

After offsetting the vessel 30 m to the northwest of Hole U1302A, Hole U1302B was spudded at 1340 h on 3 October 2004. With only 50 cm of recovery in Core 303-U1302A-1H, the bit was positioned 4.5 m above Core 303-U1302A-2H to achieve a good mudline core. A full core was obtained (Table **T1**) that did not establish the mudline. Piston coring advanced to 104.7 mbsf, recovering 102.82 m (98.2%). Hole U1302B was terminated when the APC partially stroked in the debris interval. The Tensor tool was run for core orientation beginning with Core 3H. The bit cleared the seafloor at 0200 h on 4 October, ending operations in Hole U1302B.

Hole U1302C

The vessel was offset 30 m to the northwest again, penetrating the seafloor at 0330 h on 4 October 2004, initiating Hole U1302C. Correlation of Hole U1302A and U1302B records to a previous piston core from Orphan Knoll (MD99-2237) suggested we had missed some of the upper section. Therefore, the bit was positioned 4.5 m higher than it was during spudding of Hole U1302B. A full core was obtained for 1H, suggesting that an additional section remained unsampled. Hole U1302C was advanced to 104.5 mbsf, recovering 97.06 m (92.9%) before refusal was experienced at Core 11H. Core orientation proceeded with Core 3H. Operations in Hole U1302C ended when the bit cleared the seafloor at 1540 h on 4 October.

Hole U1302D

The vessel was offset 30 m to the northwest and Hole U1302D was spudded at 1625 h. To attempt complete recovery of the upper section, the bit was positioned 9.5 m above the position of Hole U1302C. A good 3.63 m mudline core was recovered, indicating a seafloor depth of 3555.7 mbsl (3566.5 mbrf). A second core was taken to provide overlap with core breaks from the previous holes; however, only 13% (1.24 m) was recovered. With the poor recovery in Core 2H, we chose to move to Hole U1302E to ensure complete recovery of the upper section.

Hole U1302E

The ship was offset 30 m to the northwest, and the bit was positioned 4.5 m lower than in Hole U1302D. Hole U1302E was spudded at 1910 h on 4 October 2004, and a 5.6 m core was recovered, which was less than we anticipated based on bit position and recovery in Core 303-U1302D-1H. Sea state and vessel heave may have affected bit position during spudding. The seafloor depth based on recovery and bit position for this hole is 3558.1 mbsl (3568.9 mbrf). Core 2H (recovery = 94.6%) was taken to provide additional material for overlap with previous holes (see **"Composite section"**). The drill string was pulled to 2095 mbrf in preparation for transit in dynamic positioning (DP) mode, ending operations at Site U1302 at 2215 h on 4 October.

Site U1303

Hole U1303A

The 3 nmi transit from Site U1302 to Site U1303 was made in DP mode in 3.75 h. Hole U1303A was spudded at 0445 h, recovering 8.43 m, suggesting a seafloor depth of 3524.2 mbsl (3535 mbrf). The hole was advanced to 93.9 mbsf (Cores 1H through 10H) with 73.6% recovery (Table **T1**). Difficult coring (partial strokes of the APC) and poor recovery led us to terminate the hole. The drill string was pulled clear of the seafloor at 1650 h, ending operations in Hole U1303A.

Hole U1303B

The ship was offset 40 m southeast and Hole U1303B was spudded at 1849 h on 5 October 2004. The bit was positioned 15 m shallower than in Hole U1303A because correlation to Site U1302 indicated that a substantial upper section was not recovered in Hole U1303A. This first attempt recovered no core, so the bit was positioned 9.5 m lower, recovering 9.62 m in Core 1H and indicating a seafloor depth of 3517.9 mbsl (3528.7 mbrf). The hole was cored to 85.7 mbsf (Cores 1H through 9H) with 83.5% recovery. Cores were oriented starting with Core 3H. The hole was terminated when the same difficult-to-core interval from Hole U1303A was encountered. With the combined recovery at Sites U1302 and U1303 sufficient to produce a composite record (see **"Composite section"**), we decided to end coring and proceed to the Eirik Drift sites. The drill string was retrieved to the rig floor and the ship was made ready for transit at 1315 h on 6 October, ending operations at Site U1303.

Lithostratigraphy

Five holes were drilled at Site U1302, and two holes were drilled at Site U1303 (Table **T1**). All cores were

recovered using the APC. The sediments at Sites U1302 and U1303 are dominated by varying mixtures of terrigenous components and biogenic debris (primarily quartz, detrital carbonate, and nannofossils) (see **"Site U1302 and U1303 smear slides"** in "Core Descriptions;" Fig. **F7**), so the most common lithologies are clay, silty clay, silty clay with nannofossils, nannofossil silty clay, silty clay nannofossil ooze, and nannofossil ooze with silty clay (Fig. **F8**). Gradational contacts between these lithologies are much more common than well-defined boundaries. Abundances of terrigenous components, as estimated from smear slides, are quartz, 0%–80%; detrital carbonate, 0%–95%; feldspars, 0%–20%; clay minerals (including chlorite), 0%–95%; heavy minerals (especially hornblende), 0%–1%; and volcanic glass, 0%–5%. No discrete ash layers were observed. Dropstones are present throughout these cores and display a wide range of compositions, including acidic intrusive and metamorphic (granites and granitoids), basic igneous and/or metamorphic (basalts and metabasalts), and sedimentary and metasedimentary (sandstone, quartzite, limestone, and dolomite). Abundances of biogenic components, as estimated from smear slides, are nannofossils, 0%–85%; foraminifers, 0%–50%; diatoms, 0%–25%; radiolarians, 0%–10%; and sponge spicules, 0%–25%. Total carbonate contents range from 1 to 48 wt% in these cores (see **"Sedimentary geochemistry"** in "Geochemistry" and **"Site U1302 and U1303 smear slides"** in "Core Descriptions"). Pyrite (usually associated with burrows) and iron oxide coatings on grains are present locally and were the only authigenic sediment components observed.

The sediments at Sites U1302 and U1303 were designated as a single unit composed of Holocene–Pleistocene terrigenous and biogenic sediments due to the gradational interbedding of these lithologies at scales of a few meters or less. This unit was divided into two subunits. Subunit IA is composed of undisturbed sediments, whereas underlying Subunit IB contains abundant intraclasts in a matrix of sand-silt-clay and is interpreted as debris flow deposits.

Description of units

Unit I

Intervals: Sections 303-U1302A-1H-1, 0 cm, to 13H-CC, 48 cm; 303-U1302B-1H-1, 0 cm, to 11H-CC, 31 cm; 303-U1302C-1H-1, 0 cm, to 11H-CC, 22 cm; 303-U1302D-1H-1, 0 cm, to 2H-CC, 15 cm; 303-U1302E-1H-1, 0 cm, to 2H-CC, 17 cm; 303-U1303A-1H-1, 0 cm, to 10H-CC, 26 cm; and 303-U1303B-1H-1, 0 cm, to 9H-CC, 20 cm

Depths: 0–107 mbsf (0–131 meters composite depth [mcd]): Hole U1302A: 0–107.1 mbsf, Hole U1302B: 0–104.7 mbsf, Hole U1302C: 0–104.5 mbsf, Hole 1302D: 0–13.0 mbsf, Hole U1302E: 0–15.1 mbsf, Hole U1303A: 0–93.9 mbsf, and Hole 1303B: 0–85.7 mbsf

Age: Holocene–Pleistocene

Unit I is composed predominantly of clay, silty clay, silty clay with nannofossils, nannofossil silty clay, silty clay nannofossil ooze, and nannofossil ooze with silty clay. Nannofossil ooze, foraminifer silty sand, sandy foraminifer ooze, silty clay with diatoms and sponge spicules, silty nannofossil ooze with diatoms and sponge spicules, and silty clay siliceous ooze with nannofossils are present as minor lithologies. Colors are predominantly gray (5Y 5/1 and 2.5Y 5/1) and dark gray (5Y 4/1 and 2.5YR 4/1), with lesser occurrences of light gray (2.5Y 6/1 and 5Y 6/1), brownish grays (7.5YR 5/2 to 2.5YR 5/2), and reddish brown (10YR 4/1). Contacts between these lithologies are generally gradational; the most common exceptions are the sharp contacts at the base of the foraminifer silty sands and the sandy foraminifer oozes (Fig. **F9**). Contacts between the other lithologies are sometimes defined by sharp color boundaries. Bioturbation is present through most of this unit; the most common indicators are diffuse centimeter-scale mottling and millimeter-scale pyritic burrow fills. In a few cases, discrete burrows or discrete macroscopic pyritized burrows were observed. Dropstones are present throughout Unit I, and their distribution is plotted in Figure **F10.**

In Subunit IA these lithologies occur as horizontally bedded, undisturbed sediments; the only notable exception is a disturbed zone in the lower half of Core 303-U1303A-7H. In Subunit IB, these pelagic and hemipelagic lithologies are present as angular to rounded intraclasts in a deformed matrix of foraminifers, sand, silt, and clay. Extrabasinal clasts originally deposited as dropstones are also present in this interval, which is interpreted to be a debris flow deposit (Fig. **F11**). The contact between Subunits IA and IB is relatively sharp within a single hole but varies in depth (both mbsf and mcd) between holes because of relief at the uppermost part of the debris flow deposit.

Subunit IA

Intervals: Sections 303-U1302A-1H-1, 0 cm, to 10H-3, 20 cm; 303-U1302B-1H-1, 0 cm, to 10H-2, 130 cm; 303-U1302C-1H-1, 0 cm, to 10H-4, 95 cm; 303-U1302D-1H-1, 0 cm, to 2H-CC, 15 cm; 303-U1302E-1H-1, 0 cm, to 2H-CC, 17 cm; 303-U1303A-1H-1, 0 cm, to

10H-CC, 26 cm; and 303-U1303B-1H-1, 0 cm, to 9H-CC, 20 cm

Depths: 0–79 to 91 mbsf (0–103 to 106 mcd): Hole U1302A: 0–79.3 mbsf, Hole U1302B: 0–88.5 mbsf, Hole U1302C: 0–90.95 mbsf, Hole U1302D: 0–13.0 mbsf, Hole U1302E: 0–15.1 mbsf, Hole U1303A: 0–93.9 mbsf, Hole U1303B: 0–85.7 mbsf

Age: Holocene–Pleistocene

Subunit IA consists of 103–106 m of variable mixtures of terrigenous and biogenous material dominated by quartz, detrital carbonates, and nannofossils. The resulting lithologies are clay, silty clay, silty clay with nannofossils, nannofossil silty clay, silty clay nannofossil ooze, and nannofossil ooze with silty clay. Nannofossil ooze, foraminifer silty sand, sandy foraminifer ooze, silty clay with diatoms and sponge spicules, silty nannofossil ooze with diatoms and sponge spicules, and silty clay siliceous ooze with nannofossils are present as minor lithologies. The uppermost 10–15 cm in Sections 303-U1302D-1H-1, 303-U1302E-1H-1, 303-U1303A-1H-1, and 303-U1303B-1H-1 are reddish brown to brownish gray and are interpreted as surface-oxidized equivalents of the underlying lithologies (Fig. **F12**). In each of these sections, a zone of concentrated metal oxides is present at the base of the oxidized sediments. Below this surface-oxidized layer, contacts between the major lithologies are generally gradational and defined by progressive color changes. The foraminifer silty sand and the sandy foraminifer ooze form well-defined intervals ranging from 1 to ~50 cm in thickness. These coarser-grained intervals have sharp basal contacts and sharp to gradational upper contacts (Fig. **F9**). Some intervals also exhibit a fining-upward trend in grain size, as well as millimeter-scale inclined stratification. These beds, especially the thicker ones, may be turbidites. Millimeter-scale lamination, caused by changes in grain size (foraminifers versus silty clay) and/or color, is rare in Subunit IA but is present in several intervals as thick as 20 cm (Fig. **F13**). These laminated intervals may be contourites or small turbidites, or they may reflect winnowing by downslope currents. Additional analyses will be required to develop sedimentologic interpretations of these intervals. Dropstones are present throughout Subunit IA (Fig. **F10**).

Sediments in Subunit IA are predominantly horizontally bedded and undisturbed, as indicated by the orientations of lithologic contacts and color patterns. The principal exception is in Core 303-U1303A-7H, where intraclasts of the underlying horizontally bedded lithologies lie at various orientations within a deformed sandy matrix of foraminifers, sand, silt, and clay (Fig. **F14**). This interval is interpreted as a relatively small sandy debris flow unit.

Subunit IB

Intervals: Sections 303-U1302A-10H-3, 20 cm, to 13H-CC, 48 cm; 303-U1302B-10H-2, 130 cm, to 11H-CC, 31 cm; and 303-U1302C-10H-4, 95 cm, to 11H-CC, 22 cm

Depths: From 79–91 mbsf (103–106 mcd) to 104.5–107.1 mbsf (126 mcd): Hole U1302A: 79.3–107.1 mbsf, Hole U1302B: 88.5–104.7 mbsf, Hole U1302C: 90.95–106.42 mbsf

Age: Pleistocene

Subunit IB consists of angular to rounded intraclasts as large as 1 dm and composed of clay, silty clay, silty clay with nannofossils, nannofossil silty clay, silty clay nannofossil ooze, and nannofossil ooze with silty clay. These clasts display variegated colors, including shades of gray, brown, light greenish gray, and white and occur in a deformed matrix of foraminifers, sand, silt, and clay (Fig. **F11**). Rock clasts similar in size and composition to the dropstones recorded in Subunit IA are also present. This interval is interpreted to be a debris flow deposit that was sourced in sediments similar to those forming Subunit IA. However, many of the exotic clasts are much older than Quaternary.

Discussion

The Holocene and Pleistocene sediments at Sites U1302 and U1303 record repeated variations in the input rates of terrigenous and biogenic components. Conditions such as these existed prior to the record cored at Sites U1302 and U1303, as indicated by the intraclasts of similar lithologies contained in the debris flow deposit of underlying Subunit IB.

During the deposition of Subunit IA, the relative input of terrigenous and biogenous components appears to have varied on timescales of tens to hundreds of thousands of years, as indicated by repeated broad changes in the abundances of quartz, detrital carbonate, and nannofossils (as observed in smear slides) and in the distribution of dropstones. Sources of the terrigenous input can be inferred from the dominance of quartz and detrital carbonate in smear slides and supplemented by the compositions of dropstones observed throughout these cores. Dropstone compositions include acidic intrusive and metamorphic rocks, basic volcanics and metavolcanics, and sedimentary rocks including limestones and dolomites. These carbonate dropstones and the fine-grained detrital carbonate indicate sources immediately upslope or to the northwest, especially in

the regions around Hudson Bay. The granitic and gneissic dropstones and the fine-grained quartz could have been derived from nearby sources or from more distant sources; the latter could include regions to the northwest or, potentially, to the north in southern and eastern Greenland. The dropstones with more basic lithologies could have been derived from sources to the northwest or in central eastern Greenland. Input rates of the biogenic components may have varied in response to changes in the paleoceanographic conditions in the overlying and surrounding waters.

A preliminary qualitative analysis indicates that the lithologic changes recorded in Subunit IA cannot be linked consistently to glacial–interglacial stages interpreted from magnetic susceptibility and the carbonate records (see **"Composite section"** and **"Whole-core magnetic susceptibility measurements"** in "Physical properties"). For example, dropstone distribution maxima occur during apparent glacials, apparent interglacials, and apparent climatic transitions. As a result of these complexities, extracting paleoclimatic records from the range of sedimentary components will require a variety of detailed postcruise studies.

Deposition of Subunit IA was dominated by pelagic and hemipelagic processes. Episodically, however, small turbidity currents or contour currents affected the area, depositing the sharp-based coarser-grained beds of foraminifer silty sand and sandy foraminifer ooze and producing the intervals that contain weak to well-developed laminations.

One of the major goals of Expedition 303 was to extend the record of Pleistocene millennial-scale climate change beyond that obtained from conventional cores. A reasonable first step toward achieving this objective is to evaluate the ways in which the sediments at Sites U1302 and U1303 record known late Pleistocene and Holocene millennial-scale climatic events, whose commonly recognized characteristics in the North Atlantic have included a basal layer of IRD, increased detrital carbonate content, light color, and increased magnetic susceptibility. Magnetic susceptibility and bulk density data were used to identify the positions of Heinrich events H0–H6, as well as low-detrital carbonate (LDC) and detrital carbonate (DC6) layers, in Hole U1303B (Fig. **F26**). The overall color reflectance lightness (L*) values, gravel abundances, and visually observed Munsell colors of these intervals were then compared to the characteristics of the overlying and underlying sediments. The L* values show distinct peaks at the levels of H1–H5 and DC6 but do not rise above adjacent background for H0, LDC, and H6. H5 and DC6 are the only intervals that contain significantly more IRD than adjacent background, but the IRD in H5 and DC6 is disseminated throughout each interval, rather than being concentrated at its respective base. Visual color estimates show evidence of increased brown hues for H1 and H2 and lightening for H4 and H5 but no consistent pattern of color change for all of the known millennial-scale events because they are not all rich in detrital carbonate. The detrital stratigraphy at Orphan Knoll represents a proximal analog to the detrital stratigraphy of the classic central Atlantic IRD belt. Identifying and explaining the differences in manifestation of these events and refining the correlation among events will be necessary before the record of older millennial-scale climate change can be examined and interpreted in detail.

Biostratigraphy

Samples from Sites U1302 and U1303 were examined for their micropaleontologic content and revealed rich assemblages of calcareous, siliceous, and organic-walled microfossils (Figs. **F15, F16**). Coccoliths are abundant and well preserved in most samples and permit establishment of biostratigraphic schemes that are complemented by diatoms and palynologic datums. According to these schemes, the composite sequence of Site U1302 is younger than 1.16 Ma but most likely spans the last 0.95 m.y. (Fig. **F17**). The composite sequence of Site U1303 probably corresponds to an interval spanning approximately the last 0.85 m.y. (Fig. **F18**).

Beyond the biostratigraphic schemes, the micropaleontologic assemblages provide insight into paleoclimatologic and paleoceanographic conditions. In particular, the relative abundance of the planktonic foraminifer *Neogloboquadrina pachyderma* (sinistral) and some dinocyst assemblages allow identification of glacial and interglacial conditions from some core catcher samples (Figs. **F19, F20**).

Calcareous nannofossils

Site U1302

Calcareous nannofossils were examined in all core catcher samples from Holes U1302A–U1302E (Tables **T2, T3, T4, T5, T6**). Additional samples were examined from Cores 303-U1302B-7H and 8H and 303-U1302C-8H at different depths (see Tables **T3, T4**) to verify the precise depth occurrences of two marker taxa (*Emiliania huxleyi* and *Pseudoemiliania lacunosa*). All samples are characterized by well-preserved and abundant calcareous nannofossils, except Samples 303-U1302A-4H-CC and 303-U1302C-5H-CC. The assemblages are dominated by small-sized coccoliths such as *Gephyrocapsa* spp. and *Reticulofenestra* spp.

Reworked nannofossils of Cretaceous–Miocene age are found throughout the sedimentary sequence.

E. huxleyi, the marker species of Zone NN21 (0.25–0 Ma), occurs commonly in intervals 303-U1302A-1H-CC to 3H-CC, 303-U1302B-1H-CC to 2H-CC, and 303-U1302C-1H-CC to 3H-CC. The last occurrence (LO) of *P. lacunosa,* which marks the uppermost part of Zone NN19 (0.41 Ma), is detected in Samples 303-U1302A-6H-CC, 303-U1302B-7H-CC, and 303-U1302C-7H-CC (Tables **T2, T3, T4**).

Lower in the holes, *Reticulofenestra asanoi* is a characteristic feature. Its FO and LO are recorded at 1.16 and 0.85 Ma, respectively. It is present in Samples 303-U1302A-11H-CC through 13H-CC, 303-U1302B-10H-CC through 11H-CC, and 303-U1302C-11H-CC (Tables **T2, T3, T4**). The lowest occurrence of *Gephyrocapsa parallela,* which indicates an age of 0.95 Ma, is found in Sample 303-U1302A-12H-CC. We thus suggest an age spanning 0.85–0.95 Ma for the depth interval between 111 and 128.2 mcd (Fig. **F17**). Sample 303-U1302A-13H-CC (bottom of the sequence), characterized by occurrences of *R. asanoi* and by the absence of *G. parallela,* is assigned an age interval between 0.95 and 1.16 Ma. These results indicate that the sequence recovered at Site U1302 corresponds to an interval composed between 0 and <1.16 Ma, encompassing most of the last 950 k.y. (Fig. **F17**).

Site U1303

The calcareous nannofossil assemblage found at this site is similar to that observed at Site U1302. We examined calcareous nannofossils in all core catcher samples from Holes U1303A and U1303B (see Tables **T7, T8**). The assemblages are also characterized by well-preserved and abundantly occurring coccoliths, except Sample 303-U1303A-6H-CC, and by the occurrence of nannofossils reworked from the Cretaceous to the Miocene.

As at Site U1303, there is a co-occurrence of *E. huxleyi* and *P. lacunosa* (Sample 303-U1303B-8H-CC). Sample 303-U1303A-10H-CC is characterized by the LO of *R. asanoi*, which is dated 0.85 Ma. The FO of *G. parallela* (0.95 Ma) is not found in the samples, suggesting an age younger than 0.95 Ma at the base of Site U1303 (Fig. **F18**).

Planktonic foraminifers

Planktonic foraminifers were examined in all core catcher samples from Holes U1302A–U1302C, U1303A, and U1303B (Tables **T9, T10, T11, T12, T13**). The upper three core catchers of each hole contain soft sediment that was treated with tap water. Sediments of the deeper core catchers were soaked in H_2O_2 solution, which may have resulted in a higher degree of test fragmentation. Planktonic foraminiferal tests are abundant (>50% of all particles >63 µm) in most samples investigated (Tables **T9, T10, T11, T12**). Planktonic foraminiferal tests are rare in Samples 303-U1302C-5H-CC, 303-U1303A-9H-CC, and 303-U1303B-7H-CC and barren in Sample 303-U1303A-6H-CC. Test preservation is very good in the uppermost core catchers and generally decreases downhole. In Sample 303-U1303B-7H-CC, the test preservation is poor. A dwarfed assemblage characterized by many very small tests occurs in Samples 303-U1302B-5H-CC and 303-U1302C-7H-CC.

The dominant planktonic foraminiferal species are *N. pachyderma, Globigerina bulloides,* and *Globorotalia inflata* in most samples (Tables **T9, T10, T11, T12**). At both sites, *N. pachyderma* (sinistral) is abundant continuously down to the bottom of all holes (Fig. **F19**) and most of the tests are encrusted. Its occurrence indicates that the entire sequence belongs to the *N. pachyderma* (sinistral) Zone in the Pleistocene–Upper Pliocene (Weaver and Clement, 1987). Other abundant species include *Turborotalita quinqueloba* (sinistral and dextral) and *N. pachyderma* (dextral). Specimens of *Globigerinita glutinata* are rare in many of the samples investigated. All of these species are present in the modern North Atlantic. The only extinct species recovered is *Globigerina decoraperta,* whose LO was at 1.77 Ma. It occurs in Samples 303-U1302C-6H-CC, 8H-CC, and 11H-CC, 303-U1303A-7H-CC, and 303-U1303A-5H-CC, possibly due to remobilization of older sediments.

The species composition of most planktonic foraminiferal assemblages indicates that surface water conditions were largely subpolar/polar to temperate. The frequent occurrence of *G. inflata* at Sites U1302 and U1303 suggests that the hydrography of the Orphan Knoll area was dominated by fronts. The occurrence of tropical species (*Globigerinoides ruber, Globigerinoides trilobus, Globigerinella siphonifera,* and *Orbulina universa*) indicates occasional intrusion of warm surface waters, like the modern ones with warm-core eddies from the Gulf Stream entering in the northwestern North Atlantic. The presence of adult specimens of the deep-dwelling species *Globorotalia truncatulinoides* indicates subduction of intermediate to deepwater masses from the south.

Benthic foraminifers

Benthic foraminifers were examined in core catcher samples from Holes U1302A–U1302C, U1303A, and U1303B. All investigated sediments contain benthic foraminiferal tests (Table **T14**). Preservation of benthic foraminiferal tests is good, suggesting lim-

ited reworking of the sediments. *Uvigerina* spp. (*peregrine* group) and *Epistominella exigua* are the most abundant taxa. The only agglutinated species found is *Eggerelloides bradyi*.

Dominance of *E. exigua* suggests bottom water bathed by the Northeast Atlantic Deep Water. *U. peregrina* is frequent in Samples 303-U1302A-2H-CC, 303-U1302B-2H-CC, and 303-U1303B-1H-CC and 3H-CC. These samples also contain the highest frequency of the polar planktonic foraminifer *N. pachyderma* (sinistral). The occurrence of *U. peregrina* may indicate reduced North Atlantic Deep Water formation and the presence of oxygen-poor Southern Source Waters at Sites U1302 and U1303 during cold phases (Bilodeau et al., 1994).

Diatoms

Diatoms were examined on smear slides prepared from all core catchers and additional samples from Sites U1302 and U1303 (Tables **T15, T16, T17, T18, T19, T20, T21**). Overall diatom abundance is mostly low (barren to rare) at both sites but becomes common to abundant in a few samples. Diatom preservation is poor almost throughout. The silicoflagellate *Dictyocha fibula* and the siliceous dinoflagellate *Actiniscus pentasterias* are sporadically present. Sponge spicules are abundant in several samples at both sites.

Two diatom zones, *Thalassiosira oestrupii* Zone and *Proboscia curvirostris* Zone, are recognized (Koç et al., 1999). The stratigraphic marker *P. curvirostris* (LO = 0.30 Ma) is observed in several horizons at both sites (Tables **T15, T16, T17, T20, T21;** Figs. **F17, F18**) and is therefore assigned to the *P. curvirostris* Zone (Figs. **F17, F18;** 0.60–0.3 Ma) (Koç et al. 1999). *Thalassiosira jouseae,* found only in Samples 303-U1302A-8H-CC, 303-U1303B-5H, 2–65 cm, 303-U1303B-7H, 3–90 cm, and 303-U1303B-8H-CC gives a very similar age (LO = 0.30 Ma). The occurrence of *Fragilariopsis reinholdii* (LO = 0.62 Ma) in Sample 303-U1303A-8H-CC suggests that the interval below 75 mcd in Holes U1302B and U1302B belongs to the lower *P. curvirostris* Zone (0.85 to ~0.60 Ma). We cannot date other samples because of extremely rare and poorly preserved diatoms.

The major constituent of the diatom flora is *Lioloma* sp. This needle-shaped diatom dominates the assemblage in almost every sample where diatoms are either common or abundant (Tables **T15, T16, T17, T20, T21**). The dominance of *Lioloma* sp. may be related to enhanced surface circulation leading to the development of frontal systems and facilitating the concentration of diatom cells in the plankton and, consequently, greater downward flux through the water column (Kemp et al., 1995, and references therein). Entire valves of *Lioloma* sp. are very rare, reflecting bad preservation conditions of diatoms. A species-rich pelagic warm-water-related flora also occurs throughout. The main constituents of this tropical/subtropical association are *Fragilariopsis doliolus* and several species of *Azpeitia,* accompanied by some *Coscinodiscus* spp., *Roperia tesselata, Thalassiosira fere-lineata,* and *Thalassiosira lineata*. Secondary species in each horizon are *Actinocyclus curvatulus, T. oestrupii* var. *oestrupii,* and *T. oestrupii* var. *venrickae*.

The diatom flora is enriched by resting spores of *Chaetoceros,* which are indicative of high productivity in the upper water column. In addition, coastal-associated tycopelagic *A. curvatulus, Thalassionema nitzschioides* var. *nitzschioides,* and *Paralia sulcata* occur in several horizons. Typical subpolar species (*Rhizosolenia hebetata* f. *hiemalis, Thalassiosira gravida,* and *Thalassiosira trifulta*) occur throughout as trace components.

Radiolarians

Radiolarians were examined in all core catcher samples from Sites U1302 and U1303 (Tables **T22, T23**). In most samples, radiolarians are barren to rare and their preservation is moderate to poor. A few samples contain common to abundant radiolarians, notably in the middle part of Holes U1302A (Sample 303-U1302A-7H-CC), U1302B (Samples 303-U1302B-8H-CC and 9H-CC), and U1302C (Samples 303-U1302C-4H-CC and 8H-CC) and in the lower part of Holes U1303A (Sample 303-U1303A-7H-CC) and U1303B (Samples 303-U1303B-8H-CC and 9H-CC) (Tables **T22, T23**). In these samples, the diversity of species is high.

The most abundant species are *Actinomma leptodermum* and *Cycladophora davisiana davisiana*. The stratigraphically diagnostic *C. davisiana davisiana* occurs in the middle part of Holes U1302A (Samples 303-U1302A-5H-CC and 7H-CC) and U1302C (Samples 303-U1302C-4H-CC and 8H-CC) and in the middle to upper part of Hole U1302B (Samples 303-U1302B-1H-CC, 3H-CC, and 5H-CC to 9H-CC). This species also occurs in Samples 303-U1302D-2H-CC and 303-U1302E-1H-CC. The assemblages of these samples thus belong to the Upper Pliocene–Pleistocene *C. davisiana davisiana* Zone of Goll and Bjørklund (1989). *C. davisiana davisiana* is also characteristic of many samples from Holes U1303A (Samples 303-U13013A-3H-CC, 5H-CC, 7H-CC, and 8H-CC) and U1303B (Samples 303-U1303B-4H-CC, 5H-CC, 8H-CC, and 9H-CC), indicating the *C. davisiana davisiana* Zone.

Palynomorphs

Palynologic assemblages were examined in core catcher samples from Holes U1302A, U1302B, and U1303A (Tables **T24, T25, T26**). In general, samples were difficult to process because of abundant detrital and biogenic silica. Nevertheless, well-preserved pollen grains and dinoflagellate cysts were recovered in most samples. The species composition of assemblages is modern, suggesting Pleistocene age of all analyzed samples.

The pollen content is largely dominated by *Pinus* and/or *Picea,* which are related to atmospheric input from boreal forest of the adjacent northeast North American continent. Variable pollen concentrations suggest changes in the density of the forest cover in the source area and/or changes in the strength and pattern of atmospheric trajectories.

The dinocyst concentration is extremely variable, ranging from <10 cysts/cm^3 to >10^3 cysts/cm^3. Such amplitude of variations of more than three orders of magnitude suggests varying dinoflagellate productivity and sea-surface conditions through geologic time. Relatively high dinocyst concentrations characterize Quaternary interglacial and interstadial intervals in the northern North Atlantic, whereas generally low concentrations characterize glacial stages (de Vernal and Mudie, 1992).

The dinocyst assemblages show relatively low species diversity, probably partly due to the insufficient onboard sample preparation. Large changes in both species composition and dominant species from one sample to another indicate changing conditions in surface waters. Reworked palynomorphs of Paleozoic–Paleogene ages are a characteristic feature of many core catcher samples, even dominating the assemblages in some samples, indicating abundant detrital inputs that originate from older sedimentary formations.

Hole U1302A

Only seven core catcher samples from Hole U1302A were processed (Table **T24**). Five of these samples revealed more abundant reworked palynomorphs than dinocysts (Samples 1H-CC, 4H-CC, 6H-CC, 10H-CC, and 12H-CC), suggesting that detrital input dominated over pelagic flux during sedimentation at these depths. Samples 3H-CC and 8H-CC contain moderately high dinocyst content, reflecting interglacial-type conditions when pelagic flux dominates over detrital input.

Hole U1302B

All core catcher samples from Hole U1302B were prepared and examined for their palynologic content (Table **T25**). Three of the samples revealed more abundant reworked palynomorphs than dinocysts (Samples 3H-CC, 7H-CC, and 11H-CC), indicating important detrital inputs from Paleozoic–Paleogene formations and limited dinocyst fluxes. Sample 7H-CC contains abundant microscopic charcoal fragments. Samples 6H-CC, 8H-CC, and 9H-CC contain relatively rich dinocyst assemblages dominated by *Brigantedinium,* which suggests low-salinity conditions in surface waters. Samples 1H-CC and 5H-CC are characterized by rich assemblages with both neritic and oceanic components.

Hole U1303A

All core catcher samples from Hole U1303A were prepared and examined for their palynologic content (Table **T26**). Two samples revealed no dinocysts (Samples 6H-CC and 9H-CC) but contained reworked palynomorphs. Samples 5H-CC and 8H-CC possibly include palynomorphs that might be useful as biostratigraphic markers. In Sample 5H-CC, *Filisphaera filifera,* (last-appearance datum [LAD] in MIS 17) was recovered. However, this sample contains very rare and poorly preserved dinocysts, which may indicate sedimentary redeposition. In Sample 8H-CC, which contains a rich palynologic assemblage, the presence of specimens belonging to the prasinophyte *Cymatiosphaera ?invaginata* (LAD in MIS 17) may suggest an age of ≥0.7 Ma. Samples 3H-CC, 7H-CC, and 8H-CC are characterized by dinocyst assemblages typical of temperate waters and relatively low sea-surface salinity. These samples likely indicate interglacial stages.

Paleomagnetism

The natural remanent magnetization (NRM) of the archive half-core sections of Sites U1302 and U1303 were measured and remeasured after alternating-field (AF) demagnetization in peak fields of up to 20 mT. Cores 303-U1302A-1H through 7H and 303-U1302C-1H were AF demagnetized at 5, 10, 15, and 20 mT. Cores 303-U1302A-8H through 9H were AF demagnetized at 10, 15, and 20 mT. Cores 303-U1302A-10H, 303-U1302B-1H through 10H, and 303-U1302C-2H through 11H and core from Holes U1302D, U1302E, U1303A, and U1303B were AF demagnetized at 10 and 20 mT. Cores 303-U1303A-11H through 13H and 303-U1303B-11H were demagnetized at 20 mT. The number of demagnetization steps was influenced by the magnetic characteristics of the sediments and the need to maintain core flow through the laboratory. Sections completely affected by drilling disturbance were not measured. Data associated with intervals identified as drilling slurry af-

fected by drilling disturbance and exceptionally coarse deposits (see **"Lithostratigraphy"**) were culled.

The NRM intensities at both Sites U1302 and U1303 are strong with meter-scale variations of up to a factor of 3. Intensity values after demagnetization with 20 mT peak fields ranged from ~1.5×10^{-1} to 5×10^{-2} A/m in lithologic Subunit IA (down to ~106 mcd) (Fig. **F21**). NRM intensities are lower in lithologic Subunit IB (below ~106 mcd) with values after demagnetization in 20 mT peak fields varying around 1×10^{-2} A/m (Fig. **F21**).

Steep positive inclinations observed prior to demagnetization and due to the drill string magnetic overprint are removed by 10 mT peak AF demagnetization. Intensity continues to decrease between 10 and 20 mT demagnetization, although inclinations and declinations show little difference. Inclinations in lithologic Subunit IA are consistent with those expected from a geocentric axial dipole (GAD) (~67°) for the 50°10′N latitude of these sites (Fig. **F22**). Declinations (Fig. **F23**) show within-core consistency. Inclinations and declinations of Subunit IB are more variable, likely reflecting its origin as a debris flow (see **"Lithostratigraphy"**). The positive inclinations of lithologic Subunit IA are interpreted as a primary magnetization indicating normal polarity deposition entirely in the Brunhes Chron (see also **"Biostratigraphy"**). A short interval of negative inclinations and reversed declinations was observed in correlative sediments in Sections 303-U1302C-3H-5, 303-U1302B-3H-2, and 303-U1303A-3H-2. Based on shipboard stratigraphic estimates, this feature likely reflects the Iceland Basin Event with an estimated age of 187 ka (Channell et al., 1997). The polarity zones from lithologic Subunit IB are not clearly defined. Sediments with a more tranquil depositional origin were found below the debris flow deposits at the base of Subunit IB in Hole U1302A. These show reversed inclinations with relatively well defined declination over two sections underlain by positive inclination and a 180° declination shift to the base of the cored section. Biostratigraphic interpretation suggesting a late Matuyama age for these sediments is consistent with the reversed inclinations. Whether the transition to positive inclination observed in Core 303-U1302C-12H represents a true geomagnetic reversal (possibly the upper Jaramillo) is not unequivocally supported by the biostratigraphic data or the overall quality of the paleomagnetic data in Subunit IB.

Composite section

We constructed two spliced composite sections at Sites U1302 and U1303. The first includes only intervals from Site U1302, with the exception of a short segment of Core 303-U1302A-1H that was not recovered near the top of Site U1302. This segment, referred to as the "shipboard" splice, was used for shipboard reporting purposes. It was not possible to construct a complete composite record at Site U1303 because not all of the gaps in Hole U1303A could be filled by cores from Hole U1303B. Consequently, a second splice, referred to as the "sampling" splice, was constructed using the best sections from both locations regardless of whether they came from Site U1302 or Site U1303. One may question the validity of creating a spliced record using two sites located 5.68 km apart, but both sites are in the same depositional environment and the density and magnetic susceptibility signals can be easily correlated between sites. We recommend that the "sampling" splice and its composite depth scale be used for postcruise sampling and analysis because it optimizes the quality and correlation of the stratigraphic section. The "sampling" splice table has been implemented in the Janus database.

We initially depth-shifted cores on the basis of magnetic susceptibility data (magnetic susceptibility core logger [MSCL] aka "fast track") and then refined correlations once GRA density data were available from the multisensor track (MST). The offsets and composite depths differ between the shipboard and sampling spliced sections (Tables **T27, T28**). In general, the magnetic susceptibility and GRA bulk density records from all holes at both sites are nearly identical (Figs. **F24, F25**). Differences among holes can often be attributed to drilling disturbance or the occurrence of dropstones that resulted in spikes in the density and magnetic susceptibility records. For the uppermost 30 m of section, the density and magnetic susceptibility signals at Sites U1302 and U1303 were compared to piston Core MD99-2237 to assess the completeness of the stratigraphic section (Fig. **F26**). Aside from some differences resulting from differential stretching of the MD core relative to the spliced Site U1302 and U1303 record, the density signals are virtually identical, permitting the identification of all Heinrich and detrital carbonate events during the last glacial period as identified in conventional piston cores from the same location (Hillaire-Marcel et al., 1994; Stoner et al., 1996).

For both splices, cores were correlated by aligning features in GRA density and magnetic susceptibility profiles. It is impossible to align every feature in cores across all holes because of stretching and compression of the core during the coring process. Because of this effect, we selected features in magnetic susceptibility or GRA density that were present in a majority of records to anchor the correlation among

cores. An example is the density maximum at ~16 mcd that appears in six holes (Fig. F25). With this feature aligned, there is a 0.5 m mismatch of another density maximum at ~13.4 mcd in Hole U1303B. Such discrepancies are unavoidable when using the program Splicer but can be corrected postcruise using software that permits stretching and squeezing within cores.

The sections of core used for both the shipboard and sampling splices are identified in the spliced data tables (Tables T29, T30). We avoided using the tops and bottoms of each core in the splice, whenever possible, because of potential core disturbance, and were particularly wary of the first section of each core. The composite data indicate that the cores from Sites U1302 and U1303 provide a continuous stratigraphic sequence to ~107.0 mcd. Below this level, cores were appended to the base of the composite section. This level corresponds to the top of a thick debris flow. The uncorrelated cores from below the base of Core 303-U1302A-10H were given the offset of the deepest correlated core. Cores from other holes were correlated with Hole U1302A cores below the splice, but the correlation is weak.

The growth factor (GF) is the ratio of mcd to mbsf and is used to correct the mcd scale for core lengthening. An overall growth factor from both sites is calculated by linear regression of all of the data (GF = 1.13) (Fig. F27). We used this value of GF to calculate corrected meters composite depth (cmcd) presented in Table T27 to aid in the calculation of mass accumulation rates. Growth factors are somewhat different for Sites U1302 (GF = 1.15) and U1303 (GF = 1.03), and the difference may be significant at deeper depths.

Sedimentation rates were difficult to calculate because the expanded section was all deposited in a single polarity chron and there are few reliable biostratigraphic markers. Age is plotted versus depth in Figure F28 for both biostratigraphic and paleomagnetic datums. A single least-squares linear fit to the data results in an average sedimentation rate of 9.8 cm/k.y. over the interval where we have data. However, the least-squares fit line does not intercept the 0 depth point at 0 age, suggesting a higher sedimentation rate of 22.5 cm/k.y. between the seafloor and our first datum at 39 mcd.

Geochemistry

Volatile hydrocarbons

Headspace gas analysis was performed as a part of the standard protocols required for shipboard safety and pollution prevention monitoring. A total of 20 headspace samples from Holes U1302A and U1303A were analyzed (10 from each site at a sampling resolution of 1 per core) (Table T31). In general, sediments from Sites U1302 and U1303 yield low interstitial gas concentrations. Methane (C_1) concentrations are slightly higher than the atmospheric background level, ranging between 2.1 and 3.8 ppmv, and show no notable downhole trend (Fig. F29). The average C_1 concentrations for Holes U1302A and U1303A are 2.7 and 3.3 ppmv, respectively. No hydrocarbons higher than C_1 were detected.

Sedimentary geochemistry

Sediment samples were collected for the analyses of solid-phase geochemistry (inorganic carbon and elemental C, N, and S) at a sampling resolution of approximately two per core from all the holes drilled at Sites U1302 and U1303. At each site, the samples collected from multiple holes are taken to constitute a single depth profile using the composite depth scale (see "Composite section"). Figures F30 and F31 show calcium carbonate ($CaCO_3$) concentrations, total organic carbon (TOC) contents, N elemental concentrations, and organic C/N atomic ratios for Sites U1302 and U1303, respectively. Results of the coulometric and elemental analyses are reported in Table T32.

Determinations of bulk $CaCO_3$ contents by coulometry were made for 59 samples from Site U1302 and 30 samples from Site U1303. In general, carbonate contents for the sampled strata range from 1.4 to 48.6 wt% at Site U1302 (Fig. F30) and from 3.7 to 46.8 wt% at Site U1303 (Fig. F31). At Site U1302, the carbonate record is characterized by three distinct maxima of ~46 wt% at 129.8, 64.0–60.3, and 22.1–20.6 mcd, whereas minima (<10 wt%) are recognized at 107.1–91.1, 69.4, 26.7, and 10.4 mcd (Fig. F30). The carbonate contents appear to decrease gradually upward from each of the maxima toward the minima, particularly between 129.8 and 107.1 mcd, ~64 and 26.7 mcd, and ~20.6 and 5.5 mcd. In contrast, upward increases in carbonate content from each of the minima to the maxima are rapid, as observed between 69.4 and 64.0 mcd, 26.7 and 20.6 mcd, and 5.5 and 1.3 mcd. Although obscured by lower sampling resolution, the carbonate record at Site U1303 (Fig. F31) exhibits upward trend and maximum and minimum peaks that are similar to those in the Site U1302 record.

The variable carbonate contents recognized at Sites U1302 and U1303 primarily reflect relative abundance of calcareous components (i.e., nannofossils, foraminifers, and detrital carbonate) and noncarbonate materials dominated by silty clay and siliceous

microfossils (see "Lithostratigraphy"). The lithology of deep-sea sediments can be traced using various downcore physical property and color reflectance records (see "Physical properties" and "Lithostratigraphy," both in the "Site U1302–U1308 methods" chapter). To supplement the lower resolution shipboard carbonate data from Sites U1303 and U1302, we compare them to a high-resolution color reflectance L* record from Site U1302. As illustrated in Figure F32, the L* variation at Site U1302 corresponds well to the Site U1302 and U1303 carbonate profiles visually in that the high L* values (i.e., high reflectance) are associated with high carbonate contents and the low L* values correspond to low carbonate contents. Such visual correspondences between the carbonate and L* records are also recognized with other high-resolution physical property data (not shown) and, therefore, our shipboard low-resolution carbonate data document the first-order lithologic variability reasonably well.

Sedimentary total C, N, and S concentrations were determined on 36 samples from Holes U1302A–U1302E and 31 samples from Holes U1303A and U1303B. TOC content for most intervals at Sites U1302 and U1303 is <0.7 wt% (average = ~0.5 wt%) (Figs. F30, F31). Total N content at Sites U1302 and U1303 ranges from 0.03 to 0.10 wt% (average = ~0.05 wt%) (Figs. F30, F31). No significant downcore trends are recognized for TOC and N records at Sites U1302 and U1303. C/N ratio is a useful indicator to interpret origin of organic matter (i.e., marine, degraded marine, or terrestrial) in the sediments (Emerson and Hedges, 1988; Meyers, 1997). At Sites U1302 and U1303, most of the C/N values are ~4–13 ratio (Figs. F30, F31). This suggests that the organic materials preserved in the upper ~140 m of the sediments at Sites U1302 and U1303 are marine in origin (i.e., C/N = ~4–10 ratio) (Meyers, 1997). We recognize a sporadic occurrence of high C/N values (~20 ratio) that appears to be associated with intervals of high carbonate content. These relatively high C/N values could represent oxidized and degraded marine organic matter. None of the analyzed samples contained measurable S.

Interstitial water chemistry

We collected a total of 16 interstitial water samples from whole-round sediment sections from Sites U1302 and U1303. Seven samples from Hole U1302A and nine samples from Holes U1303A and U1303B were processed for routine shipboard geochemical analyses. For Site U1303, the samples from the two holes are taken to constitute a single depth profile using the composite depth scale. Besides whole-round samples, interstitial water samples were collected from small plug (~10 cm^3) sediment samples for the upper ~100 mbsf for shore-based studies. Results of interstitial water analyses for Sites U1302 and U1303 are reported in Table T33 and Figure F33. Interstitial water chemistry data from Sample 303-U1303A-10H-1, 145–150 cm (i.e., 92.58 mcd), is not considered for further discussion due to clear evidence of core disturbance (see "Site U1302 and U1303 visual core descriptions" in "Core Descriptions") and contamination by drill fluid in the sample evident in several interstitial water chemistry parameters shown in Figure F33.

Chloride, sodium, salinity, and pH

The Cl^- records from Site U1302 and U1303 interstitial water are similar in terms of the overall trends, although some offsets exist between them because of low sampling resolution at each site (Fig. F33). In the upper ~40 mcd of the sediments, Cl^- increases downhole from ~555 to ~567 mM, returning to the near-seawater values in the underlying sediments to ~110 mcd. Previous workers have attributed the chlorinity maximum of ~40–50 mbsf to a remnant of higher-salinity bottom water masses during the Last Glacial Maximum (LGM) preserved in the sediment pore spaces (e.g., McDuff, 1985; Adkins et al., 2002; Adkins and Schrag, 2003). The overall downhole trends of our shipboard pore fluid chlorinity data in the upper ~100 m of the sediment columns are similar to those reported from other deep-sea sections. This implies that conservative chemical proxies preserved in the interstitial water samples collected from Sites U1302 and U1303 may record properties of bottom water masses prevailed during the LGM.

Downhole profiles of pore fluid Na^+ concentrations derived from charge balance calculation for Sites U1302 and U1303 exhibit trends that are roughly similar to those of Cl^- (Fig. F33). The Na^+ values at the sites range from 468 to 486 mM. The pH profiles at Sites U1302 and U1303 do not exhibit any significant downhole trends, with values ranging from 7.4 to 7.7 (Fig. F33). Salinity (not shown) is generally higher at Site U1303 than Site U1302 in the upper ~60 mcd while exhibiting decreasing trend downhole at both sites.

Alkalinity, sulfate, ammonium, and dissolved silica

Alkalinity increases with depth from 4.5–10.4 mM in the upper ~30 mcd at Site U1303, followed by relatively constant values at ~10.5 mM downhole (Fig. F33). Alkalinity values at Site U1302 are generally lower than those at Site U1303 by ~1 mM overall and decrease slightly from 9.7 mM at 36.4 mcd to 8.7 mM at 110.7 mcd. Sulfate profiles from Sites

U1302 and U1303 are in concert with one another in terms of their values and downhole trends (Fig. F33). In general, SO_4^{2-} concentrations decrease steadily downhole over the entire drilled sequences, ranging from 26.7 mM at ~2.3 mcd to ~5.8 mM at ~110.7 mcd. The downhole trends in NH_4^+ show antithetic relationships to SO_4^{2-} (Fig. F33). NH_4^+ concentrations at Site U1303 are slightly higher than those at Site U1302 and exhibit a downward increasing trend in the upper 70 m, ranging from 165 to 977 µM. Below ~70 mcd, NH_4^+ decreases by ~150 µM at Site U1302. The downhole increases in alkalinity and NH_4^+ and decrease in SO_4^{2-} at Sites U1302 and U1303 primarily reflect decomposition of organic materials driven by SO_4^{2-} reduction. The highest alkalinity values (i.e., ~10.6 mM) below ~40 mcd at Sites U1302 and U1303 are not as high as expected from the degree of SO_4^{2-} reduction (i.e., ~42 mM), implying that alkalinity produced through SO_4^{2-} reduction is being consumed in the sediments.

Dissolved silica concentrations at Sites U1302 and U1303 increase with depth from 579 µM at 2.3 mcd to 880 µM at ~79.7 mcd (Fig. F33). The elevated dissolved H_4SiO_4 at Sites U1302 and U1303 likely reflects the presence and dissolution of biogenic H_4SiO_4 in the sediments. The lowest dissolved H_4SiO_4 concentration of ~327 µm recognized at 110.7 mcd in Hole U1302A coincides with an interval of opal-free silty clay sediments (see **"Lithostratigraphy"** and **"Biostratigraphy"**).

Calcium, strontium, lithium, magnesium, and potassium

At Site U1303, pore fluid calcium (Ca^{2+}) concentrations decrease downhole gradually from the near-seawater value of ~9.8 mM at ~2.3 mcd to ~4.6 mM at ~60.8 mcd (Fig. F33). A similar downhole trend is recognized at Site U1302, but values are offset and higher than those at Site U1303 by ~0.8 mM. The most depleted Ca^{2+} values are recognized at 60.8 and 79.7 mcd at Sites U1303 and U1302, respectively. The Sr^{2+} and Li^+ trends resemble one another in terms of overall downhole trends (Fig. F33); the highest values close to the seawater average are recognized at the top of the interstitial water profiles, decrease gradually downward to ~40–80 mcd, and increase slightly toward the bottom of the recovered sections. The parallel downhole trends recognized in the Ca^{2+}, Sr^{2+}, and Li^+ profiles suggest the uptake in a diagenetic phase. These trends and the consumption of alkalinity likely reflect precipitation of carbonate minerals. However, biogenic carbonate dissolution and recrystallization are not important diagenetic processes at the sites because Sr^{2+} does not increase with depth (e.g., Baker et al., 1982).

Mg^{2+} and K^+ concentrations decrease steadily and consistently with depths at the two sites (Fig. F33). By the deepest sample at Site U1303 (i.e., at 68.9 mcd), Mg^{2+} decreases by ~13% to 44.8 mM and K^+ decreases by ~17% to 10.1 mM from the near-seawater values at the topmost sample. These correlating profiles (r = 0.83, n = 15) indicate that Mg^{2+} and K^+ ions are being consumed in a related process perhaps through reactions with silicate minerals (i.e., clay diagenesis) within or below the cored interval. Another possible explanation for the downhole decreasing trend in the Mg^{2+} concentrations is precipitation of authigenic dolomite. However, dolomite precipitation may not be a significant diagenetic process governing the Mg^{2+} profiles at the sites because the magnitude of downhole decrease in Mg^{2+} concentrations is small relative to Ca^{2+}.

Manganese, iron, boron, and barium

The Mn^{2+} profile at Site U1303 is characterized by a maximum concentration (52.2 µM) at the shallowest sample and subsequent rapid decrease to 17.0 µM at 8.9 mcd (Fig. F33). Below ~10 mcd, Mn^{2+} concentrations decrease moderately downhole at Sites U1302 and U1303, reaching a minimum concentration of ~6 µM at ~60–80 mcd. The downhole Mn^{2+} profiles suggest that we may have sampled the lowermost part of the manganese reduction zone. Pore fluid Fe profiles at Sites U1302 and U1303 exhibit downhole decreasing trends, ranging from 18.3 µM in the shallowest sample to 1.4 µM at 68.9 mcd (Fig. F33). In particular, the Fe profile at Site U1302 shows relatively uniform and very low concentrations of ~2–3 µM from 36.4 mcd toward the bottom of the recovered sections. At these sites, available Fe is probably rapidly precipitated into iron sulfides, which are ubiquitous in the sediments (see **"Lithostratigraphy"**).

Boron concentrations, mostly as boric acid (H_3BO_3), in the interstitial water samples at Sites U1302 and U1303 (not shown), exhibit a wide variety of values ranging from 496 to 623 µM, while no significant downhole trends are recognized. Barium (Ba^{2+}) concentrations (not shown) are very low (<1.0 µM) as expected within the sulfate reduction zone, as available Ba^{2+} is sequestered in barite.

Physical properties

Physical properties were measured at Sites U1302 and U1303 following the procedures described in **"Physical properties"** in the "Site U1302–U1308 methods" chapter. Two measurements of magnetic susceptibility were conducted, along with GRA, natural gamma radiation (NGR), and *P*-wave velocity (PWS3). Thermal

conductivity was measured on whole cores with a frequency of one per section for each core, and moisture and density (MAD) property samples were measured on two samples per core, usually at the bottom of Section 1 and the top of Section 6.

Whole-core magnetic susceptibility measurements

Trends in magnetic susceptibility are similar between those obtained from the "Fast Track" MSCL and the MST (Fig. F34). One exception occurs in Hole U1303A between 72.8 and 76.2 mcd, where MSCL values are similar between both holes at Site U1303 but the MST record shows a different pattern. Some data are missing because of failure of the MST magnetic susceptibility loop. Peak magnetic susceptibility values range from 280×10^{-5} to 300×10^{-5} SI in lithologic Subunit IA (down to ~106 mcd) (Fig. F34) and coincide with peaks in GRA bulk density (Fig. F35).

Density

Site U1302 and U1303 sediments display a relatively uniform increase in bulk density and decrease in water content downcore. Discrete bulk densities agree well with the primary trends in GRA bulk density (Fig. F36). GRA density varies between 2 and 2.5 g/cm^3 and is positively correlated with susceptibility in lithologic Subunit IA. Underlying lithologic Subunit IB and coinciding with a mass flow deposit, the covariance between magnetic susceptibility and GRA density is not as clear. However, magnetic and peak density values found below the debris flow deposits at the base of Subunit IB at Site U1302 show the same covarying behavior.

Natural gamma radiation

NGR and magnetic susceptibility measurements were used to correlate among holes from the two sites (Fig. F37). These proxies provide a means of evaluating the relative amounts of clay and carbonate in the sediments. At both sites, NGR is positively correlated with both magnetic susceptibility and GRA density measurements. NGR counts range from 20 to 49 cps, with the majority of the values between 40 and 49 cps. Low NGR counts (20–22 cps) correspond to low magnetic susceptibility and GRA values, suggesting that these intervals are associated with increased carbonate sedimentation.

P-wave velocity

P-wave velocity was not measured with the MST-mounted *P*-wave logger (PWL) at these sites because of an instrument malfunction. However, discrete measurements were performed with the PWS3 on every section where the sediment was not disturbed by the coring process. *P*-wave velocities range from 1400 to 1650 m/s, averaging 1541–1566 m/s at Site U1302 and 1549 m/s at Site U1303, slightly higher than the standard velocity of sound in seawater (1531 m/s). Prominent maxima correspond to levels where peak GRA density values were measured. In Subunit IB (100–106 mcd at Site U1302), scatter in the measurements becomes more pronounced with sound velocities up to 1800 m/s (Fig. F38), coinciding with bulk density and magnetic susceptibility peaks.

Thermal conductivity

Discrete thermal conductivity measurements were made usually on Section 4 of each core from Sites U1302 (Table T34) and U1303 (Table T35). Thermal conductivity is variable throughout the cores, showing an average value of 1.03–1.06 W/(m·K) at the top of Holes U1302D, U1302E, and U1303A, increasing to values of ~1.22–1.25 W/(m·K) downcore (Fig. F36). Thermal conductivity is strongly correlated with other physical properties of the sediments, including bulk density, *P*-wave velocity, and porosity.

Porosity

Porosity was calculated from the MST GRA density measurements (see **"Physical properties"** in the "Site U1302–U1308 methods" chapter) and compared with the porosity results generated from discrete MAD samples (Fig. F39). The porosity values are highly variable and range between 30% and 80%. Highest velocities and lowest porosities are associated with clay-rich layers in this interval. Porosity also decreases gradually downhole from 60%–70% at the top to 40%–50% at the bottom of the hole.

Discussion

Physical property records allow identification of high-resolution lithologic variability that results largely from variations in the input of terrigenous and biogenic components to the region. Generally, magnetic susceptibility and density peaks coincide with increased delivery of terrigenous sediments. The NGR variations are sufficient to resolve millennial-scale events and glacial–interglacial cycles extending back to MIS 17 (Fig. F35). In some cases, low magnetic susceptibility, density, and NGR values correspond to deposition of more carbonate rich sediments (see **"Lithostratigraphy"**) in Subunit IA. Physical properties were used to identify the last six Heinrich events as well as several other older ice-rafting episodes by comparison with previously studied

records from nearby IMAGES Core MD95-2024 and Cores HU91-045-094 (e.g., Hillaire-Marcel et al., 1994; Stoner et al., 1995, 2000) and MD99-2237 (Turon et al., 1999). These rapidly deposited detrital layers, intercalated with background hemipelagic sediments, provide a record of the effects of Laurentide Ice Sheet instability and associated paleoceanographic changes. Sites U1302 and U1303 constitute a proximal analog to the detrital stratigraphy developed for the central North Atlantic IRD belt.

References

Adkins, J.F., and Schrag, D.P., 2003. Reconstructing last glacial maximum bottom water salinities from deep-sea sediment pore fluid profiles. *Earth Planet Sci. Lett.,* 216:109–123. **doi:10.1016/S0012-821X(03)00502-8**

Adkins, J.F., McIntyre, K., and Schrag, D.P., 2002. The salinity, temperature and $\delta^{18}O$ of the glacial deep ocean. *Science,* 298:1769–1773. **doi:10.1126/science.1076252**

Aksu, A.E., and Hiscott, R.N., 1992. Shingled Quaternary debris flow lenses on the northeast Newfoundland slope. *Sedimentology,* 39:193–206.

Baker, P.A., Gieskes, J.M., and Elderfield, H., 1982. Diagenesis of carbonates in deep-sea sediments—evidence from Sr^{2+}/Ca^{2+} ratios and interstitial dissolved Sr^{2+} data. *J. Sediment. Petrol.,* 52:71–82.

Bilodeau, G., de Vernal, A., and Hillaire-Marcel, C., 1994. Benthic foraminiferal assemblages in Labrador Sea sediments: relations with deep-water mass changes since deglaciation. *Can. J. Earth Sci.,* 31:128–138.

Broecker, W.S., Bond, G.C., Mieczyslawa, K., Clark, E.A., and McManus, J., 1992. Origin of the northern Atlantic's Heinrich events. *In* Kelts, K.R. (Ed.), *Past and Present Climate Dynamics: Reconstruction of Rates of Change.* Clim. Dyn. 6(3–4):265–273. **doi:10.1007/BF00193540**

Channell, J.E.T., Hodell, D.A., and Lehman, B., 1997. Relative geomagnetic paleointensity and $\delta^{18}O$ at ODP Site 983 (Gardar Drift, North Atlantic) since 350 ka. *Earth Planet. Sci. Lett.,* 153:103–118. **doi:10.1016/S0012-821X(97)00164-7**

Chian, D., Reid, I.D., and Jackson, H.R., 2001. Crustal structure beneath Orphan basin and implications for nonvolcanic continental rifting. *J. Geophys. Res,* 106:10923–10940. **doi:10.1029/2000JB900422**

Chough, S., Hesse, R., and Müller, J., 1987. The northwest Atlantic mid-ocean channel of the Labrador Sea, IV. Petrography and provenance of the sediments. *Can. J. Earth Sci.,* 24:731–740.

de Vernal, A., and Mudie, P.J., 1992. Pliocene and Quaternary dinoflagellate cyst stratigraphy in Labrador Sea: paleocological implications. *In* Head, M.J., and Wrenn, J.H. (Eds.), *Neogene and Quaternary Dinoflagellate Cysts and Acritarchs:* Salt Lake City (Publisher's Press), 329–346.

Emerson, S., and Hedges, J.I., 1988. Processes controlling the organic carbon content of open ocean sediments. *Paleoceanography,* 3:621–634.

Goll, R.M., and Bjørklund, K.R., 1989. A new radiolarian biostratigraphy for the Neogene of the Norwegian Sea: ODP Leg 104. *In* Eldholm, O., Thiede, J., Taylor, E., et al., *Proc. ODP, Sci. Results,* 104: College Station, TX (Ocean Drilling Program), 697–737. [**PDF**]

Heinrich, H., 1988. Origin and consequences of cyclic ice rafting in the northeast Atlantic Ocean during the past 130,000 years. *Quat. Res.,* 29:142–152. **doi:10.1016/0033-5894(88)90057-9**

Hesse, R., Khodabakhsh, S., Klaucke, I., and Ryan, W.B.F., 1997. Asymmetrical turbid surface plume deposition near ice-outlets of the Pleistocene Laurentide Ice Sheet in the Labrador Sea. *Geo-Mar. Lett.* 17:179–187.

Hillaire-Marcel, C., and Bilodeau, G., 2000. Instabilities in the Labrador Sea water mass structure during the last climatic cycle. *Can. J. Earth Sci.,* 37:795–809.

Hillaire-Marcel, C., de Vernal, A., Bilodeau, G., and Weaver, A.J., 2001a. Absence of deep-water formation in the Labrador Sea during the last interglacial period. *Nature (London, U. K.),* 410:1073–1077. **doi:10.1038/35074059**

Hillaire-Marcel, C., de Vernal, A., Bilodeau, G., and Wu, G., 1994. Isotope stratigraphy, sedimentation rates, deep circulation, and carbonate events in the Labrador Sea during the last ~200 ka. *Can. J. Earth Sci.,* 31:63–89.

Hillaire-Marcel, C., de Vernal, A., Candon, L., and Bilodeau, G., 2001b. Changes of potential density gradients in the northwestern North Atlantic during the last climatic cycle based on a multiproxy approach. In *The Oceans and Rapid Climage Change: Past, Present and Future.* Geophys. Monogr., 126:83–100.

Hiscott, R.N., Aksu, A.E., Mudie, P.J., and Parsons, D.F., 2001. A 340,000 year record of ice rafting, paleoclimatic fluctuations, and shelf-crossing glacial advances in the southwestern Labrador Sea. *Global Planet. Change,* 28:227–240. **doi:10.1016/S0921-8181(00)00075-8**

Hiscott, R.N., and Aksu, A.E., 1996. Quaternary sedimentary processes and budgets in the Orphan Basin, southwestern Labrador Sea. *Quat. Res.,* 45:160–175. **doi:10.1006/qres.1996.0017**

Keen, C.E., and Beaumont, C., 1990. Geodynamics of rifted continental margins. *In* Keen, M.J., and Williams, G.L. (Eds.), *The Geology of North America: Geology of the Continental Margin of Eastern Canada.* Geol. Soc. Am., 2:391–472.

Kemp, A.E.S., Baldauf, J.G., and Pearce, R.B., 1995. Origins and paleoceanographic significance of laminated diatom ooze from the eastern equatorial Pacific Ocean. *In* Pisias, N.G., Mayer, L.A., Janecek, T.R., Palmer-Julson, A., and van Andel, T.H. (Eds.), *Proc. ODP, Sci. Results,* 138: College Station, TX (Ocean Drilling Program), 641–645.

Koç, N., Hodell, D.A., Kleiven, H., and Labeyrie, L., 1999. High-resolution Pleistocene diatom biostratigraphy of Site 983 and correlations with isotope stratigraphy. *In* Raymo, M.E., Jansen, E., Blum, P., and Herbert, T.D. (Eds.), 1999. *Proc. ODP, Sci. Results,* 162: College Station, TX (Ocean Drilling Program), 51–62. [**HTML**]

McDuff, R.E., 1985. The chemistry of interstitial waters, Deep Sea Drilling Project Leg 86. *In* Heath, G.R.,

Burckle, L.H., et al., *Init. Repts. DSDP,* 86: Washington (U.S. Govt. Printing Office), 675–687.

Meyers, P.A., 1997. Organic geochemical proxies of paleoceanographic, paleolimnologic, and paleoclimatic processes. *Org. Geochem.,* 27:213–250. **doi:10.1016/S0146-6380(97)00049-1**

Sato, T., Kameo, K., and Mita, I., 1999. Validity of the latest Cenozoic calcareous nannofossil datums and its application to the tephrochronology. *Earth Sci.,* 53:265–274.

Smith, W.H.F., and Sandwell, D.T., 1994. Bathymetric prediction from dense satellite altimetry and sparse shipboard bathymetry. *J. Geophys. Res.,* 99:21803–21824. **doi:10.1029/94JB00988**

Stoner, J.S., Channell, J.E.T., and Hillaire-Marcel, C., 1995. Late Pleistocene relative geomagnetic paleointensity from the deep Labrador Sea: regional and global correlations. *Earth Planet. Sci. Lett.,* 134:237–252. **doi:10.1016/0012-821X(95)00134-X**

Stoner, J.S., Channell, J.E.T., and Hillaire-Marcel, C., 1996. The magnetic signature of rapidly deposited detrital layers from the deep Labrador Sea: relationship to North Atlantic Heinrich layers. *Paleoceanography,* 11:309–325. **doi:10.1029/96PA00583**

Stoner, J.S., Channell, J.E.T., and Hillaire-Marcel, C., 1998. A 200 ka geomagnetic chronostratigraphy for the Labrador Sea: indirect correlation of the sediment record to SPECMAP. *Earth Planet. Sci. Lett.,* 159:165–181. **doi:10.1016/S0012-821X(98)00069-7**

Stoner, J.S., Channell, J.E.T., Hillaire-Marcel, C., and Kissel, C., 2000. Geomagnetic paleointensity and environmental record from Labrador Sea Core MD95-2024: global marine sediment and ice core chronostratigraphy for the last 110 kyr. *Earth Planet. Sci. Lett.,* 183:161–177. **doi:10.1016/S0012-821X(00)00272-7**

Toews, M.W., and Piper, D.J.W., 2002. Recurrence intervals of seismically triggered mass-transport deposits at Orphan Knoll continental margin off Newfoundland and Labrador. *Curr. Res.—Geol. Surv. Can.,* E17:1–8.

Turon, J.-L., Hillaire-Marcel, C., and Shipboard Participants, 1999. IMAGES V mission of the *Marion Dufresne,* Leg 2, 30 June to 24 July 1999. *Geol. Surv. Canada,* Open File 3782.

Weaver, P.P.E., and Clement, B.M., 1987. Magnetobiostratigraphy of planktonic foraminiferal datums, DSDP Leg 94, North Atlantic. *In* Ruddiman, W.F., Kidd, R.B., Thomas, E., et al., *Init. Repts. DSDP,* 94: Washington (U.S. Govt. Printing Office), 815–829.

Wei, W., 1993. Calibration of upper Pliocene–lower Pleistocene nannofossil events with oxygen isotope stratigraphy. *Paleoceanography,* 8:85–99.

Publication: 9 September 2006
MS 303306-103

Figure F1. Location of Orphan Knoll (from Toews and Piper, 2002).

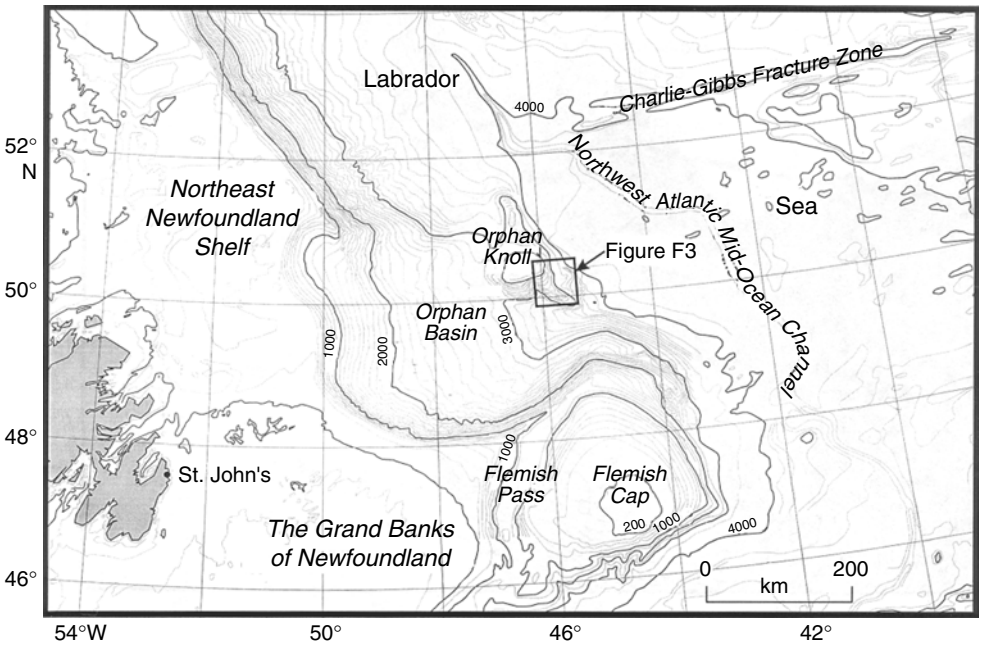

Figure F2. Location of Sites U1302 and U1303 relative to DSDP Site 111 located on the crest of Orphan Knoll (bathymetry from Smith and Sandwell, 1994) (50 m contour lines on multibeam bathymetry image).

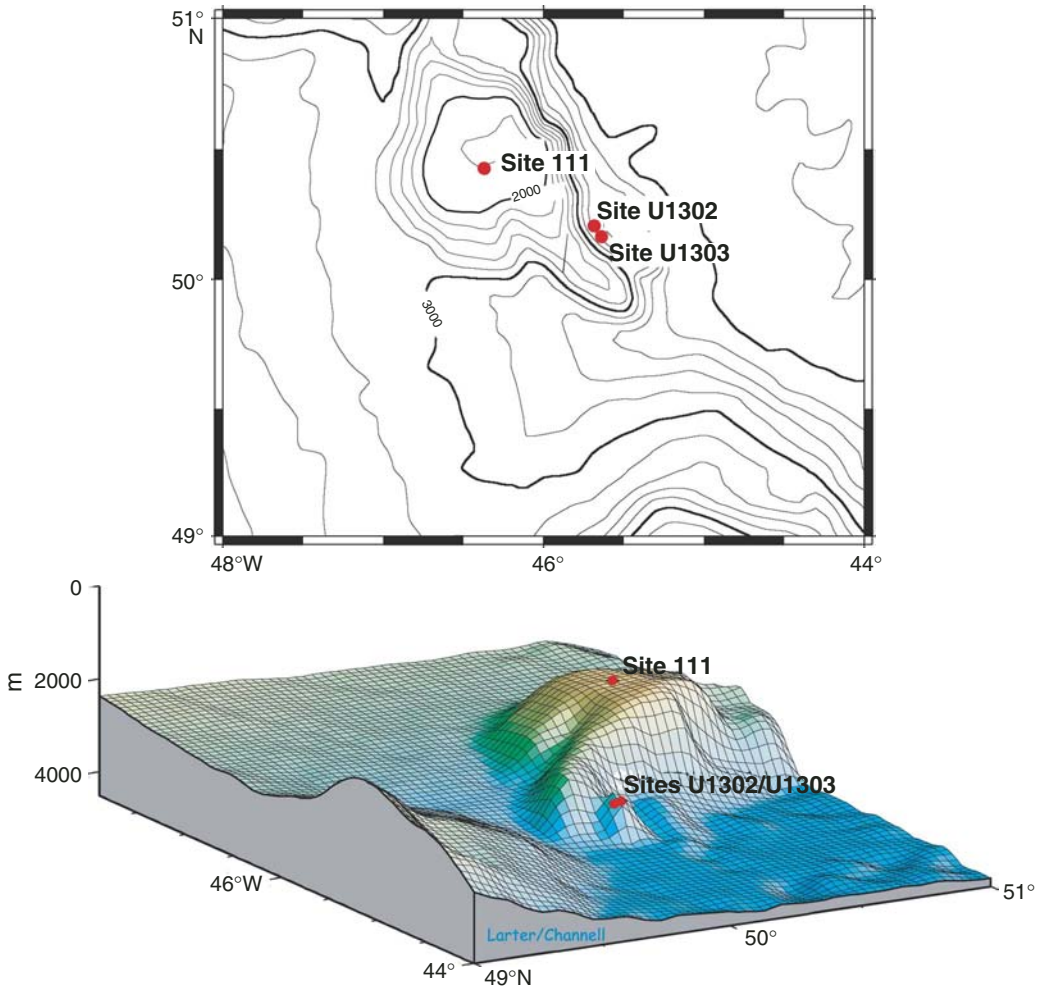

Figure F3. Bathymetric map of the site survey shiptrack close to Sites U1302 and U1303. Arrows indicate conduits for mass transport deposits (from Toews and Piper, 2002) (50 m contour lines on multibeam bathymetry image).

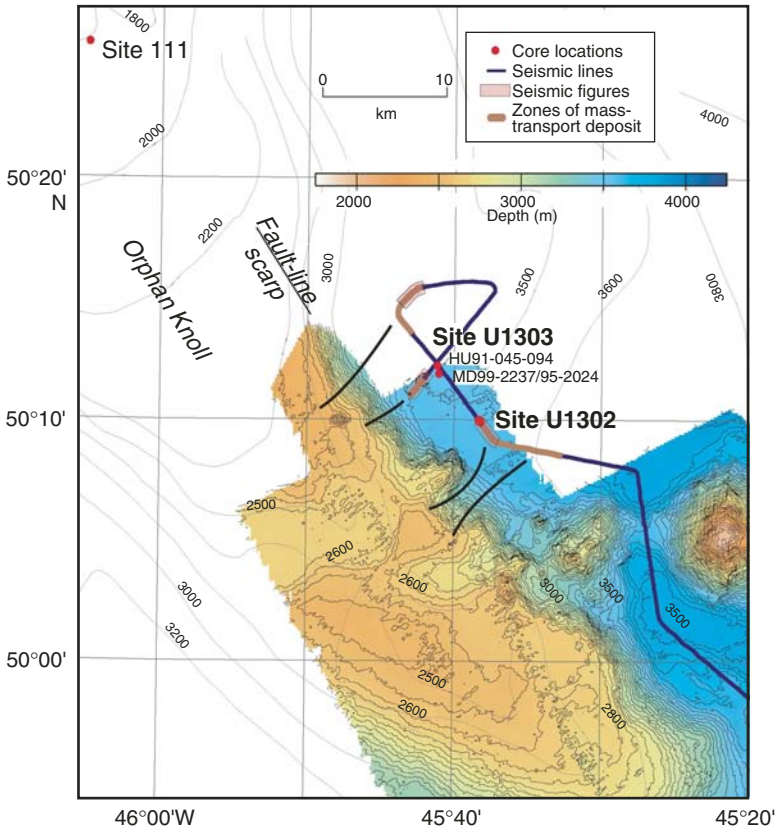

Figure F4. Volume magnetic susceptibility for three piston cores collected at Site U1303 (from Turon et al., 1999).

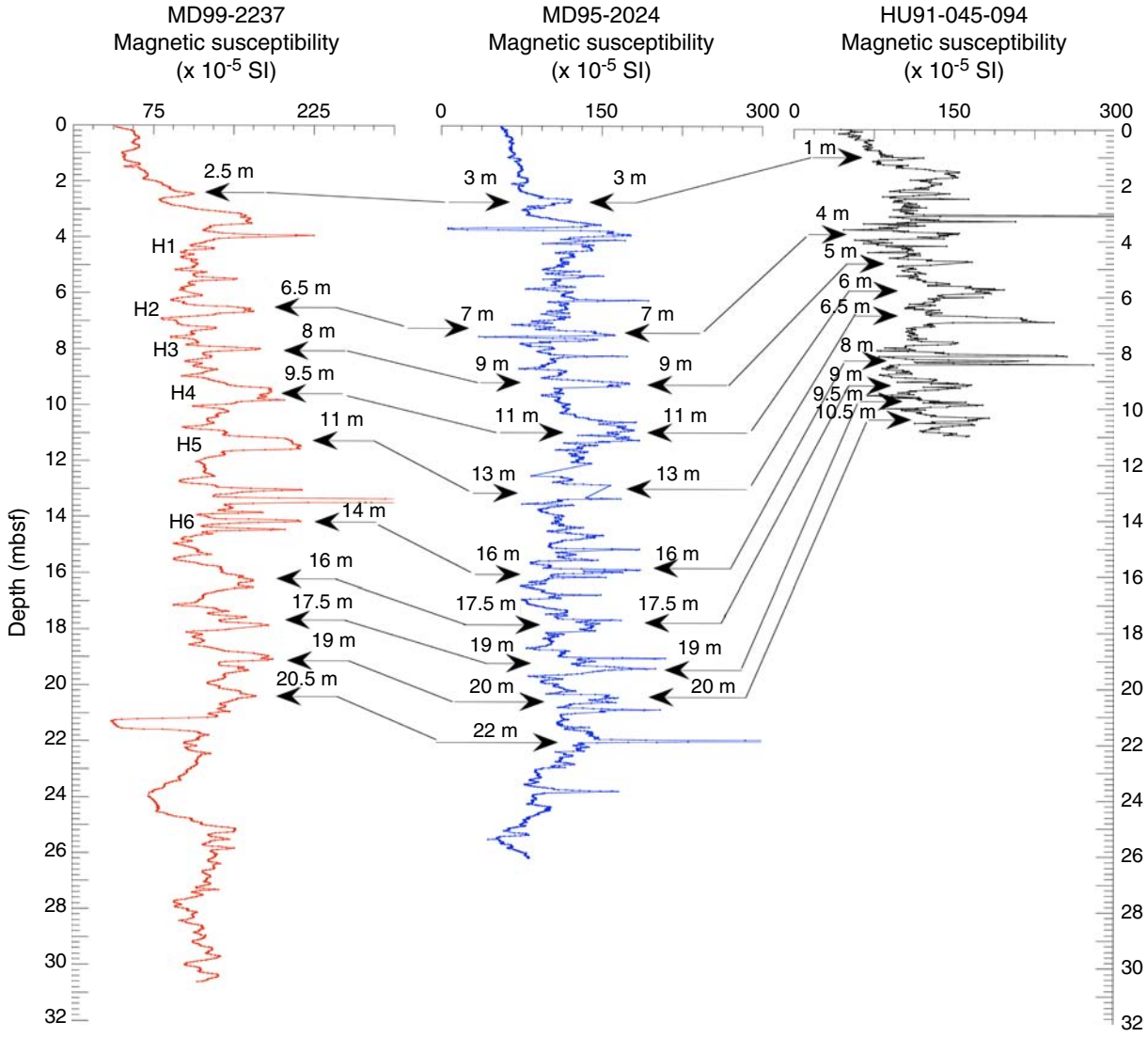

Figure F5. Single-channel air gun data on the ship's track (Fig. F3) between Sites U1302 and U1303 (see Toews and Piper, 2002).

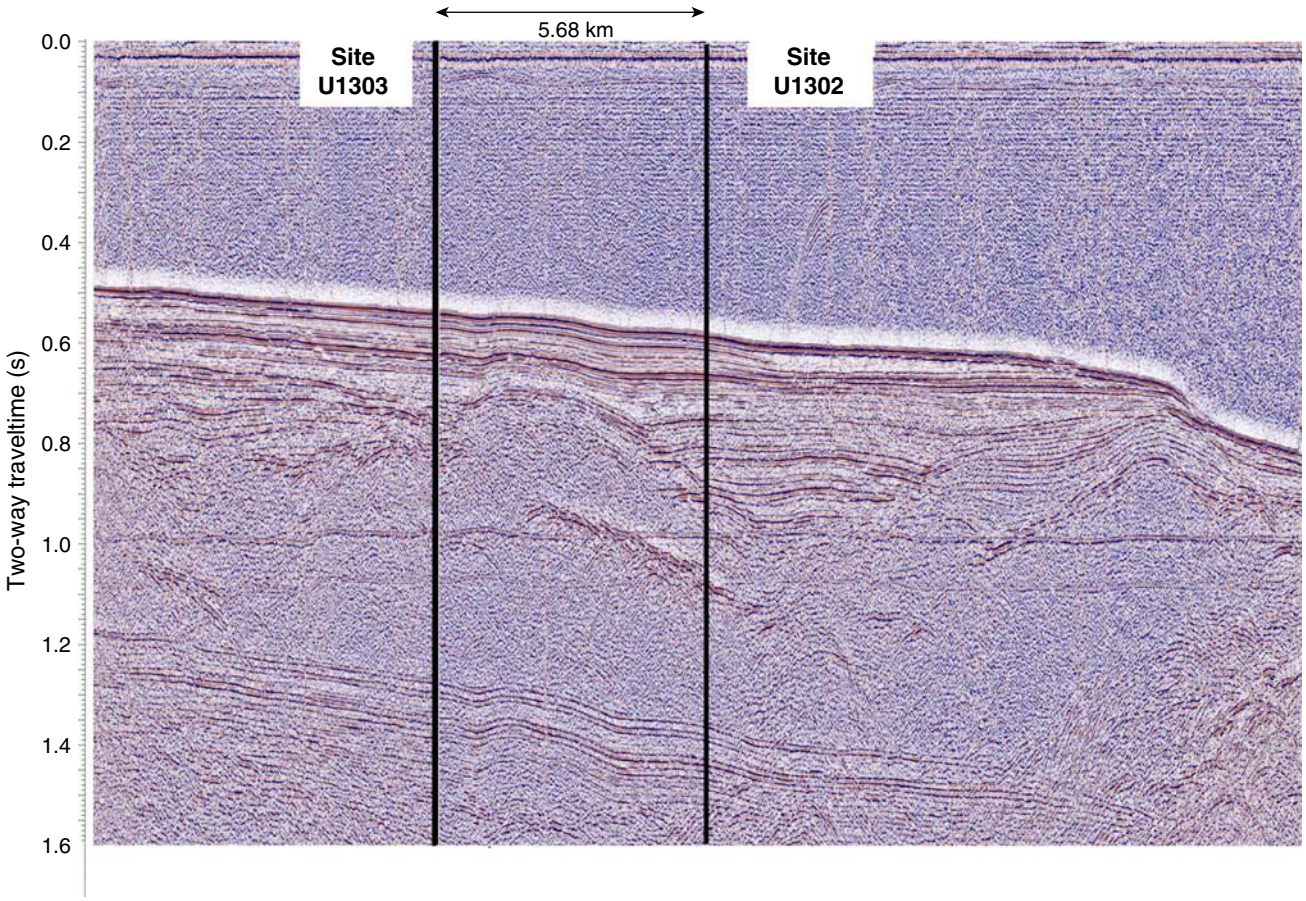

Figure F6. Huntec sparker profiles in the vicinity of Sites U1302 and U1303. Interpretation of reflectors by correlation to Core MD99-2237 and mass transport deposits (yellow) from Toews and Piper (2002). See Figure F3 for section locations (boxed areas).

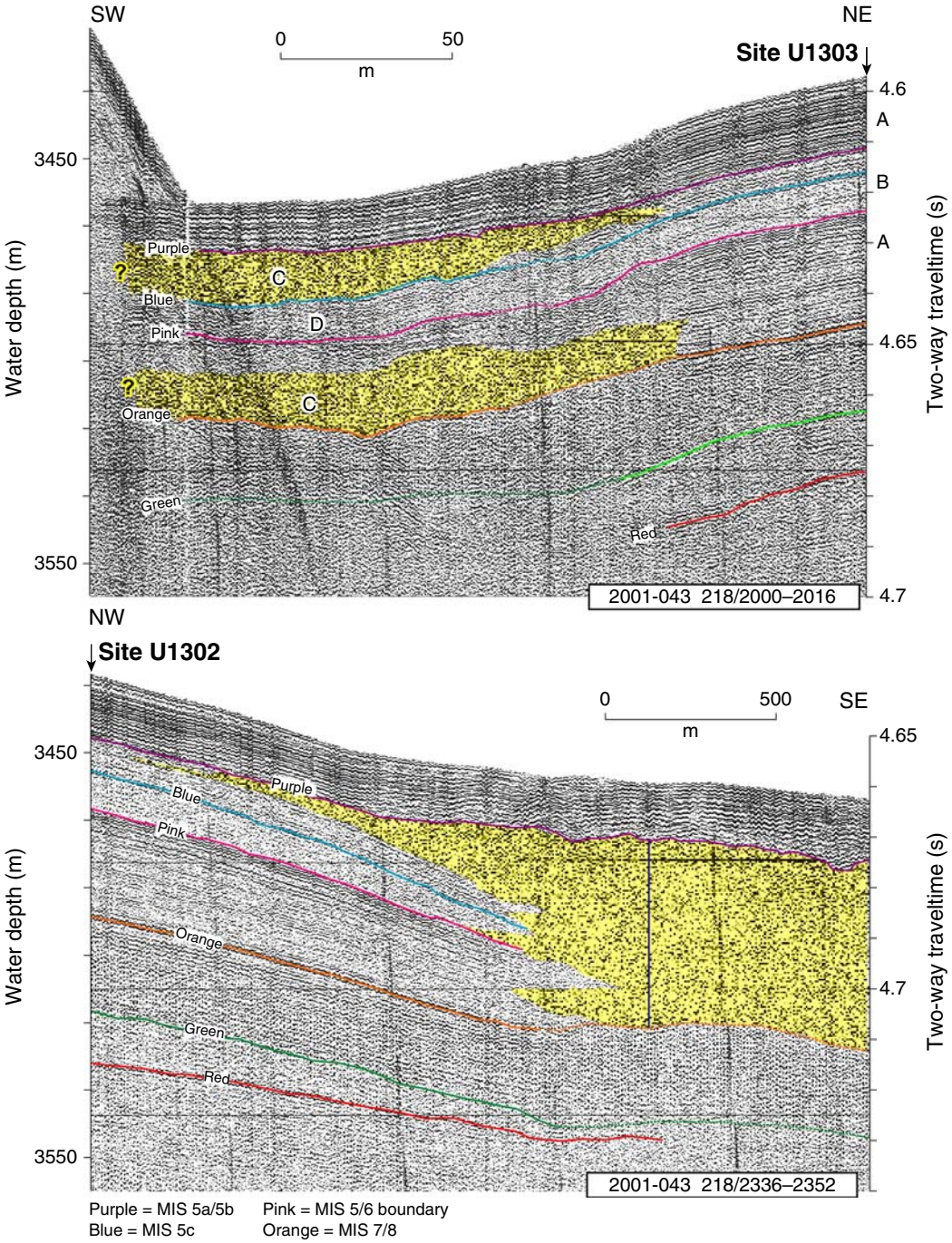

Figure F7. Abundances of quartz, inorganic calcite, and nannofossils, Site U1302. Triangle = Hole U1302A data, square = Hole U1302B data, circle = Hole U1302C data.

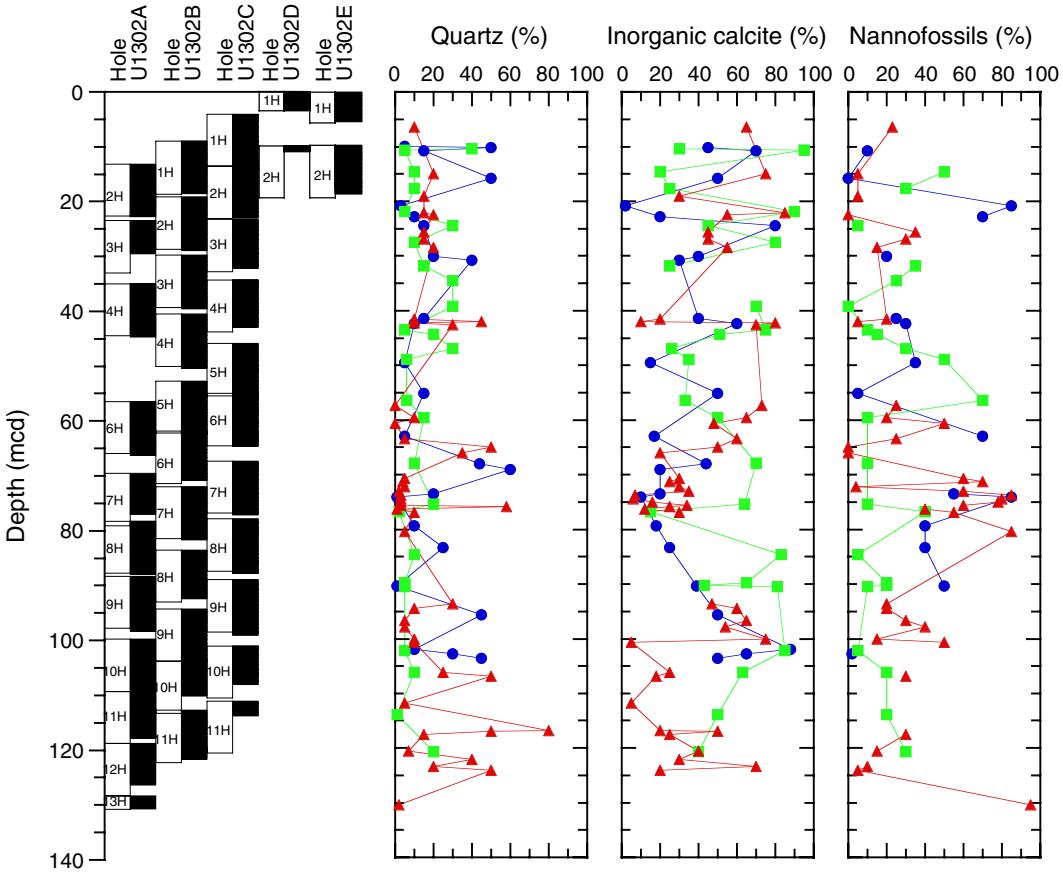

Figure F8. Graphic summary of the lithologies recovered at Sites U1302 and U1303.

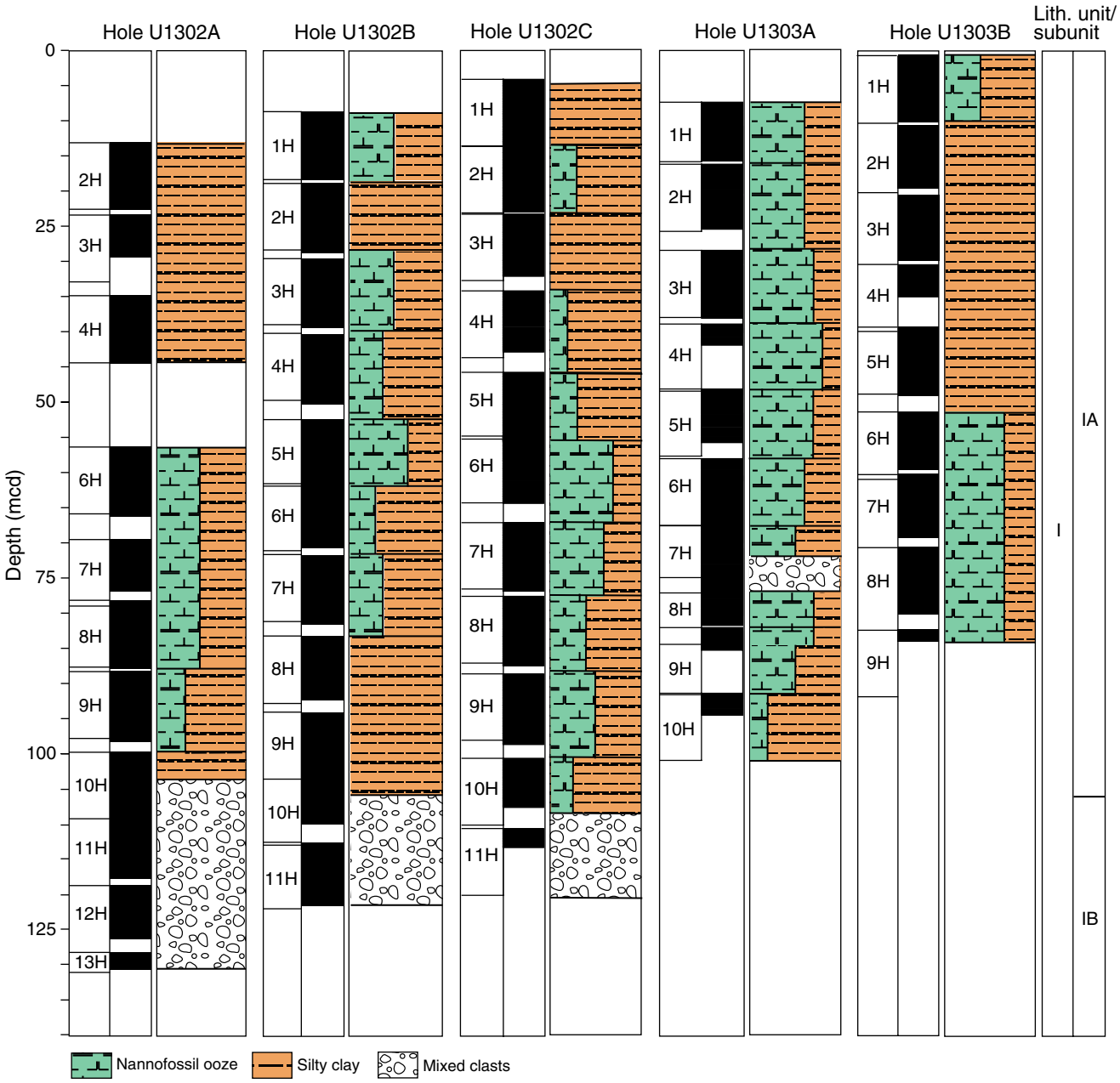

Figure F9. Foraminifer silty sand bed with sharp base and sharp to gradational top (interval 303-U1302C-6H-4, 0–23 cm).

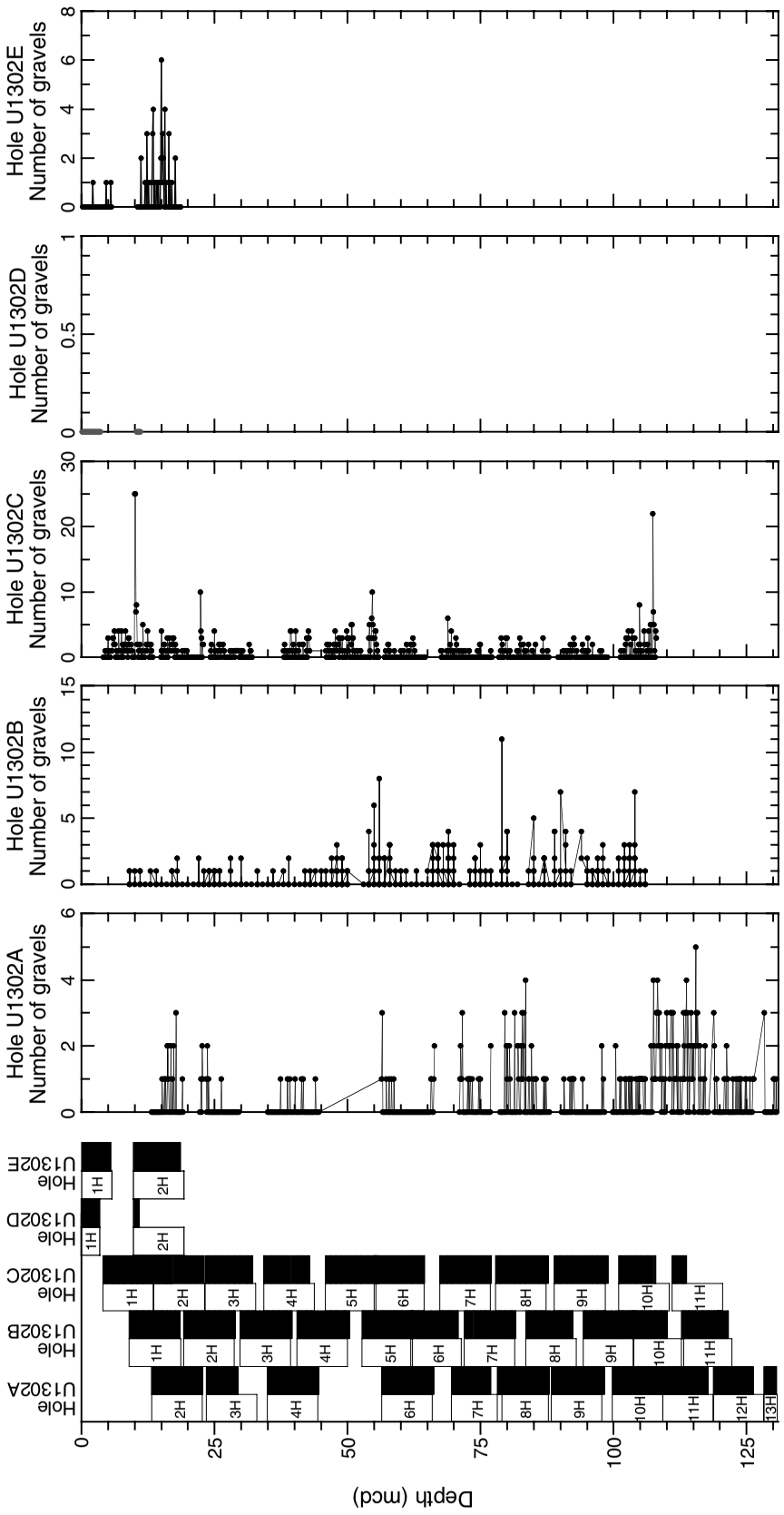

Figure F10. Abundance of gravel-sized grains (number of grains/10 cm length of core), Site U1302.

Figure F11. Intraformational conglomerate of Subunit IB, showing intraclasts, exotic clasts, and the sandy matrix (interval 303-U1302A-10H-6, 75–100 cm).

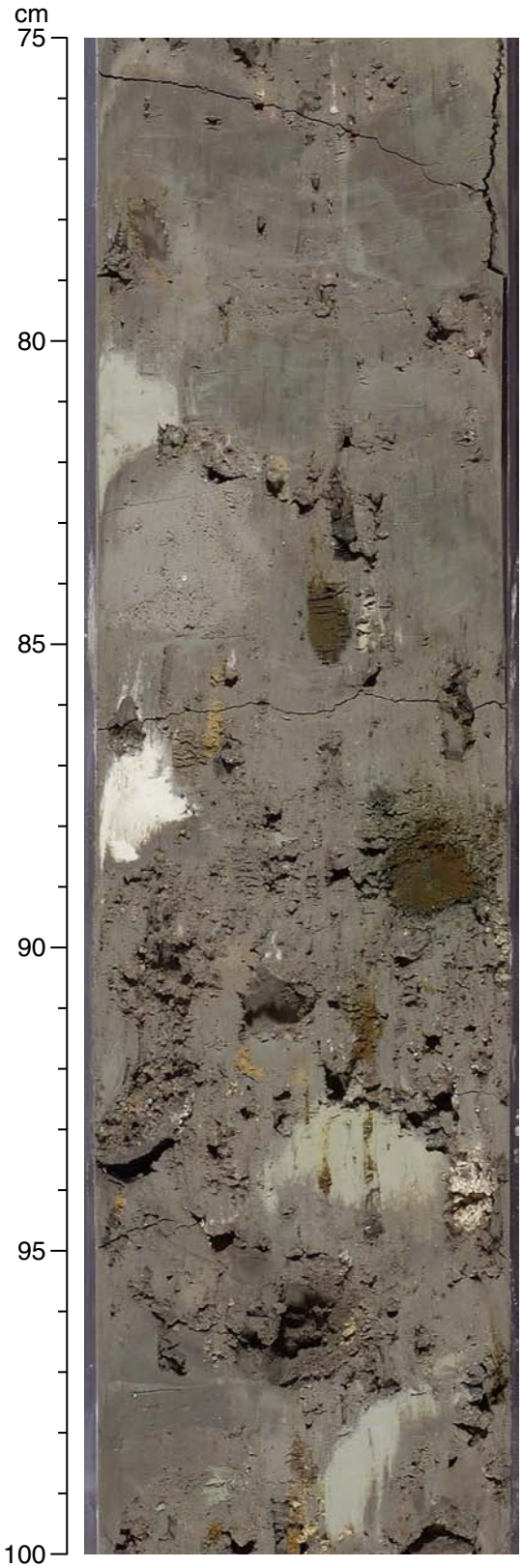

Figure F12. Oxidized layer at the uppermost part of Subunit IA (interval 303-U1302E-1H-1, 0–20 cm).

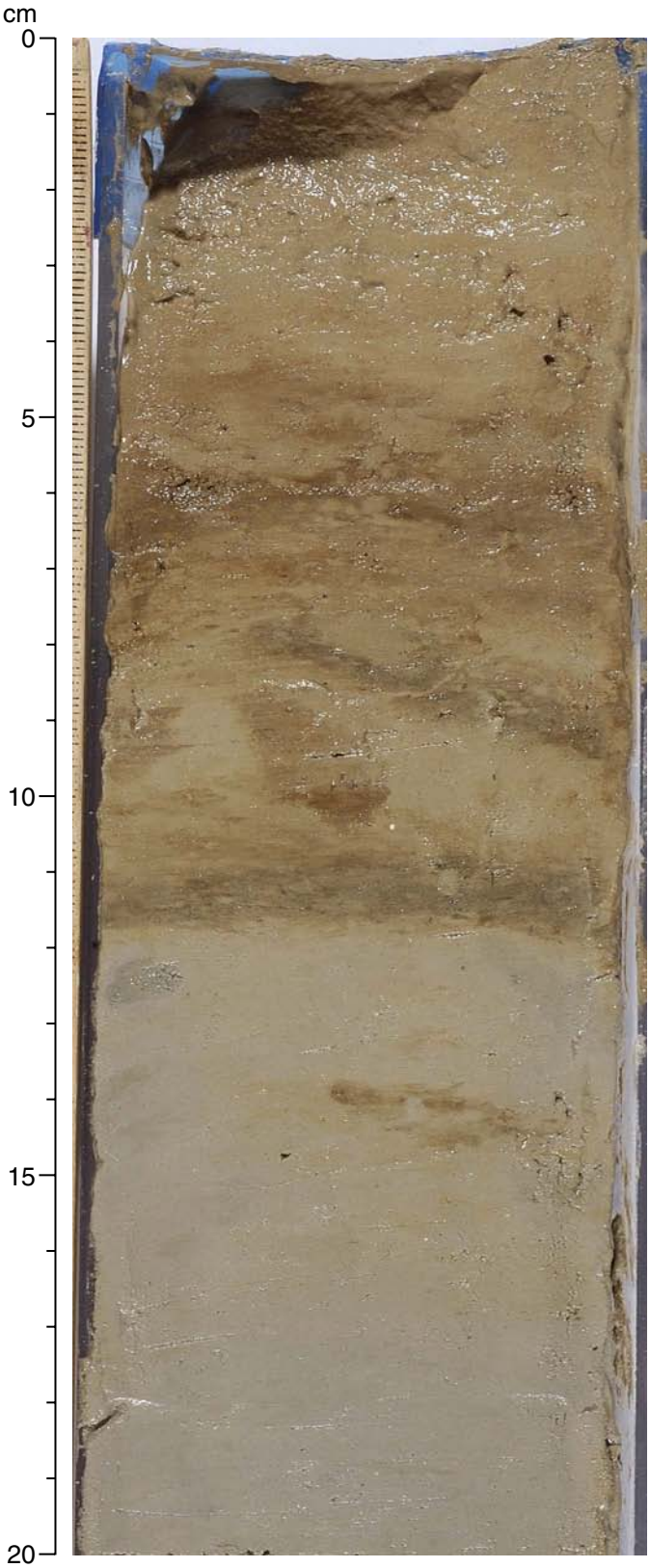

Figure F13. Millimeter-scale laminae in Subunit IA (interval 303-U1302C-5H-1, 100–130 cm).

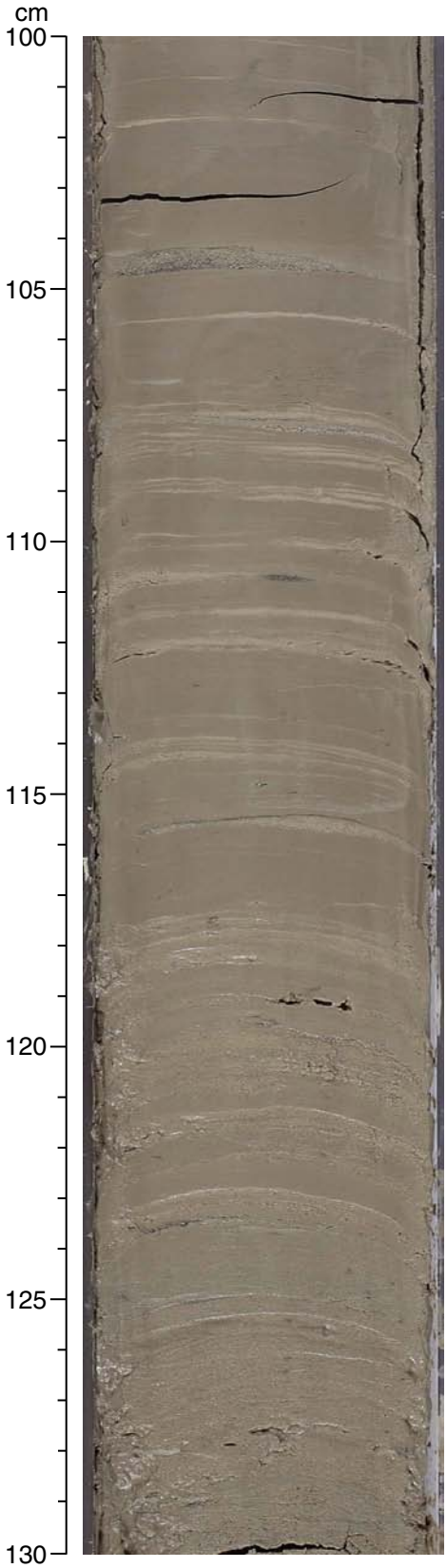

Figure F14. Part of the intraclast conglomerate with a sandy matrix in lithologic Subunit IA (interval 303-U1303A-7H-3, 115–142 cm).

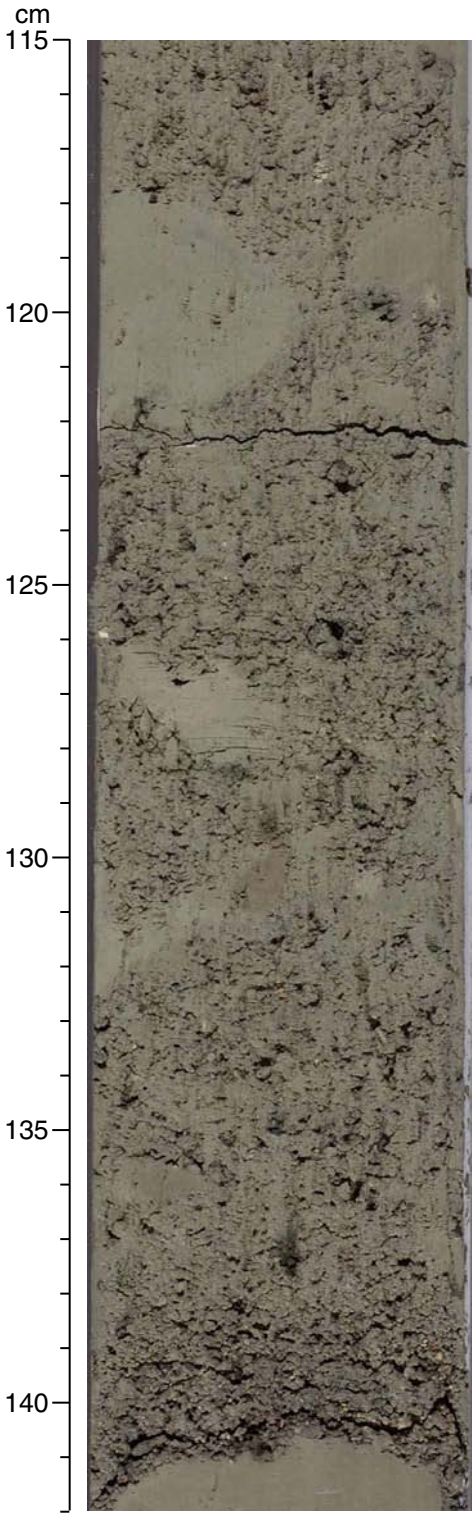

Figure F15. Site U1302 relative downcore abundance of coccoliths, planktonic foraminifers, diatoms, radiolarians, and palynomorphs. Abundance scale refers to Tables T2–T26. × = reworked pollen.

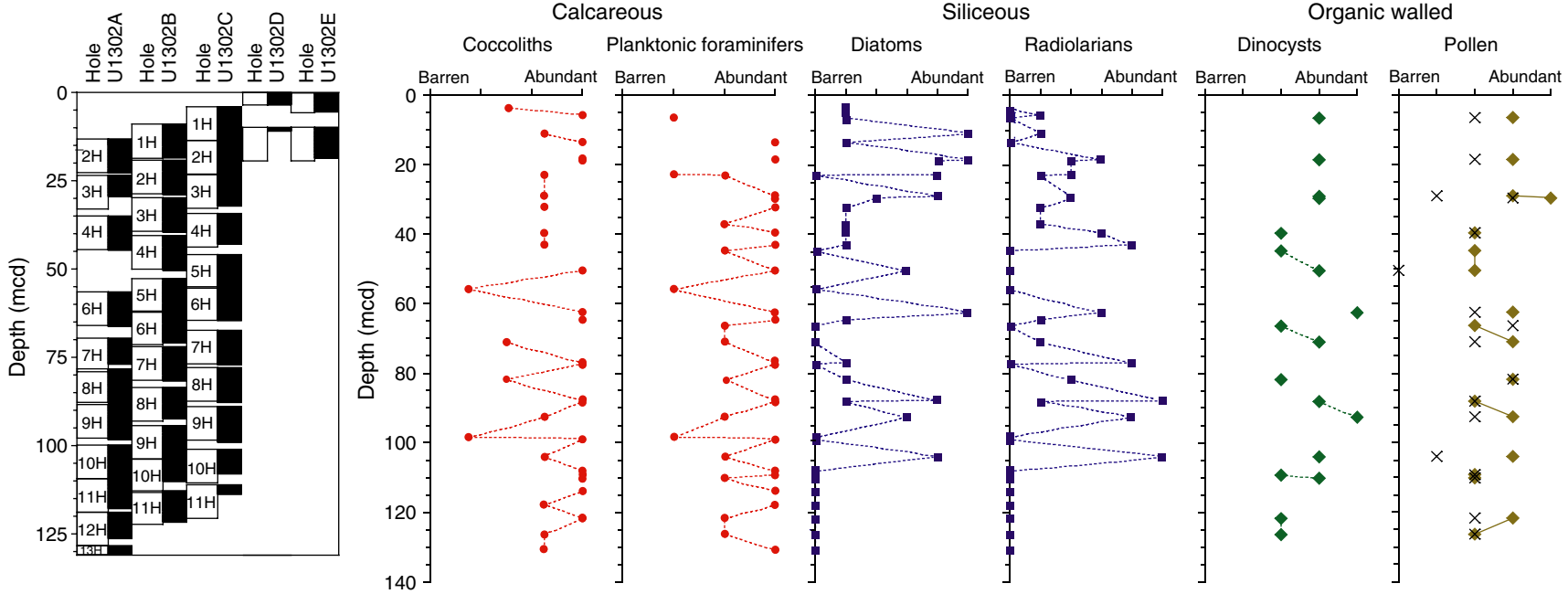

Figure F16. Site U1303 downcore relative abundance of calcareous nannofossils, planktonic foraminifers, diatoms, radiolarians, and palynomorphs. Abundance scale refers to Tables T2–T26. × = reworked pollen.

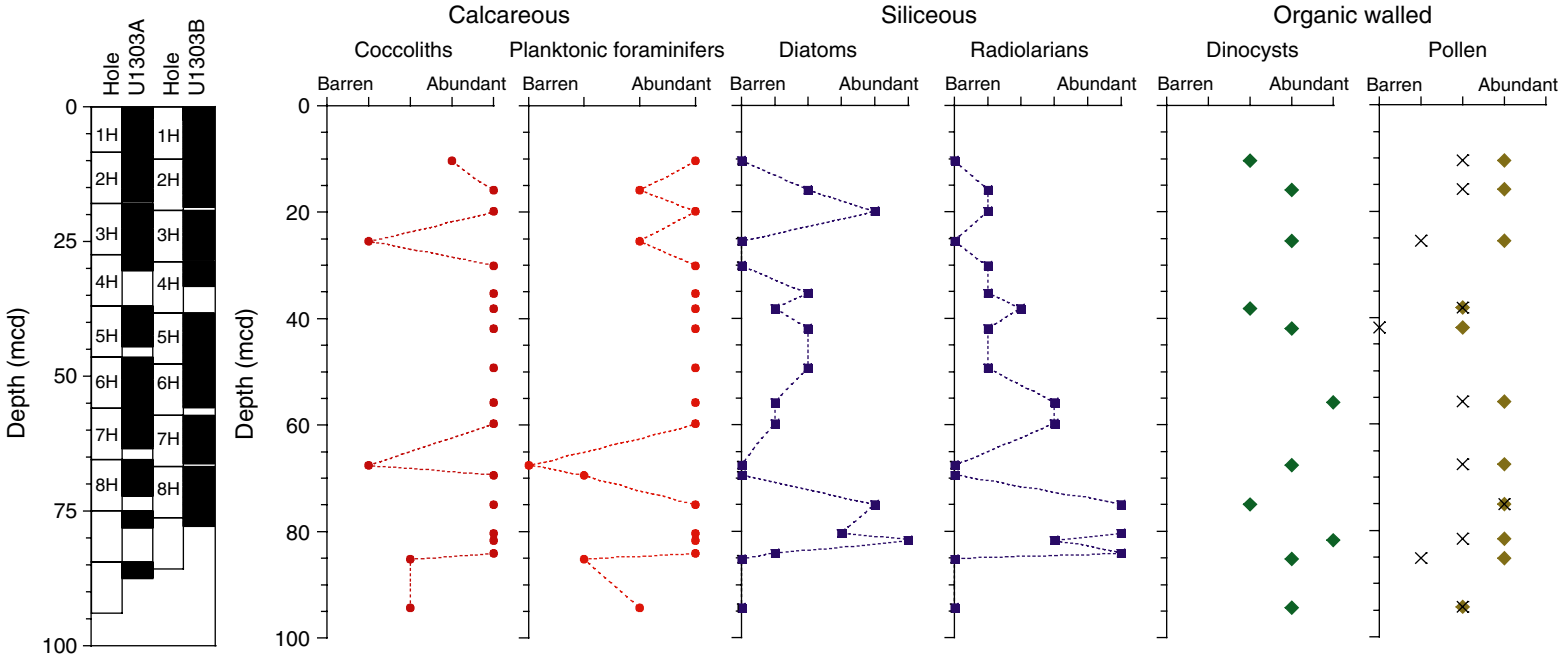

Figure F17. Chronostratigraphic correlation of Holes U1302A, U1302B, and U1302C based on calcareous nannofossils and diatoms. Relationship to magnetostratigraphy is shown in the left panel. MIS = marine isotope stage, LO = last occurrence, FO = first occurrence.

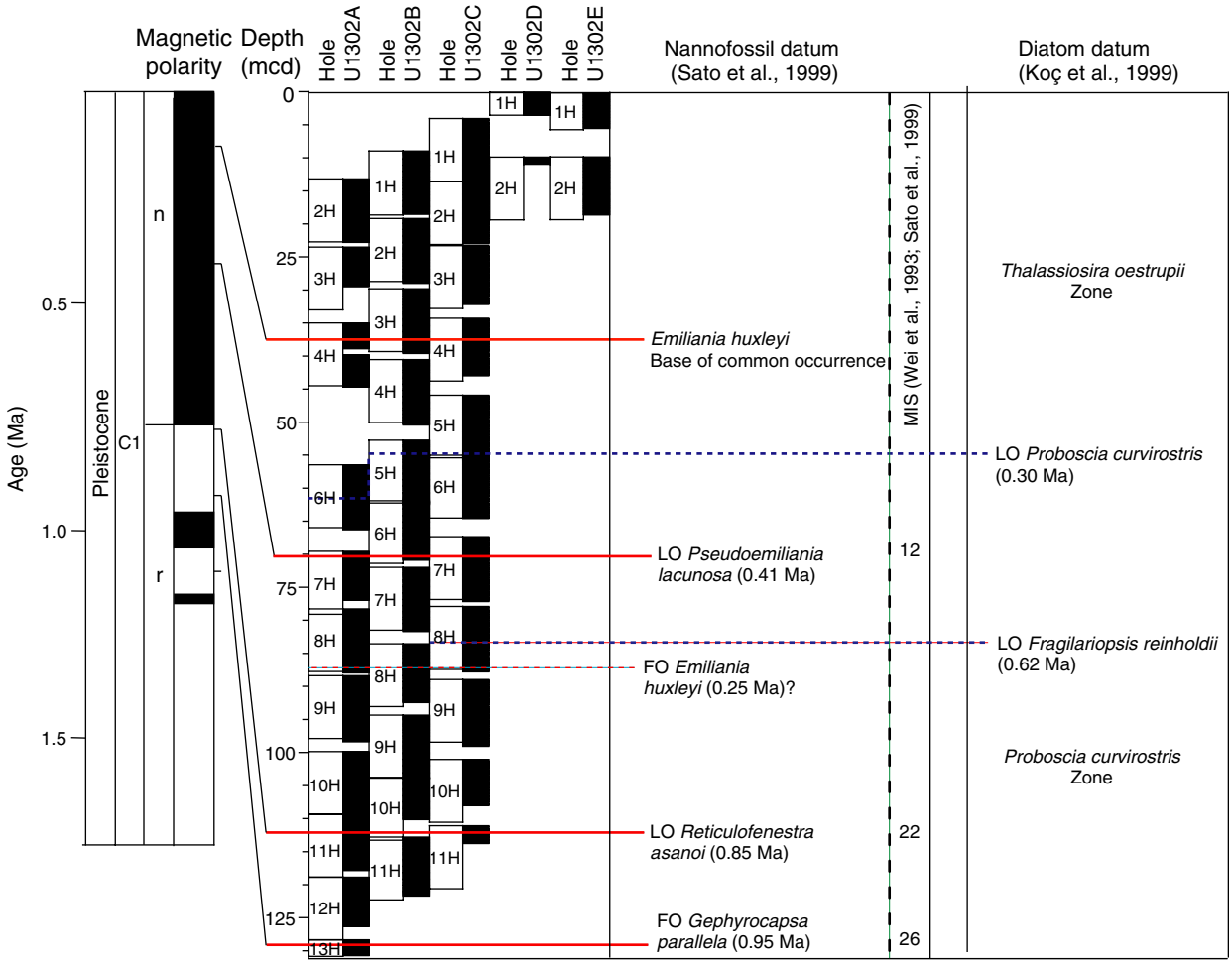

Figure F18. Chronostratigraphic correlation of Holes U1303A and U1303B based on calcareous nannofossils, diatoms, and palynomorphs. Relationship to magnetostratigraphy is shown in the left panel. MIS = marine isotope stage, LO = last occurrence, FO = first occurrence.

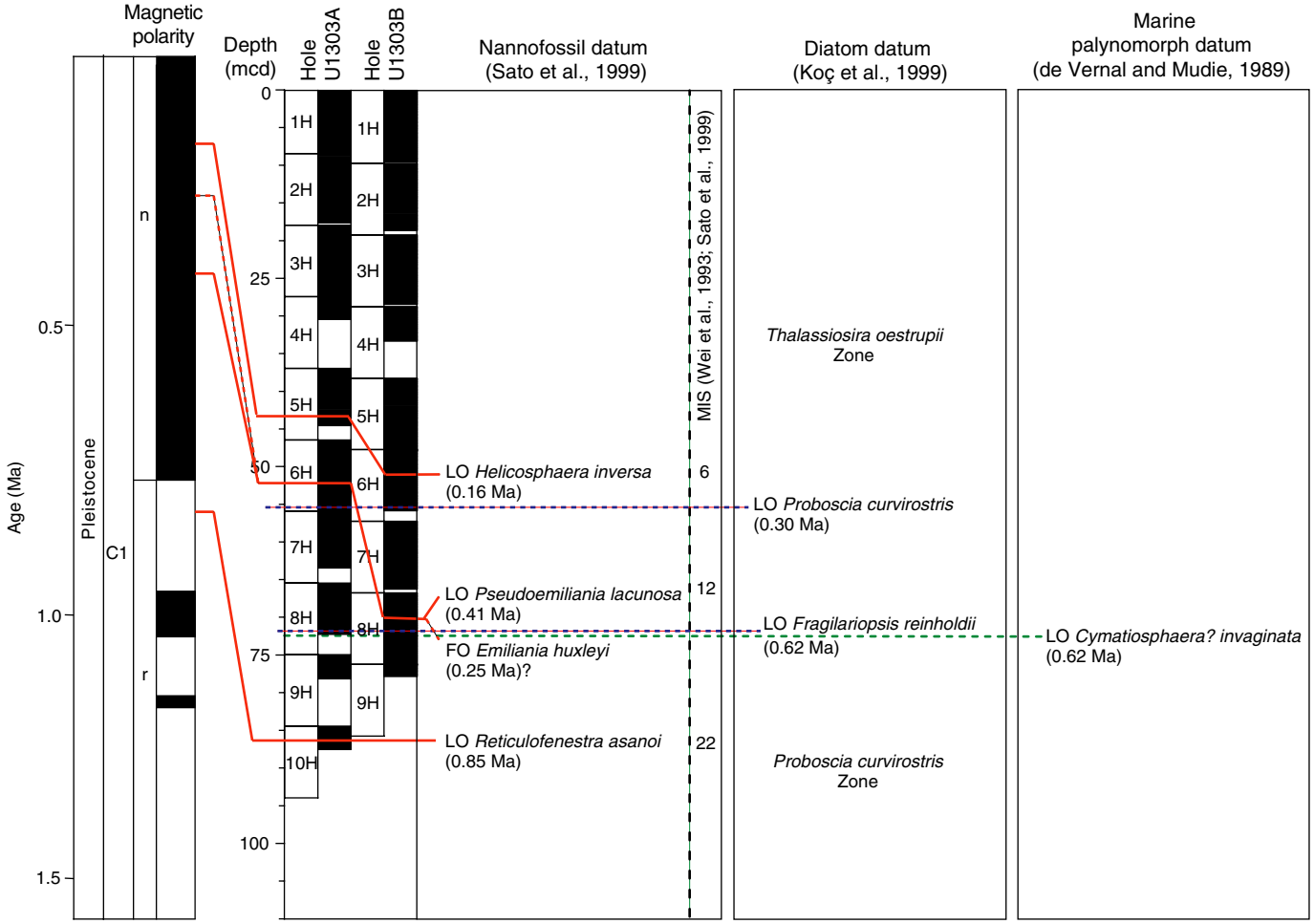

Figure F19. Site U1302 downcore relative abundance of the polar planktonic foraminifer *Neogloboquadrina pachyderma* (sinistral) and concentration of dinocysts. The dominant occurrence of *Uvigerina peregrina* (*U.p.*) suggests northward penetration of Antarctic Bottom Water and reduced North Atlantic Deep Water formation (cf. Bilodeau et al., 1994). In the dinocyst assemblages, the dominance of *Nematosphaeropsis labyrinthea* (Sample 303-U1302B-5H-CC) and the common occurrence of *Spiniferites mirabilis* (Sample 303-U1302B-9H-CC) permits identification of interglacial intervals.

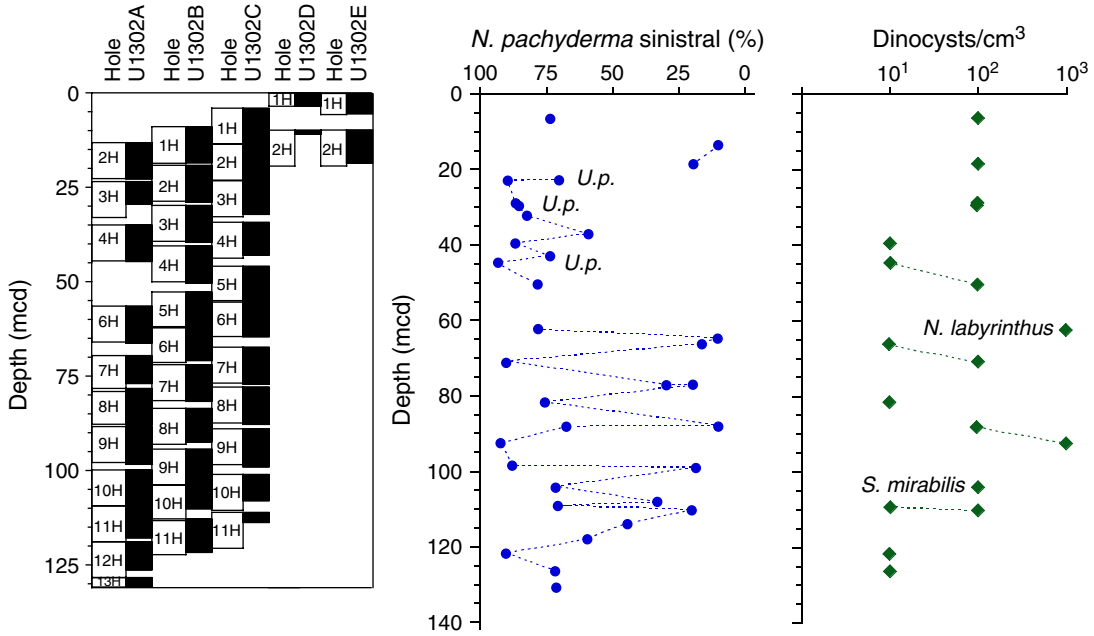

Figure F20. Site U1303 downcore relative abundance of the polar planktonic foraminifer *Neogloboquadrina pachyderma* (sinistral). The dominant occurrence of *Uvigerina peregrina* (*U.p.*) suggests northward penetration of Antarctic Bottom Water and reduced NADW (cf. Bilodeau et al., 1994).

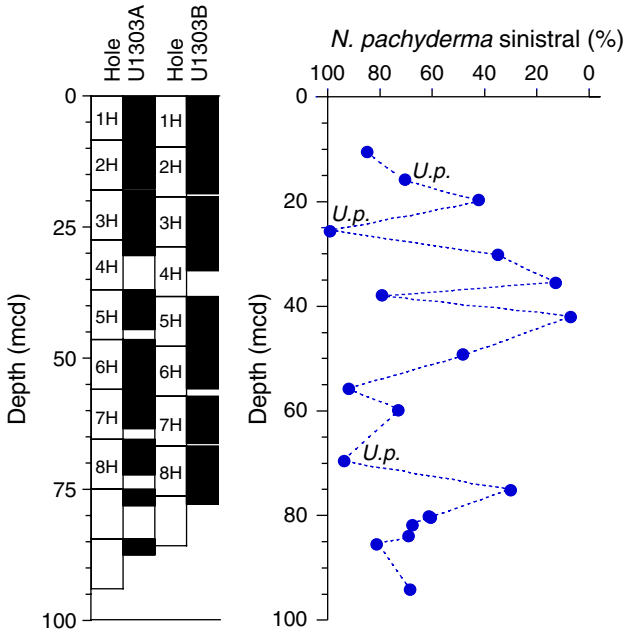

Figure F21. Site U1302 and U1303 NRM intensity (Int.) after 20 mT peak AF demagnetization versus depth (mcd refers to shipboard mcd; see "Composite section"). Core recovery is shown in the left panel. **A.** Site U1302. (Continued on next page.)

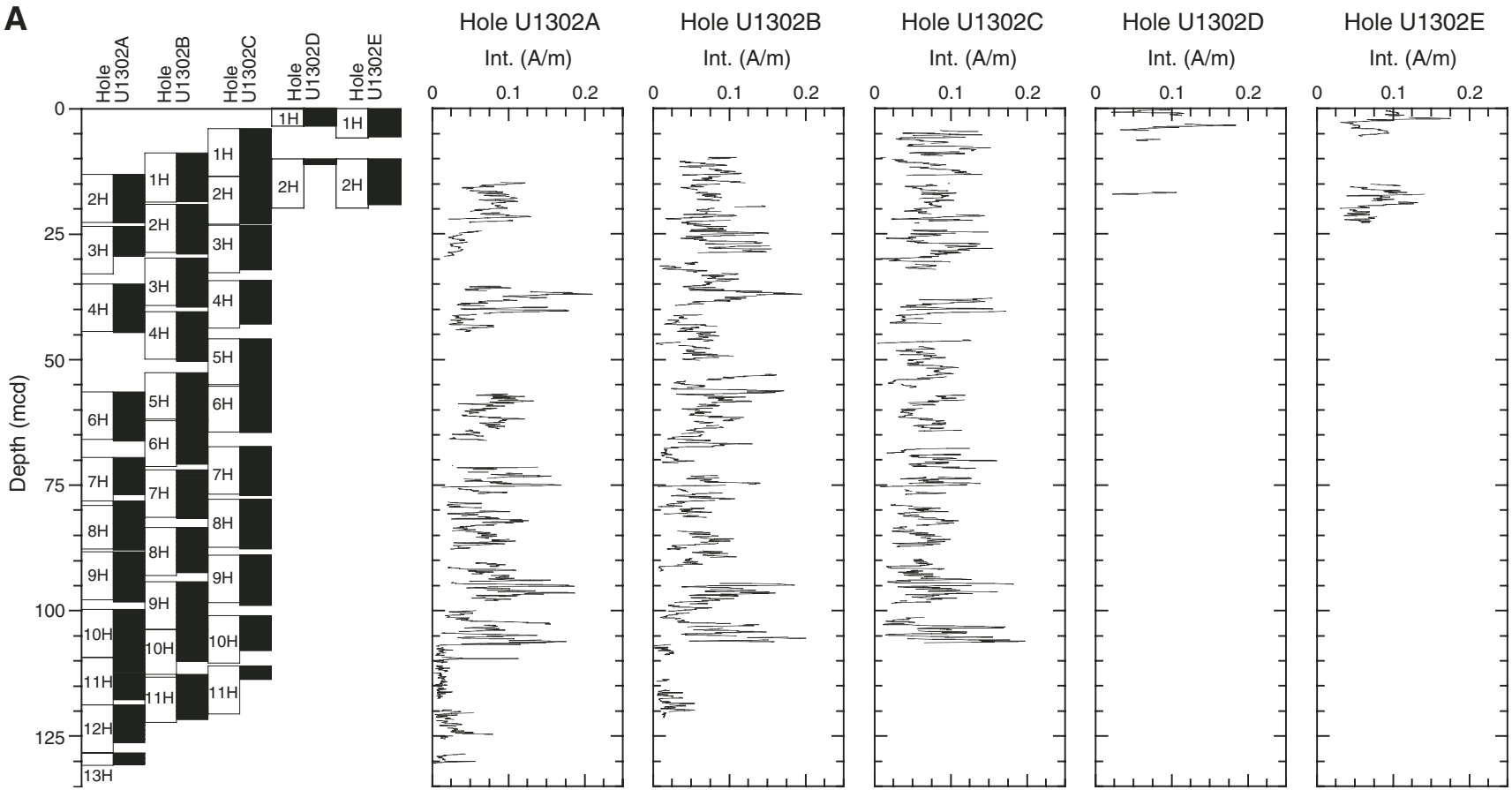

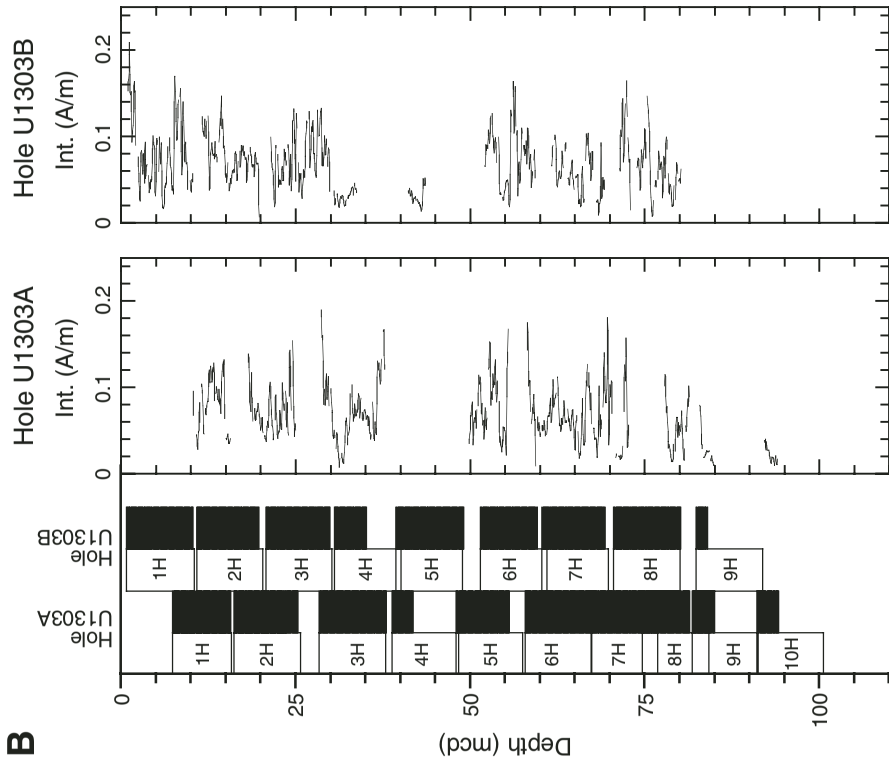

Figure F21 (continued). B. Site U1303.

Figure F22. Site U1302 and U1303 inclination after 20 mT peak AF demagnetization versus depth (mcd refers to shipboard mcd; see **"Composite section"**). Core recovery is shown in the left panel. **A.** Site U1302. (Continued on next page.)

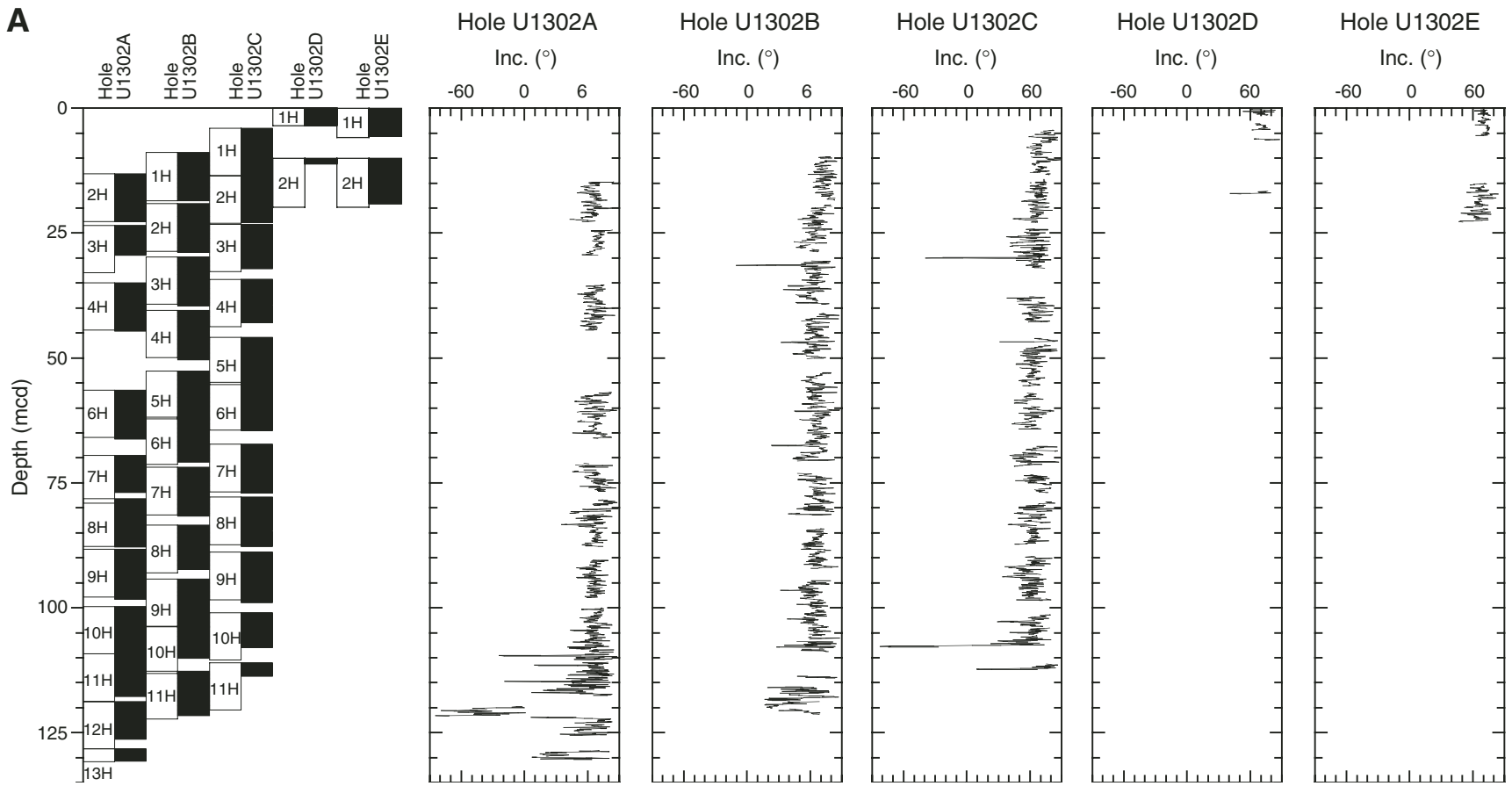

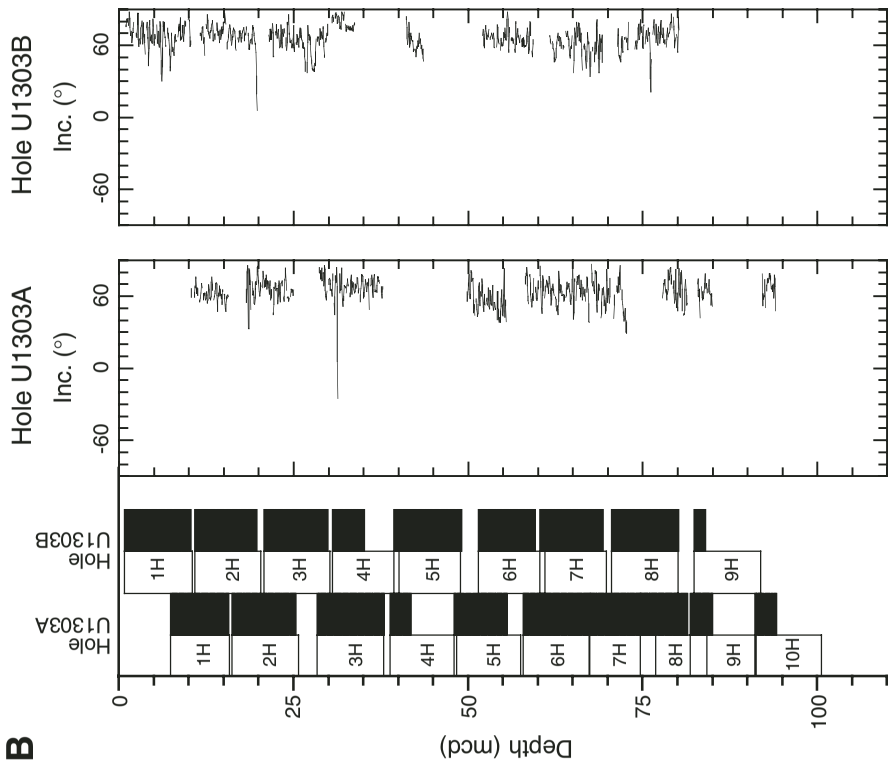

Figure F22 (continued). B. Site U1303.

Figure F23. Site U1302 and U1303 declination after 20 mT peak AF demagnetization versus depth (mcd refers to shipboard mcd; see **"Composite section"**). No Tensor tool correction was applied. Core recovery is shown in the left panel. **A.** Site U1302. (Continued on next page.)

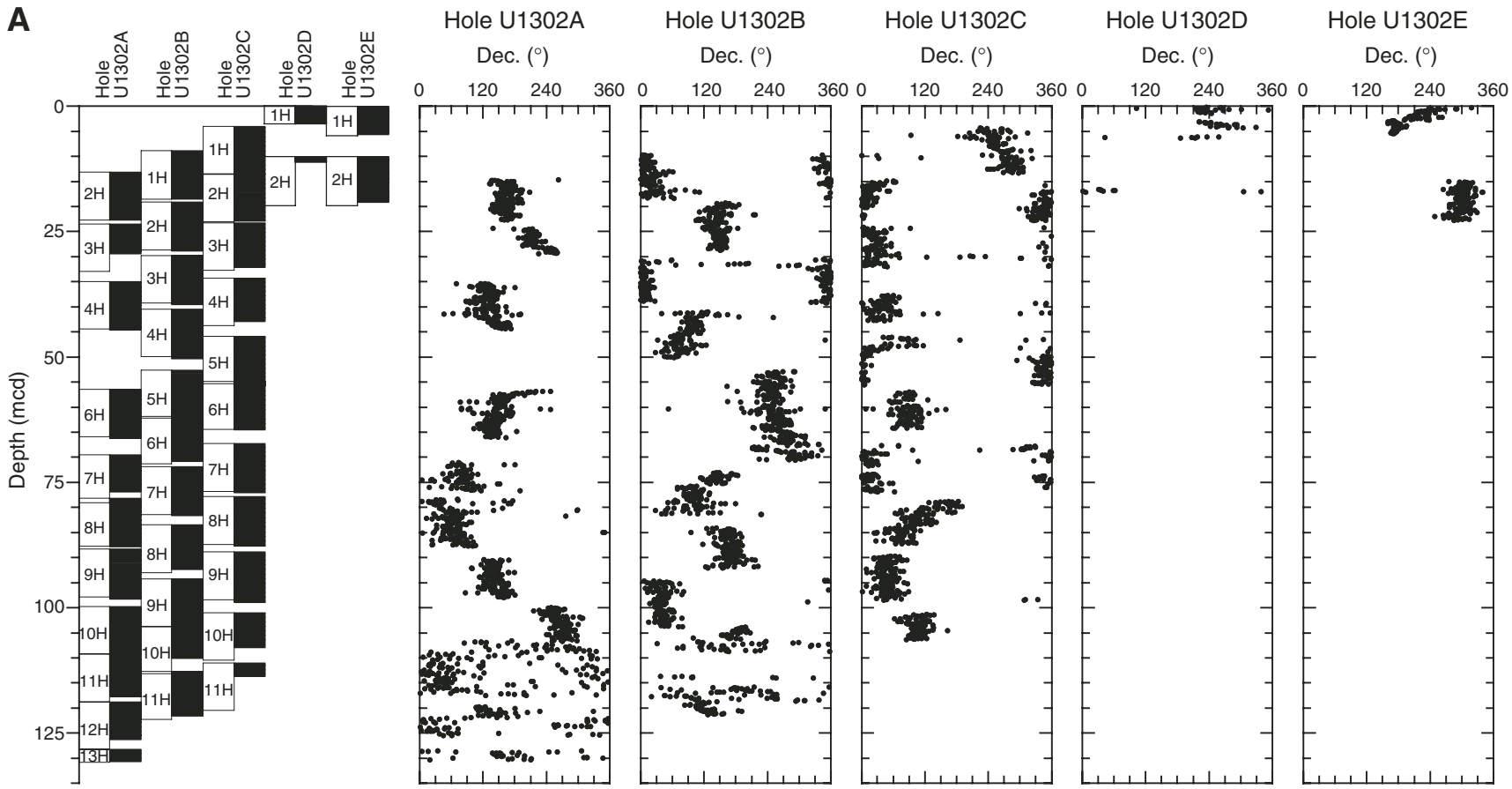

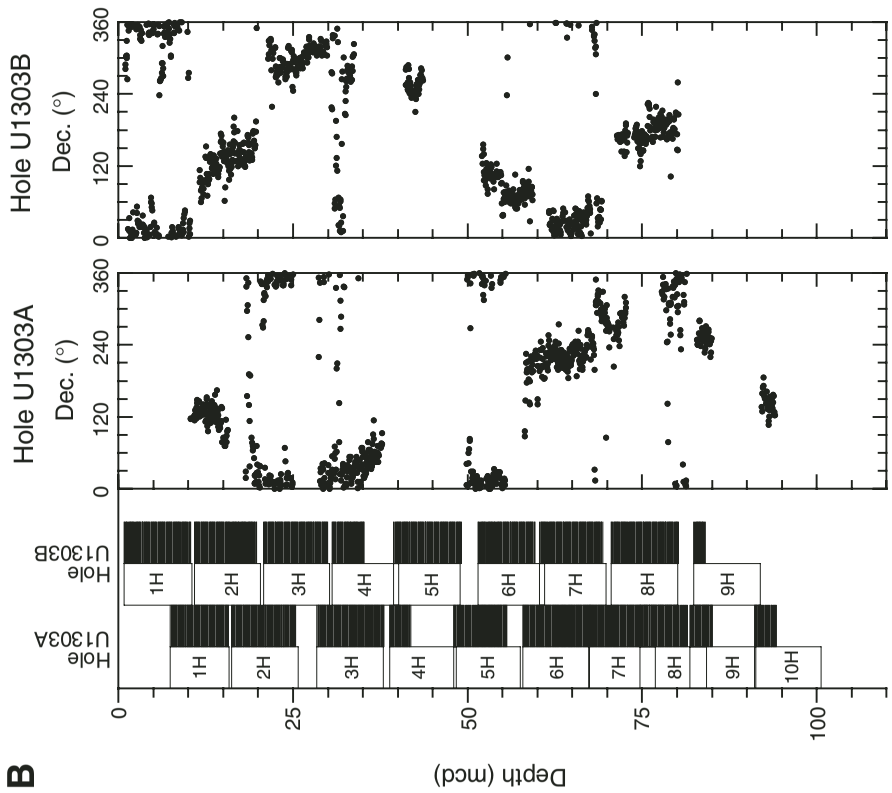

Figure F23 (continued). B. Site U1303.

Figure F24. Gamma ray attenuation (GRA) density, Sites U1302 and U1303. Upper panel shows composite GRA density record indicating which hole was used to form the splice. Letters refer to holes at Site U1302 unless otherwise indicated. Numbers shown below curves indicate core number. **A.** 0–20 mcd. (Continued on next five pages.)

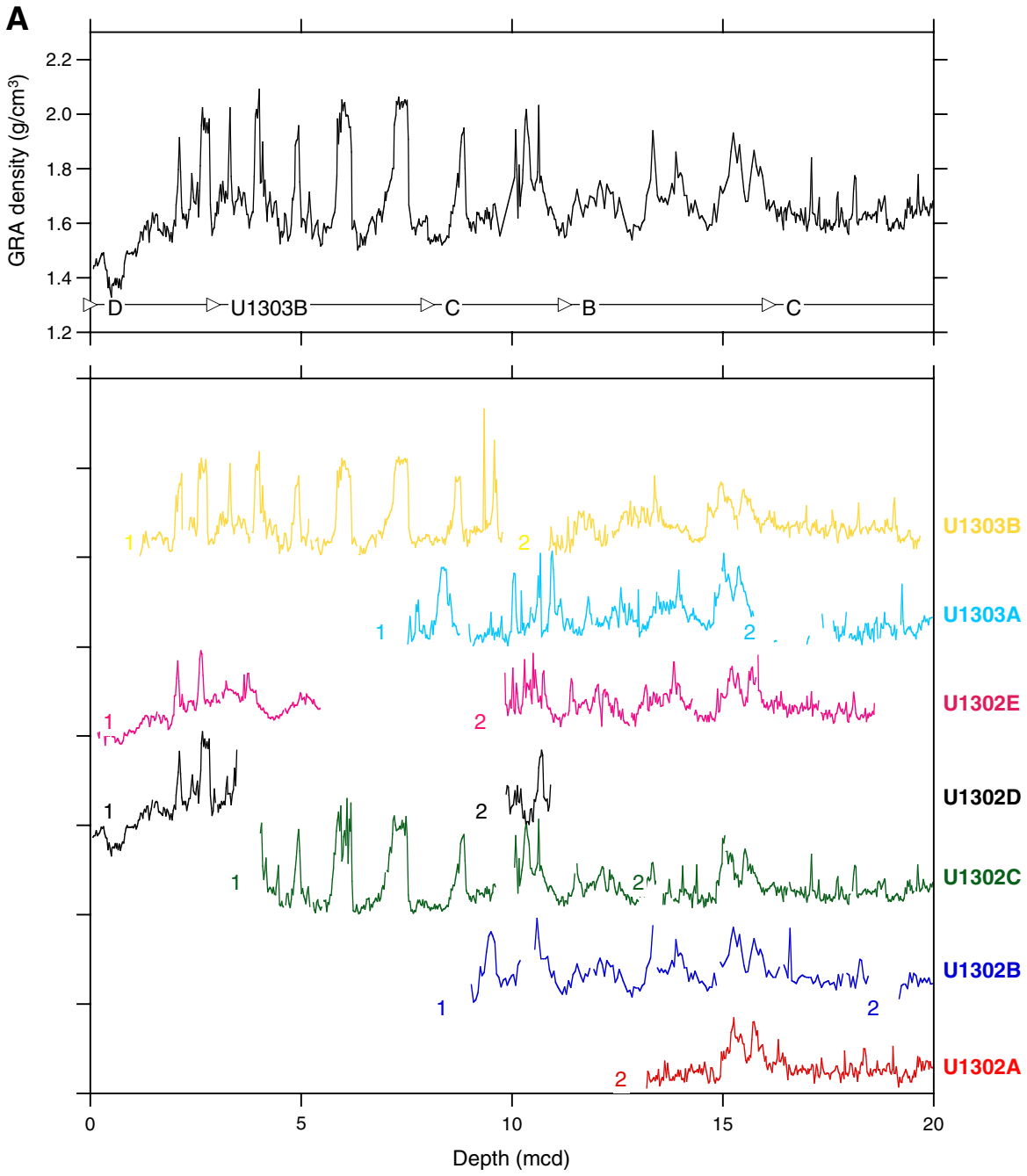

Figure F24 (continued). B. 20–40 mcd.

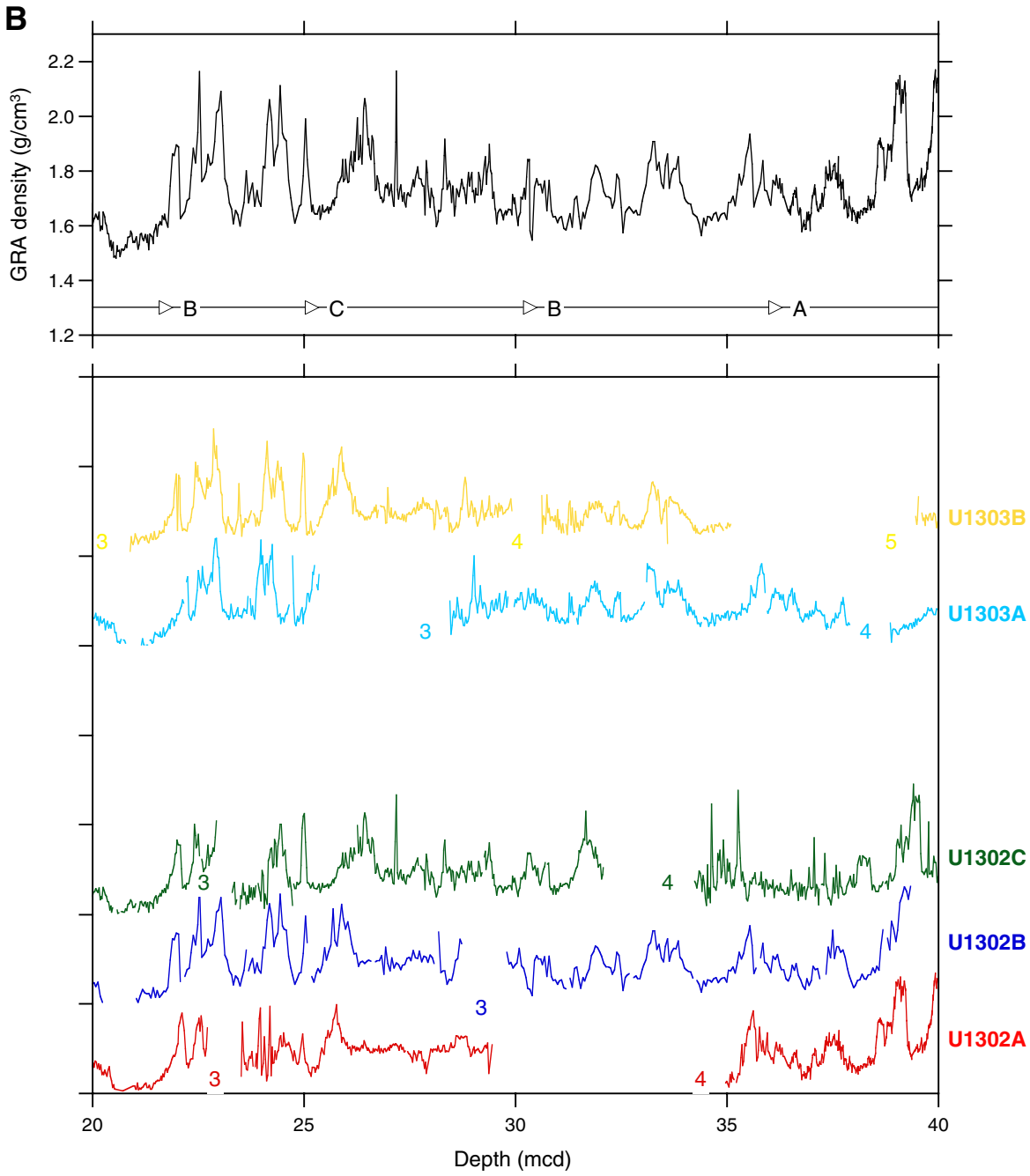

Figure F24 (continued). C. 40–60 mcd.

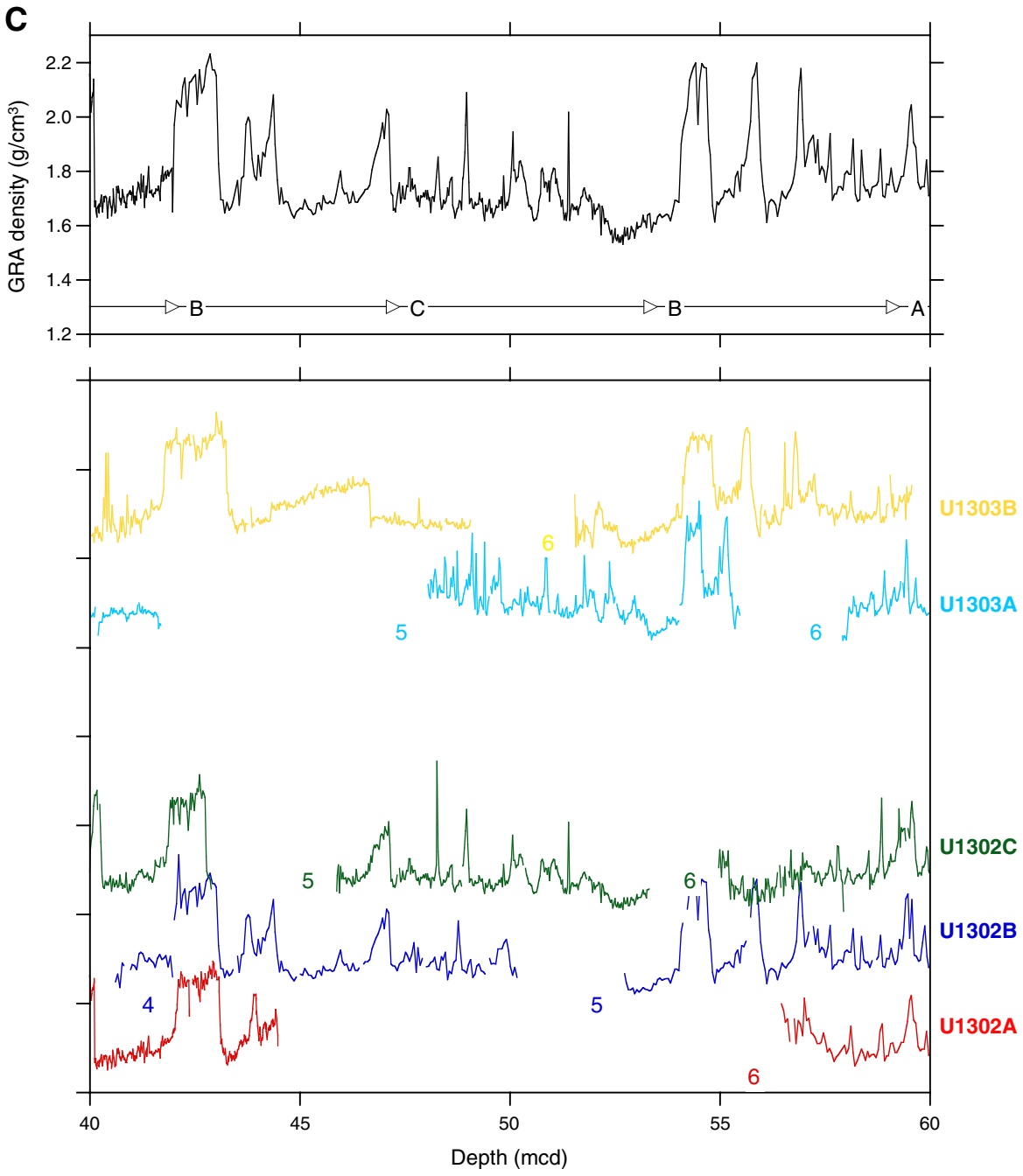

Figure F24 (continued). D. 60–80 mcd.

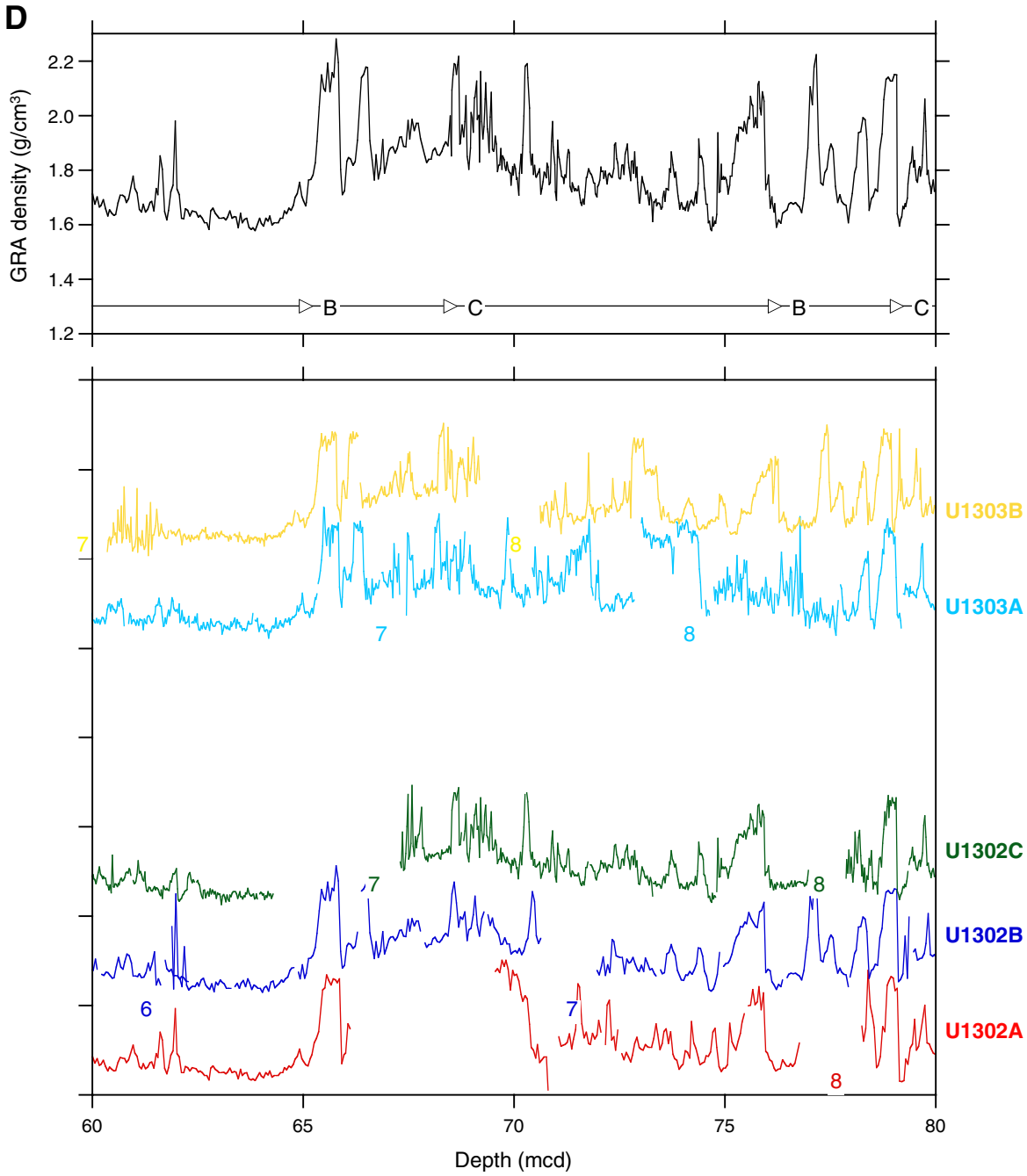

Figure F24 (continued). E. 80–100 mcd.

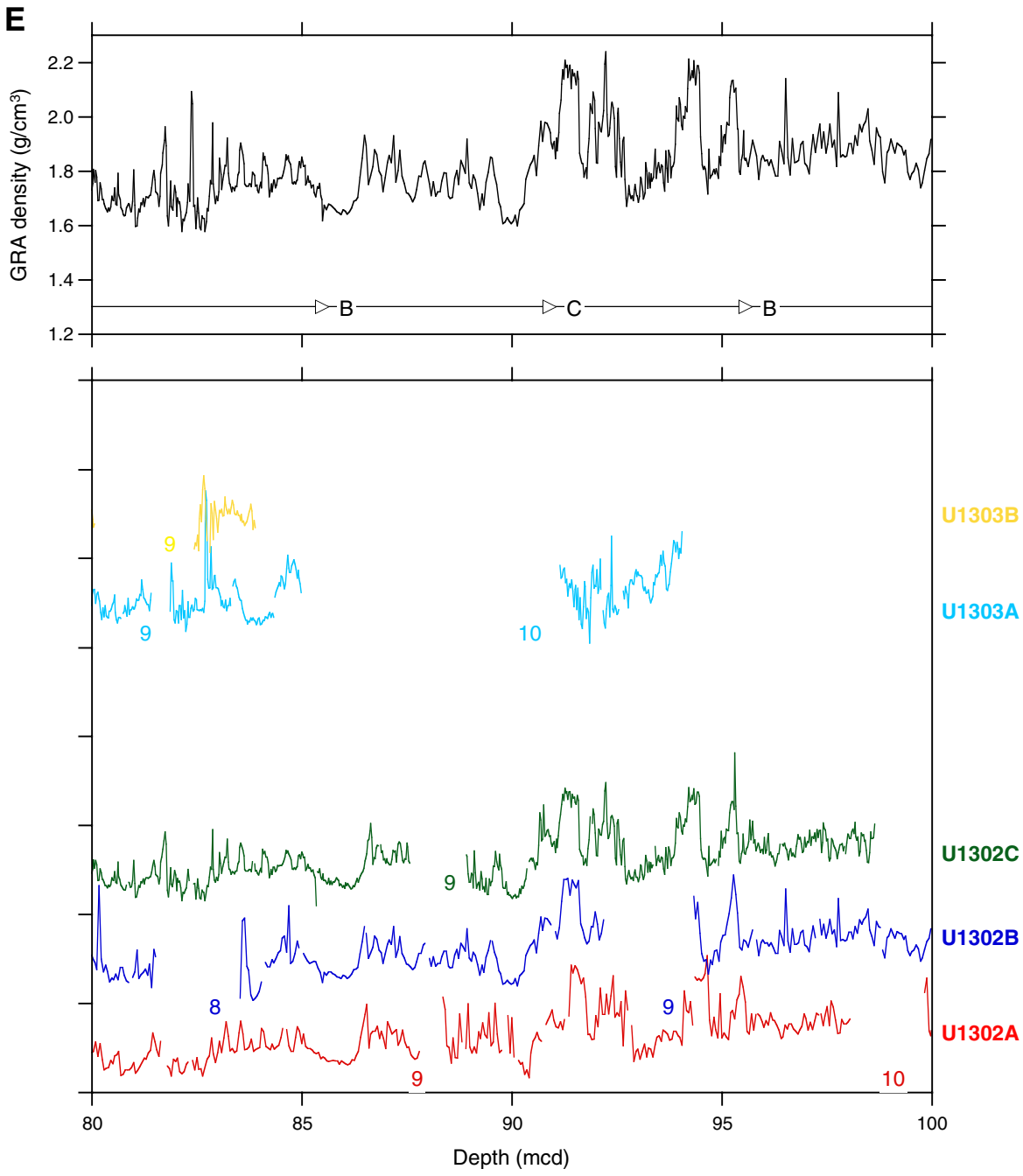

Figure F24 (continued). F. 100–120 mcd.

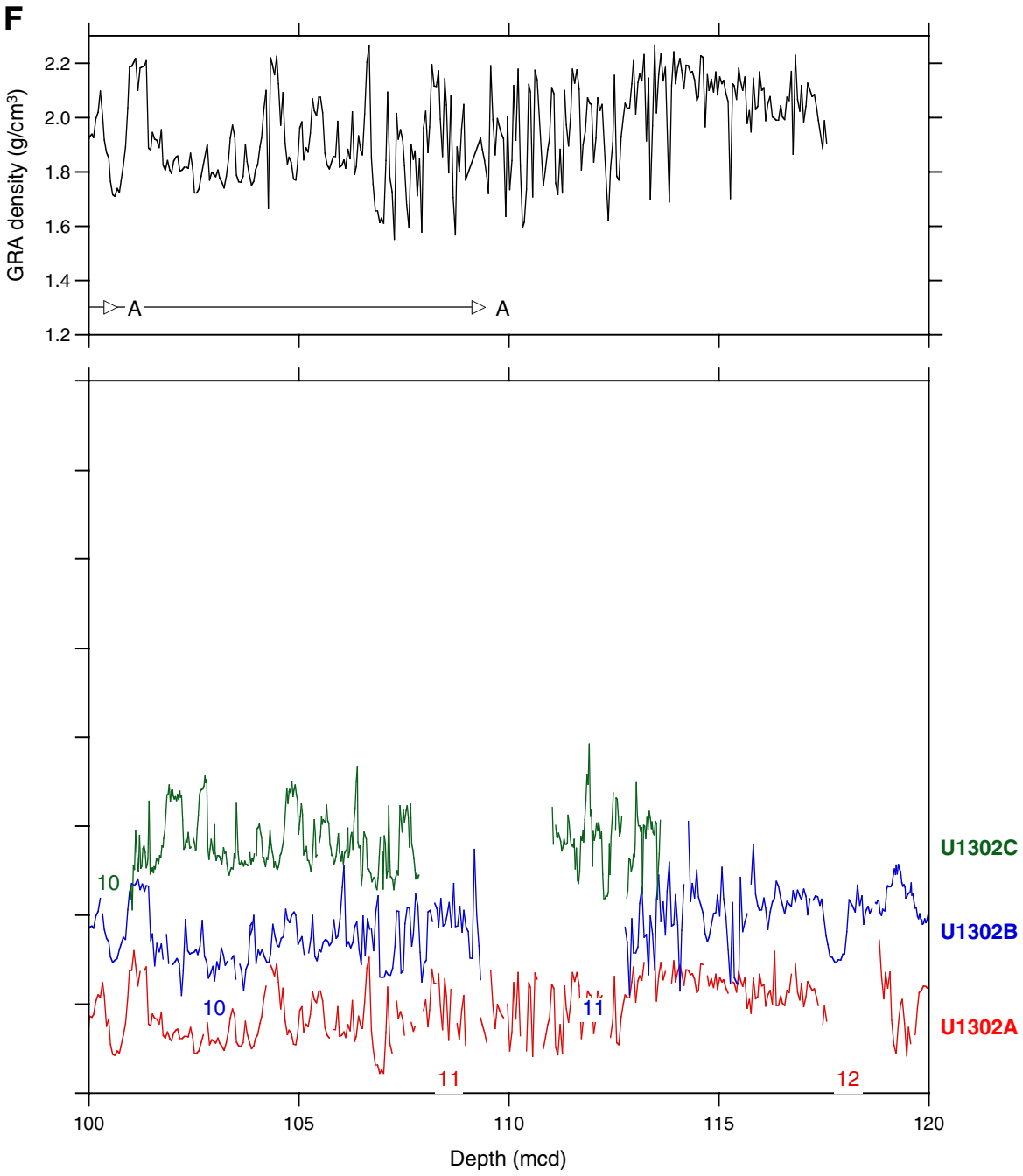

Figure F25. Magnetic susceptibility (MS), Sites U1302 and U1303. Upper panel shows composite MS record indicating which hole was used to form the splice. Letters refer to holes at Site U1302 unless otherwise indicated. Numbers shown below curves indicate core number. **A.** 0–20 mcd. (Continued on next five pages.)

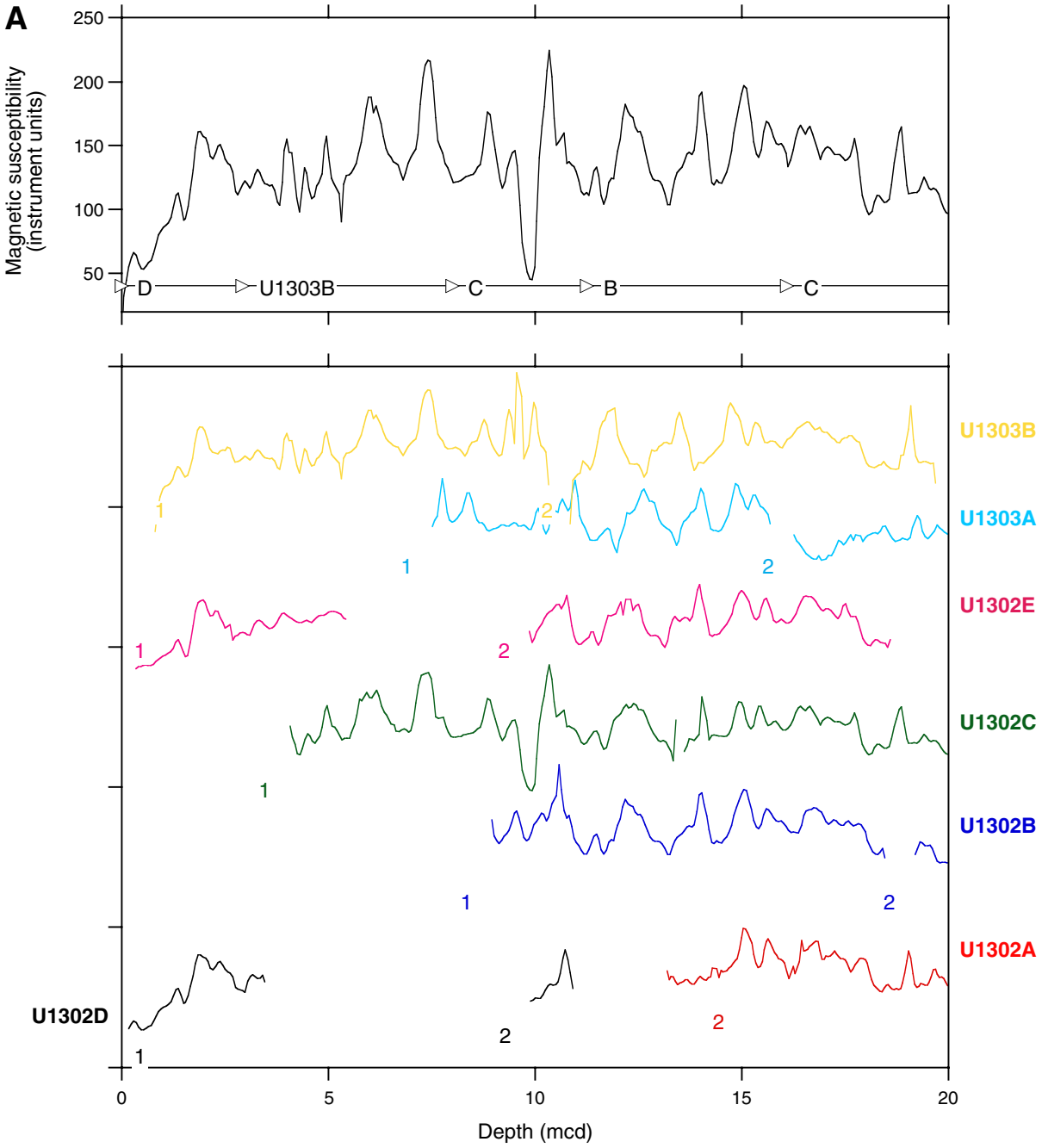

Figure F25 (continued). B. 20–40 mcd.

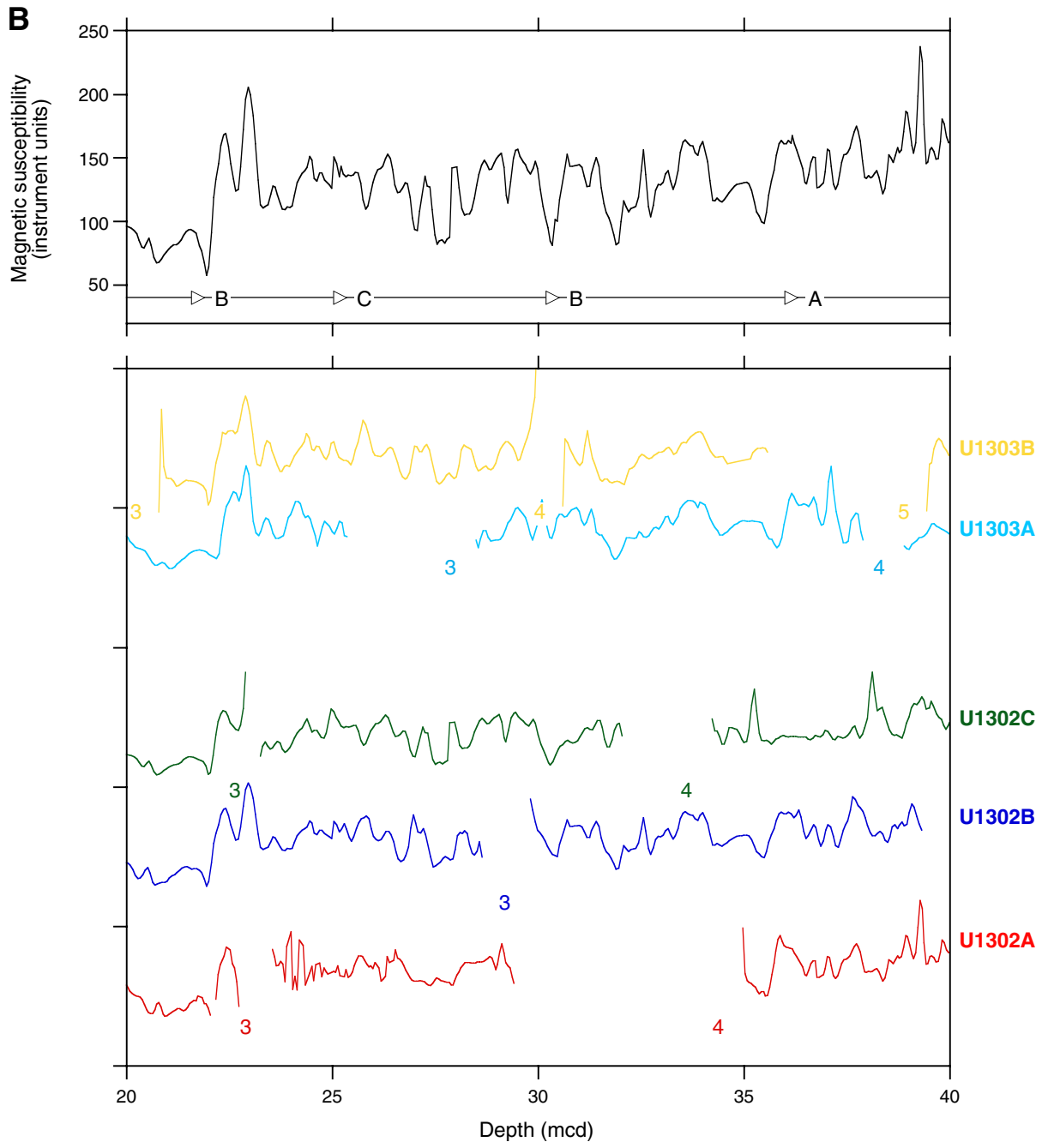

Figure F25 (continued). C. 40–60 mcd.

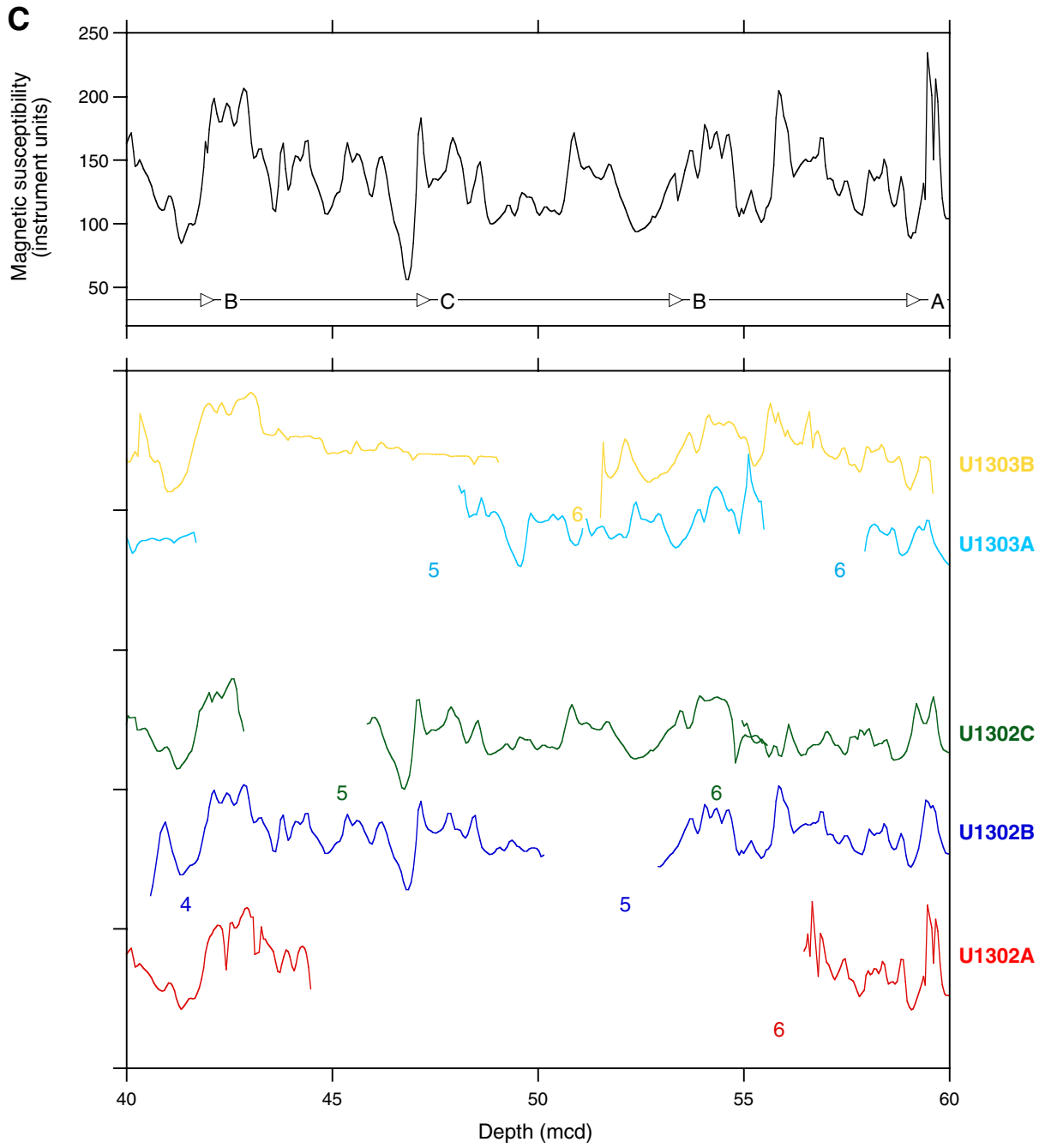

Figure F25 (continued). D. 60–80 mcd.

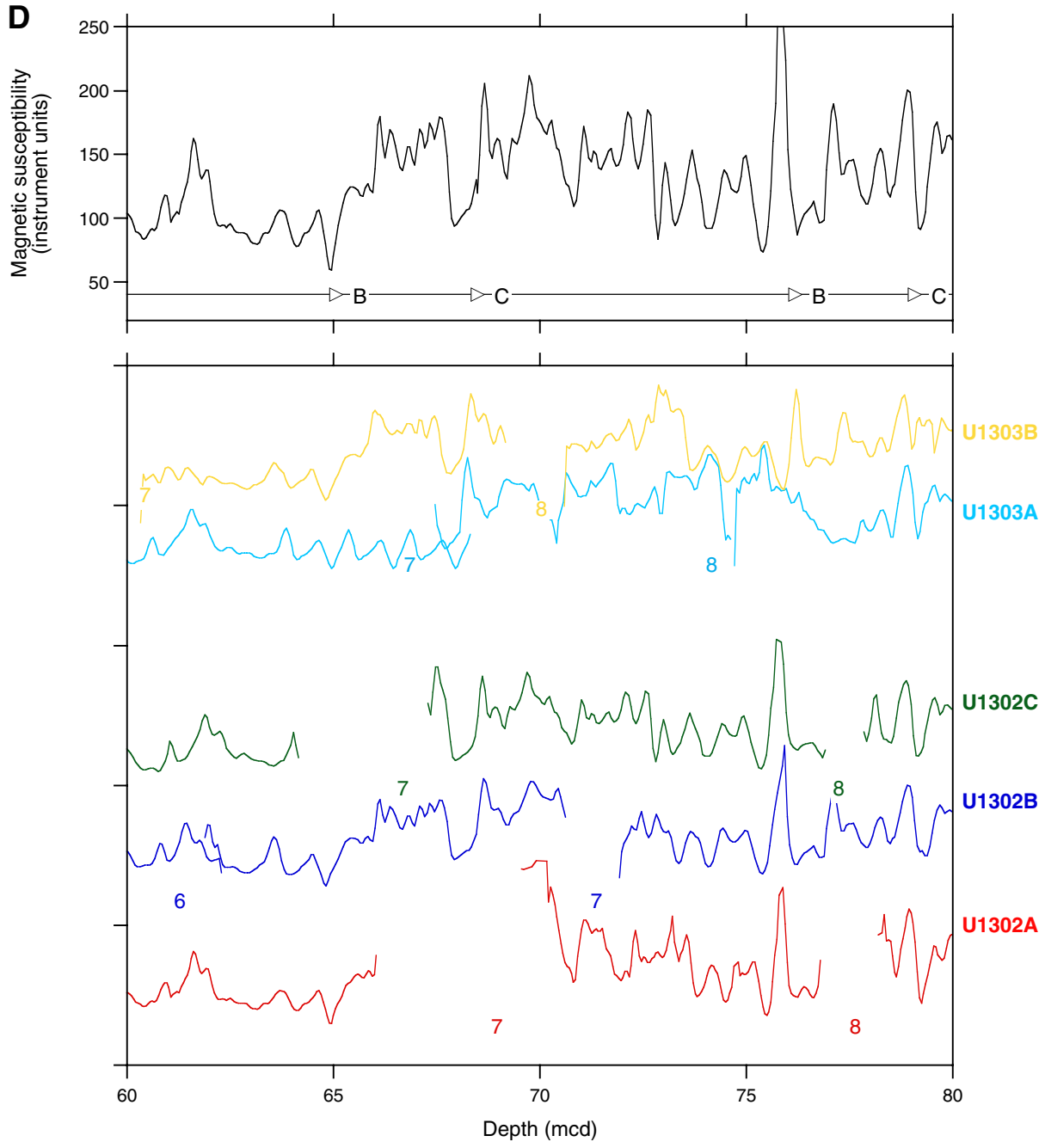

Figure F25 (continued). E. 80–100 mcd.

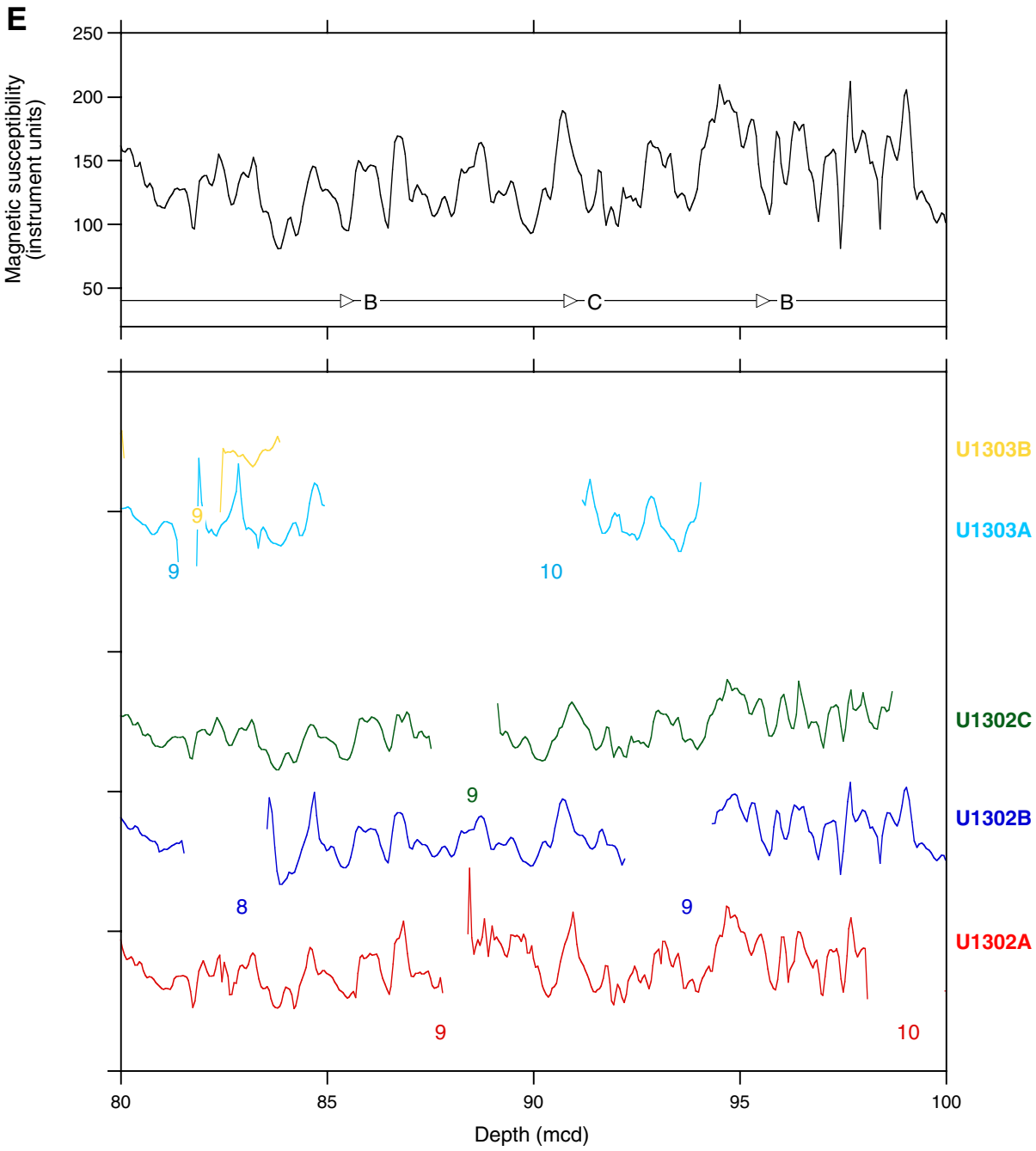

Figure F25 (continued). F. 100–120 mcd.

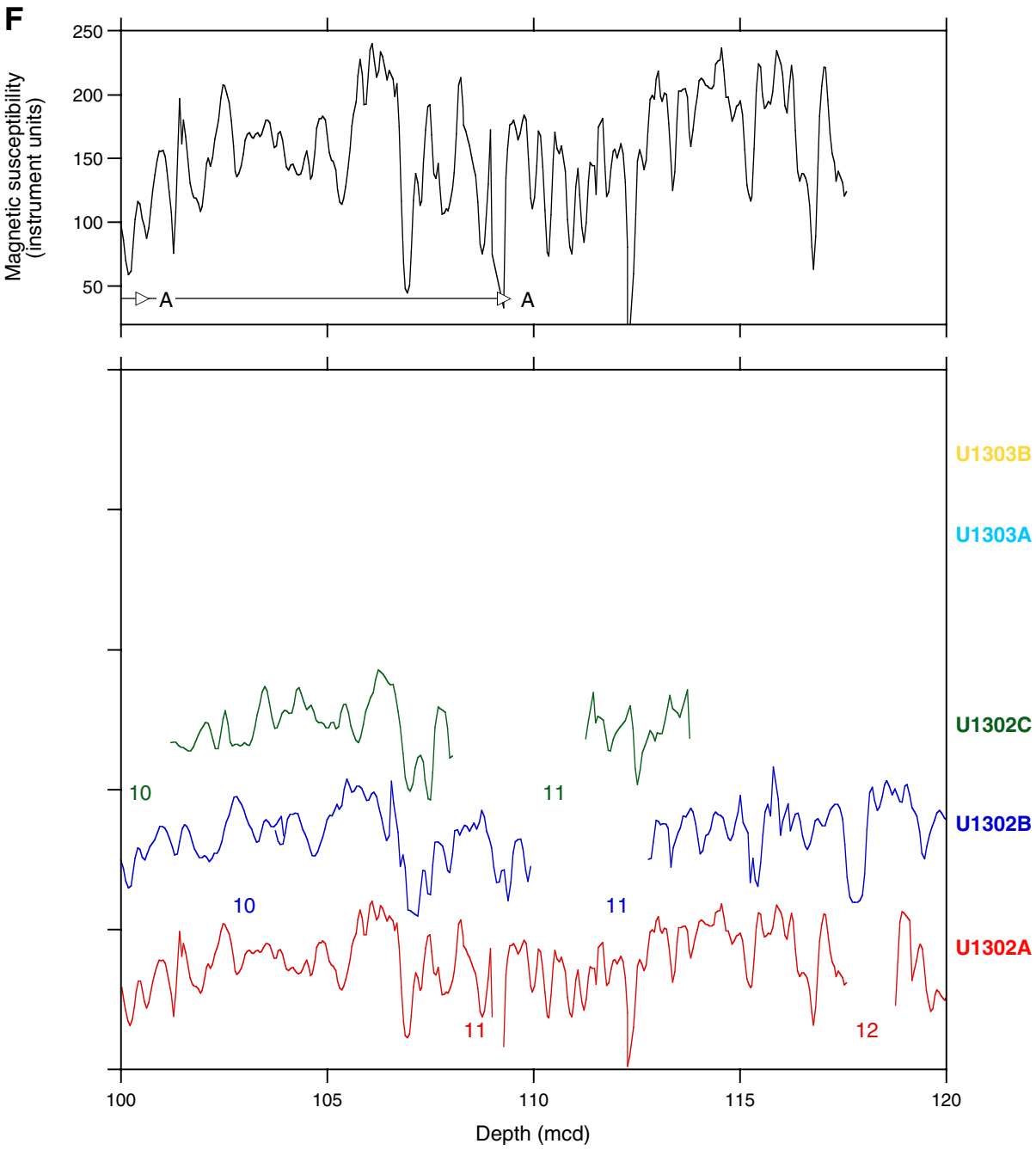

Figure F26. Correlation of gamma ray attenuation (GRA) density records between Sites U1302 and U1303 and Core MD99-2237 (Turon et al., 1999). Density maxima correspond to Heinrich events (H0–H6), low detrital carbonate (LDC) events, and detrital carbonate (DC) events following the nomenclature of Stoner et al. (1996). Density data from Core MD 99-2237 after Turon et al. (1999).

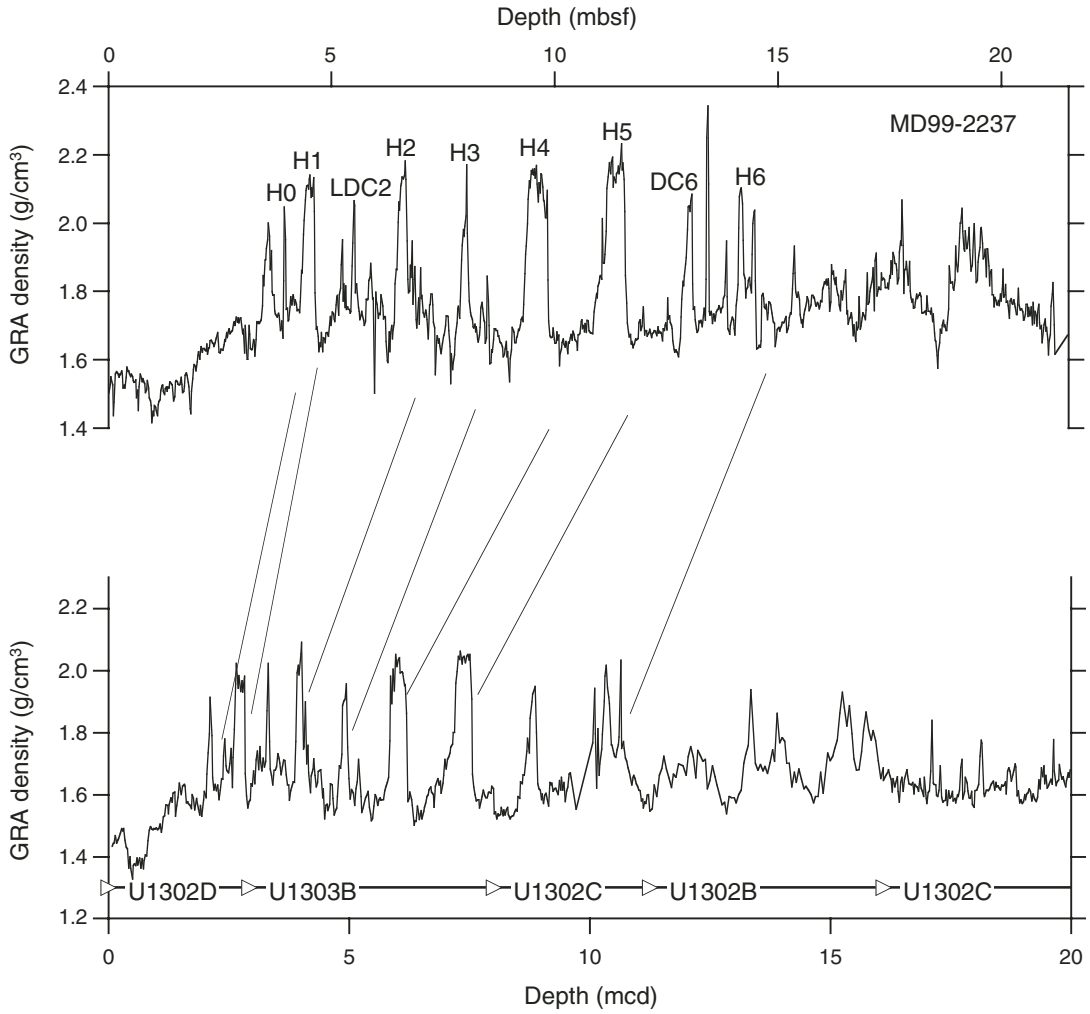

Figure F27. Meters composite depth (mcd) versus meters below seafloor (mbsf) for tops of cores at Sites U1302 and U1303. The growth factor (GF) is the slope of the regression line for Sites U1302 and U1303 and for both sites combined. On average, the mcd of the spliced section is 13% greater than meters below seafloor.

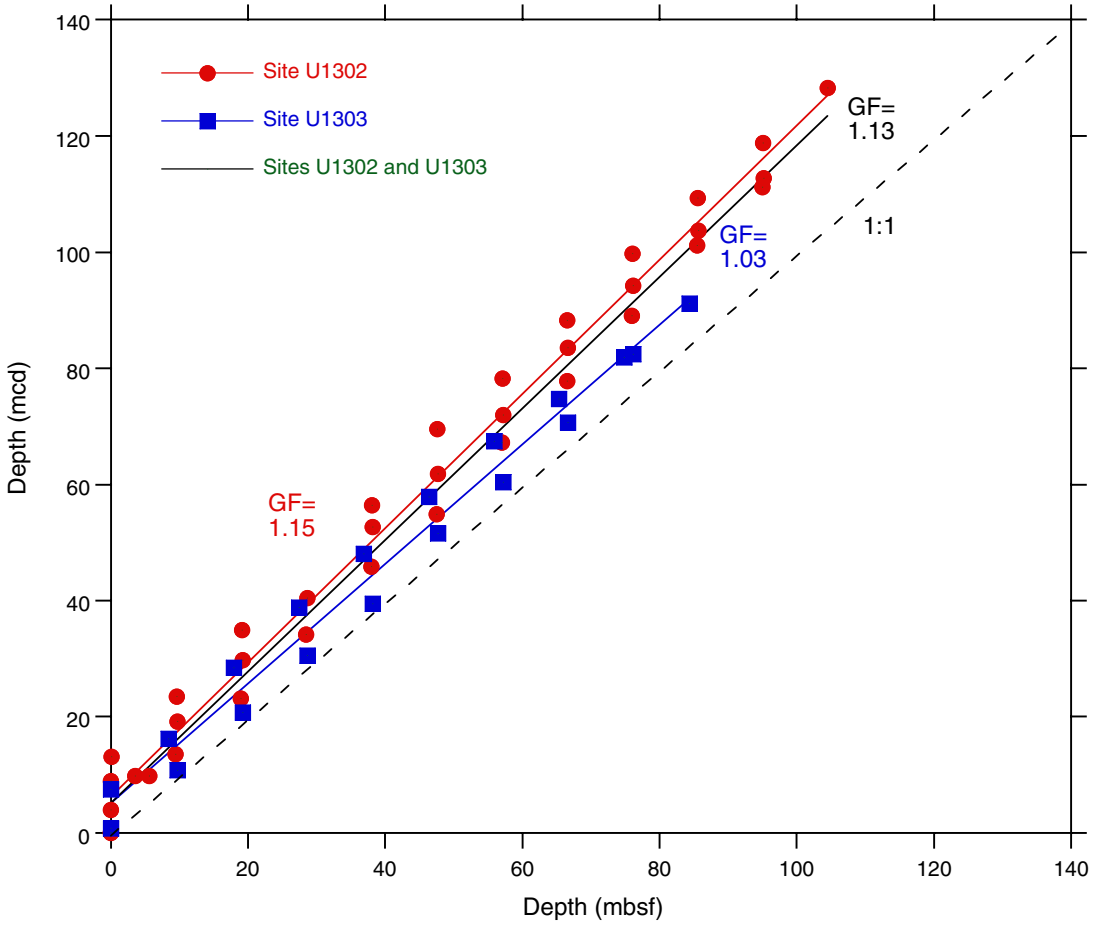

Figure F28. Age versus depth of paleomagnetic and biostratigraphic datums at Sites U1302 and U1303. Line = least squares linear fit to all data. Sed. = sedimentation rate.

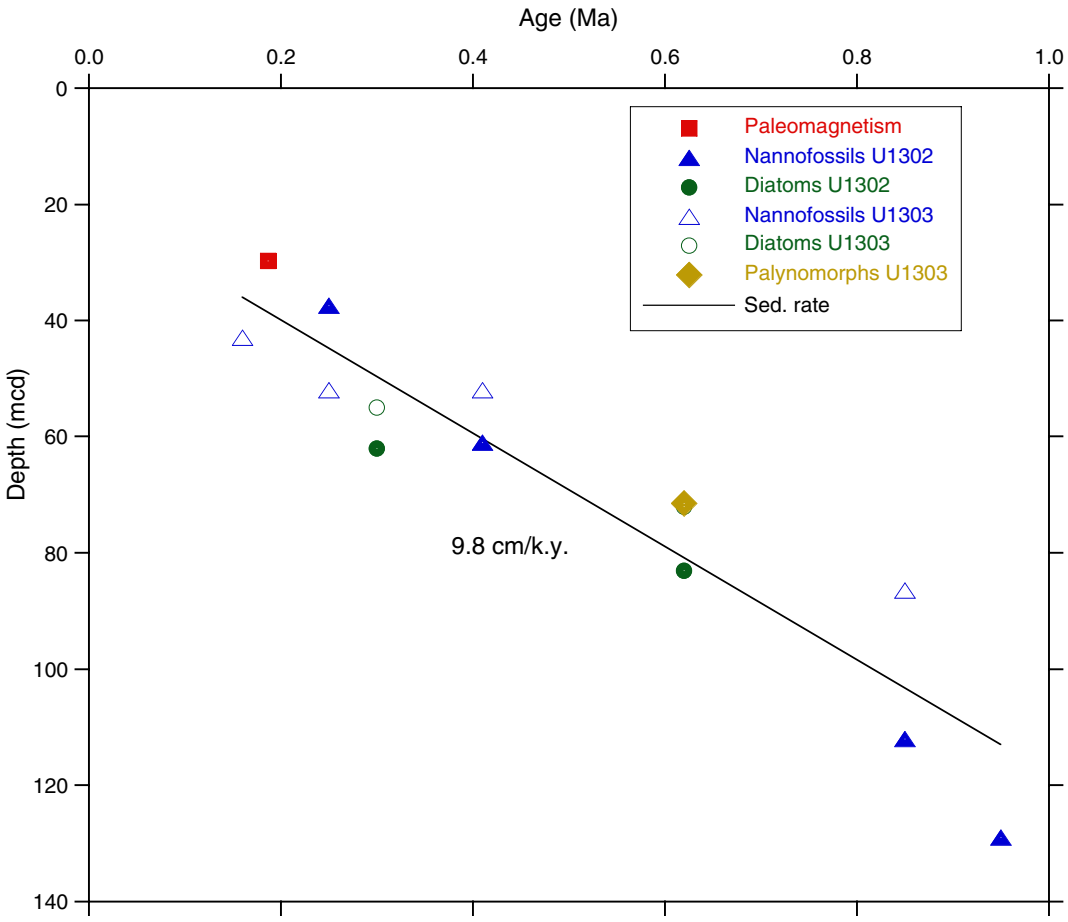

Figure F29. Headspace methane concentrations for Holes U1302A and U1303A. mcd = shipboard mcd (see "Composite section").

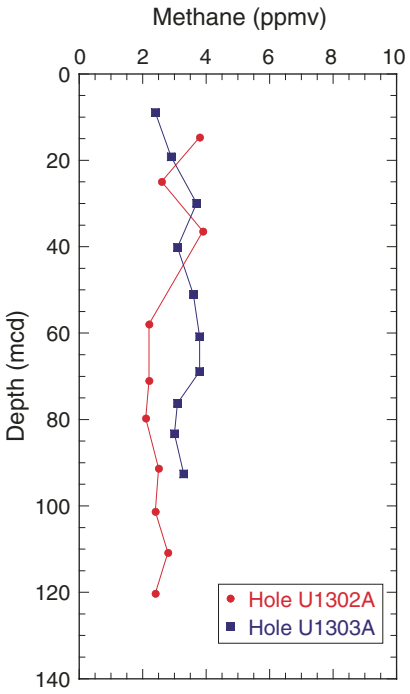

Figure F30. Site U1302 (**A**) calcium carbonate, (**B**) total organic carbon (TOC), (**C**) elemental nitrogen, and (**D**) organic C/N atomic ratio. mcd = shipboard mcd (see **"Composite section"**).

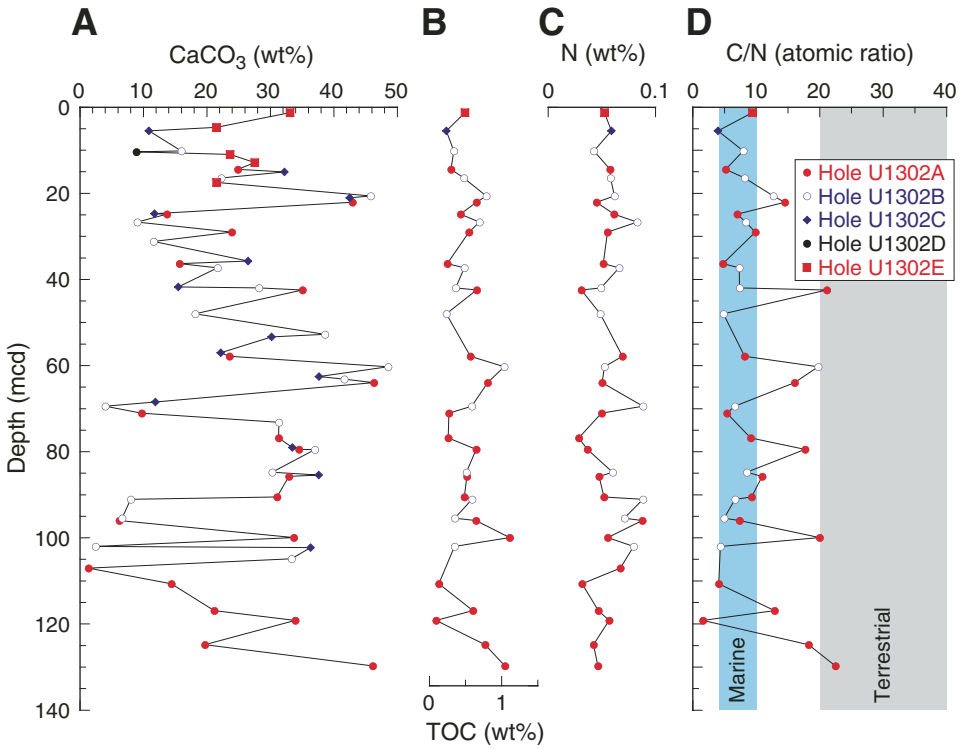

Figure F31. Site U1303 (**A**) Calcium carbonate, (**B**) total organic carbon (TOC), (**C**) elemental nitrogen, and (**D**) organic C/N atomic ratio. mcd = shipboard mcd (see **"Composite section"**).

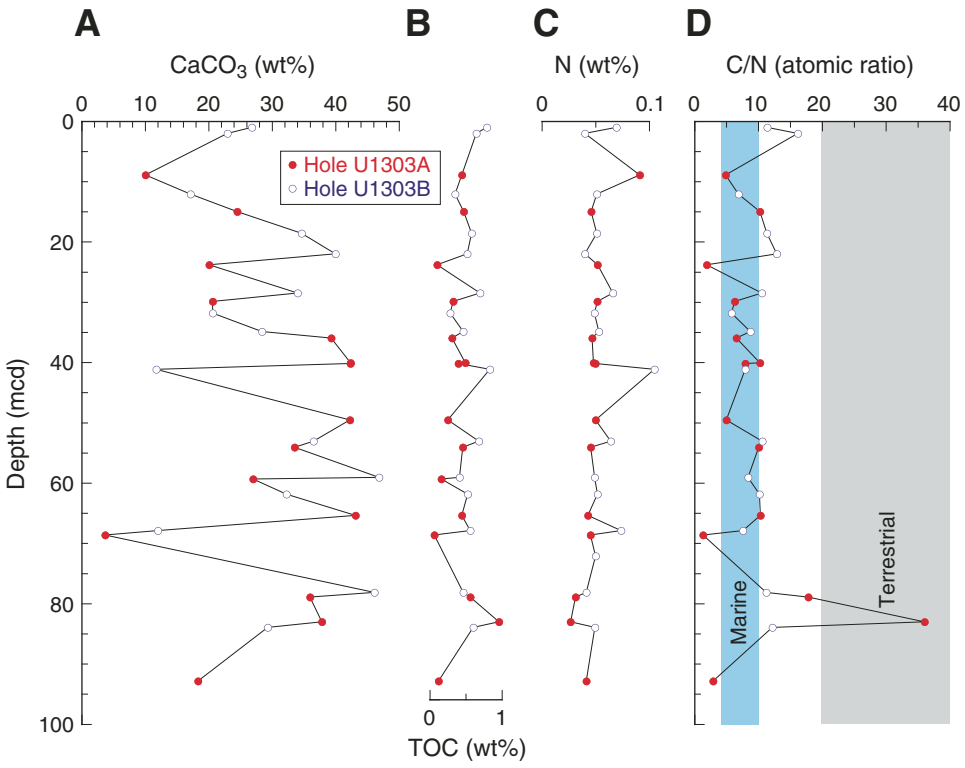

Figure F32. A. Lightness (L*) from Site U1302. Carbonate content from Sites (**B**) U1302 and (**C**) U1303. Pink shaded areas = intervals of high L* values and carbonate content. The L* record is a smoothed weighted moving average calculated using raw data from Holes U1302A–U1302C and U1302E. mcd = shipboard mcd (see "Composite section").

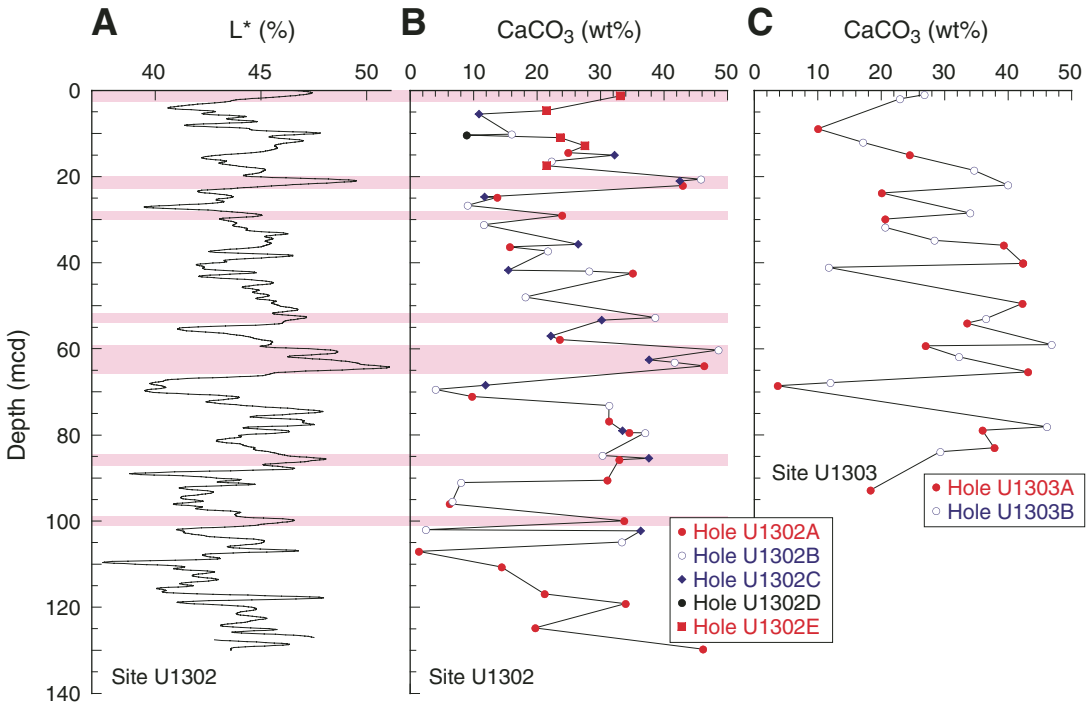

Figure F33. Profiles of chemical constituents in interstitial waters from Holes U1302A, U1303A, and U1303B. Data from Sample 303-1303A-10H-1, 145–150 cm, which was contaminated by drill fluid, are plotted in open gray squares. **A.** Chloride. **B.** Sodium. **C.** pH. **D.** Alkalinity. **E.** Sulfate. **F.** Ammonium. **G.** Dissolved silica. **H.** Calcium. **I.** Strontium. **J.** Lithium. **K.** Sr/Ca ratio. **L.** Magnesium. **M.** Potassium. **N.** Manganese. **O.** Iron. mcd = shipboard mcd (see **"Composite section"**).

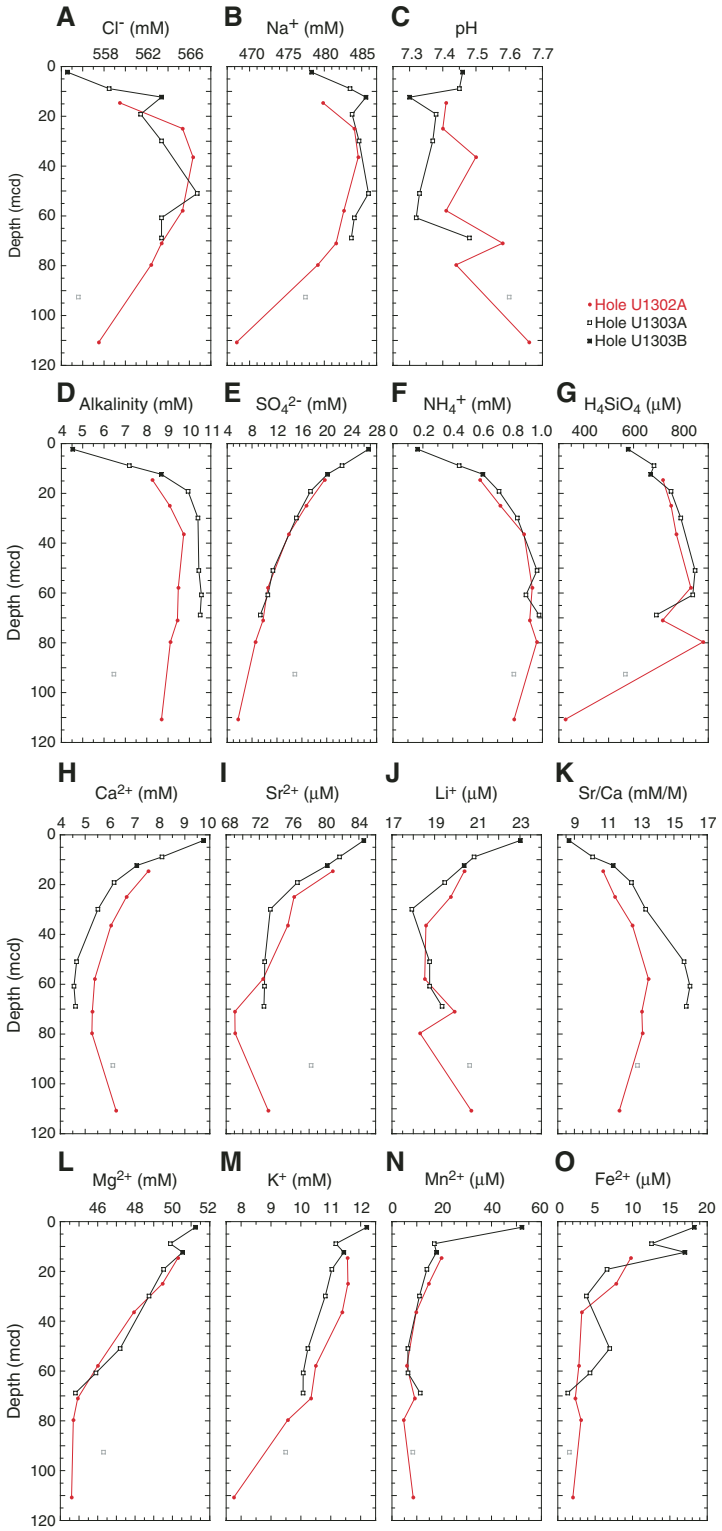

Figure F34. Magnetic susceptibility (MS) records. Core recovery columns are represented on the left side. Black = MST record, red = MSCL record. **A.** Site U1302. (Continued on next page.)

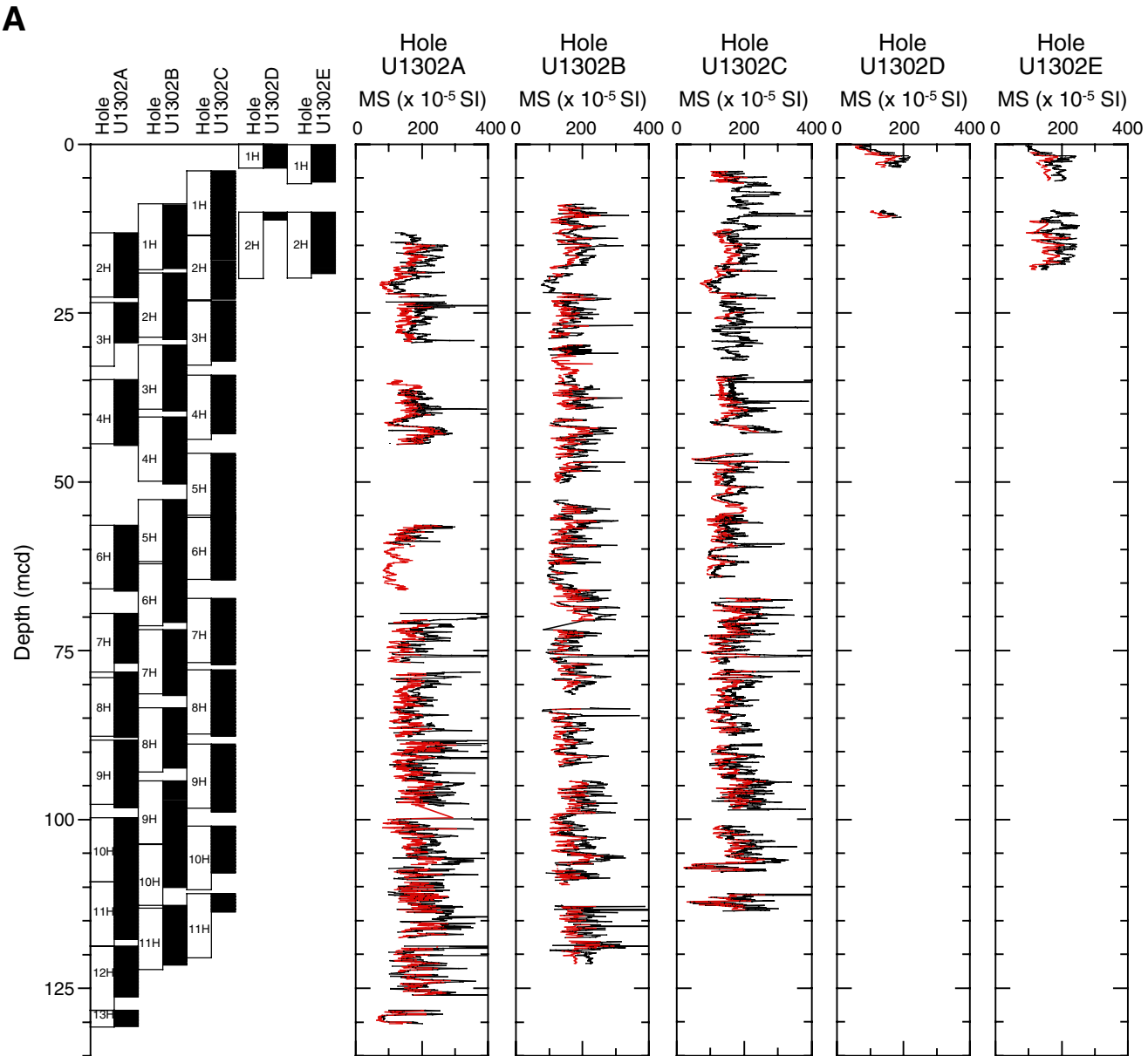

Figure F34 (continued). B. Site U1303.

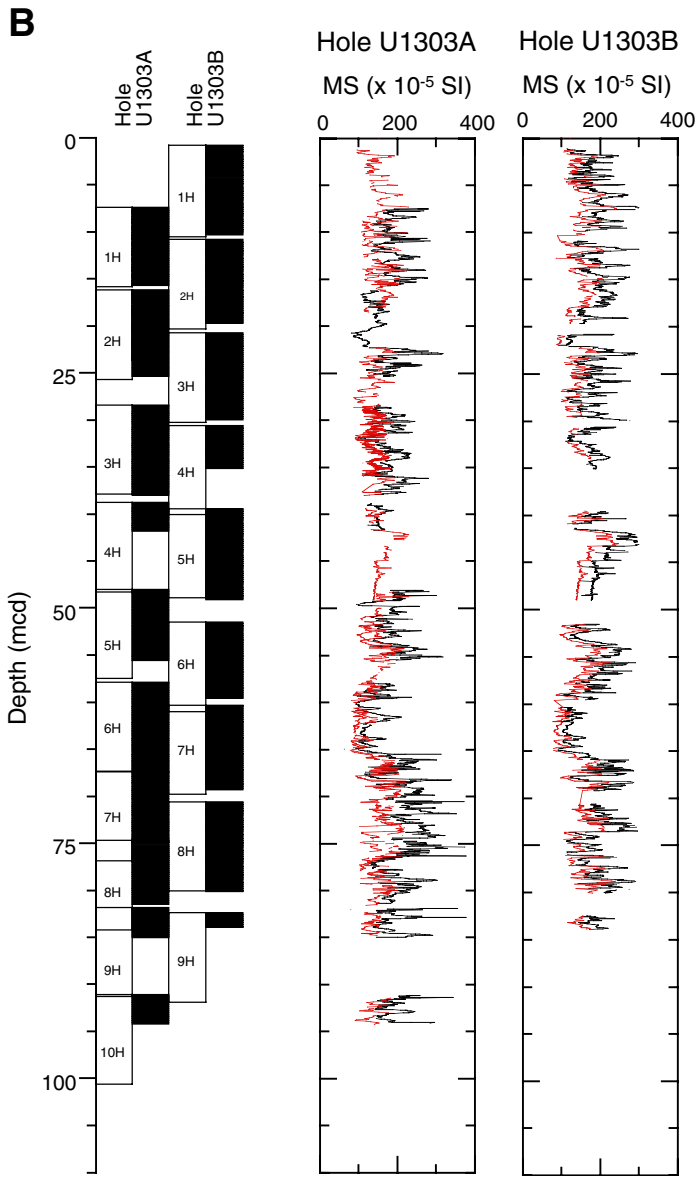

Figure F35. Combined plots of the spliced records of reflectance (lightness [L*]) in the 650–700 nm band, natural gamma ray (NGR), "fast track" magnetic susceptibility (MS), and gamma ray attenuation (GRA) density from Sites U1302 and U1303 (see **"Lithostratigraphy"**). **A.** 0–60 mcd. (Continued on next page.)

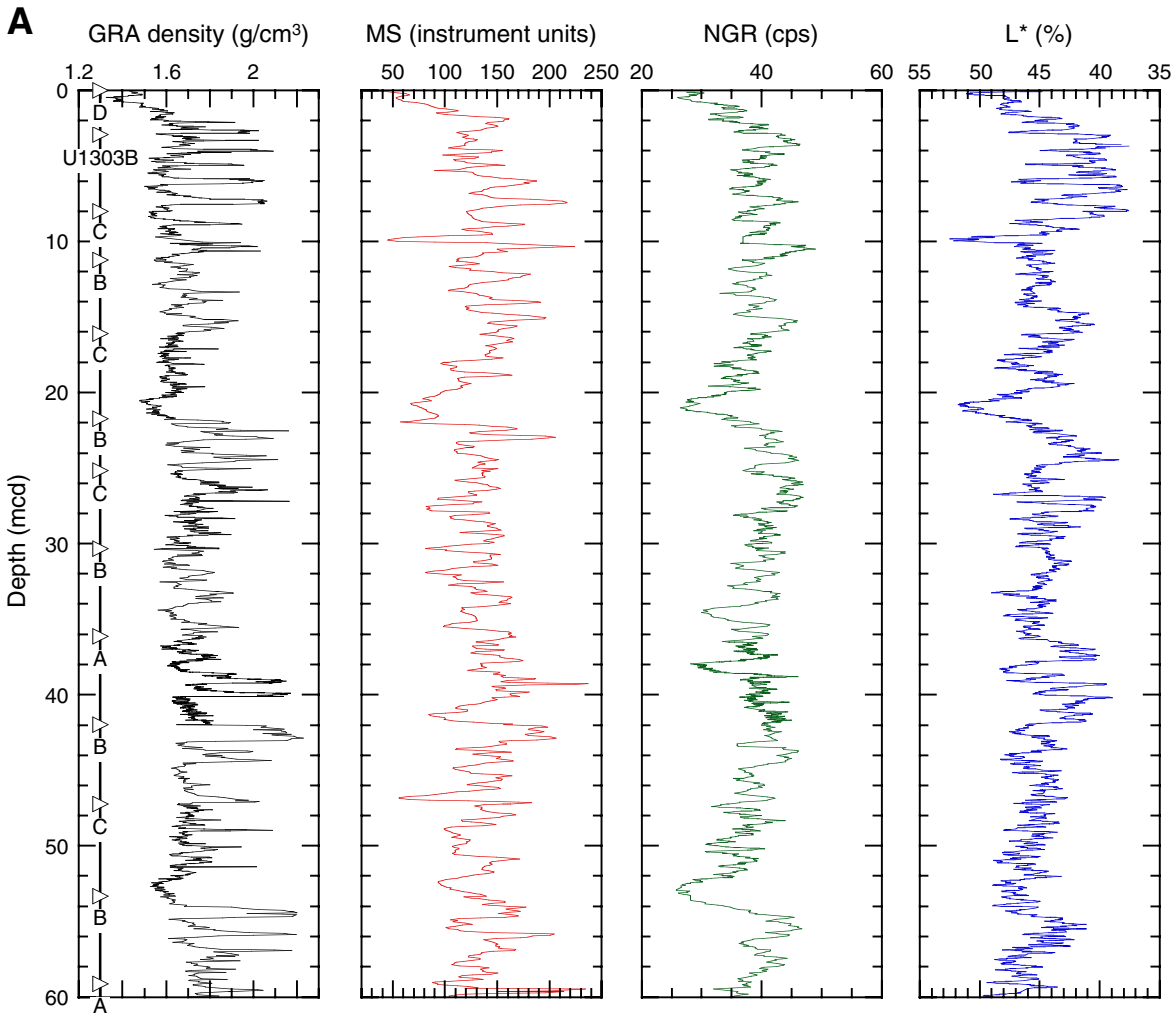

Figure F35 (continued). B. 60–107 mcd.

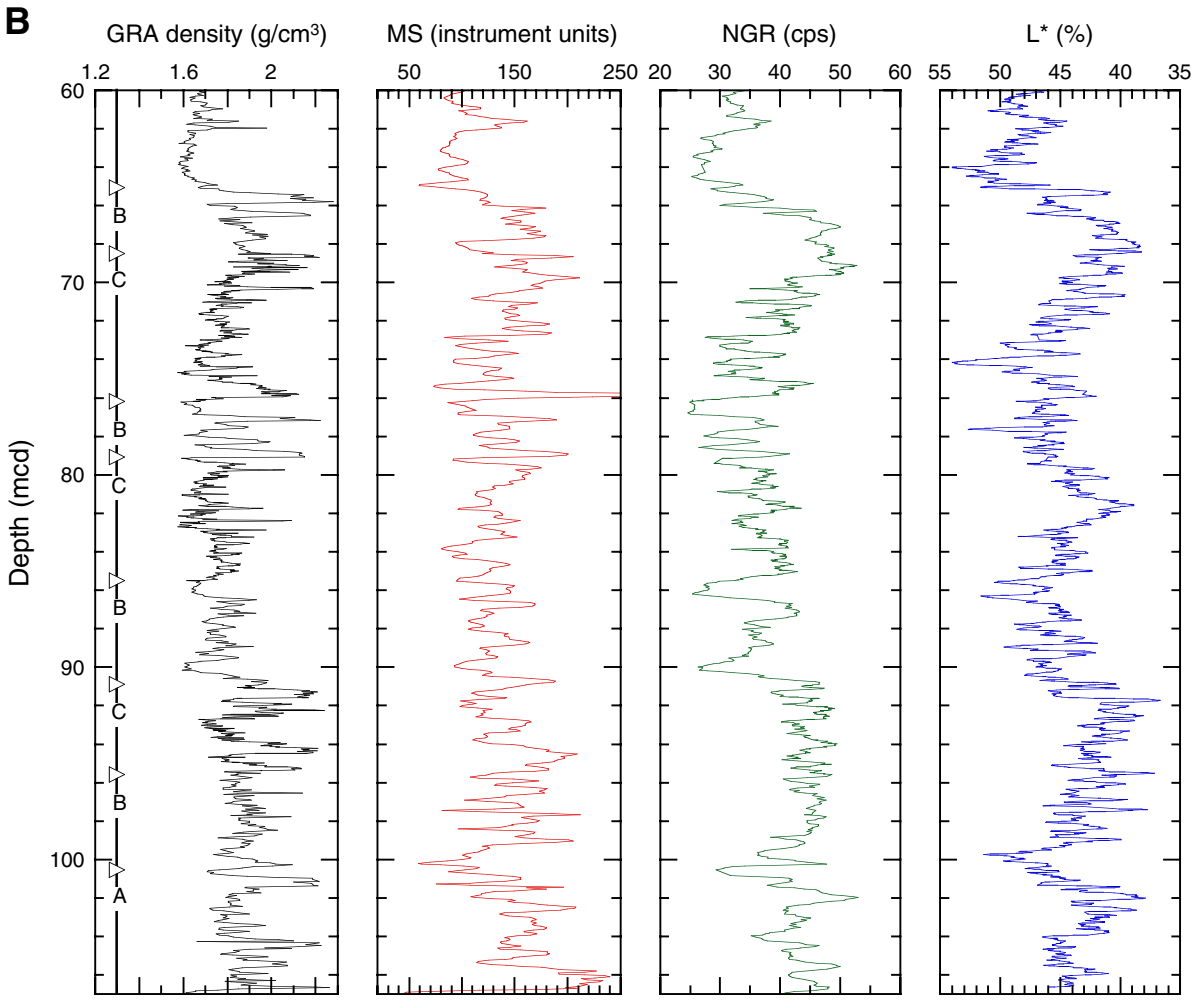

Figure F36. A. Site U1302: Combined gamma ray attenuation density measurements from the MST and bulk density from discrete measurements (red circles). Comparison with thermal conductivity (TC) measurements. (Continued on next page.)

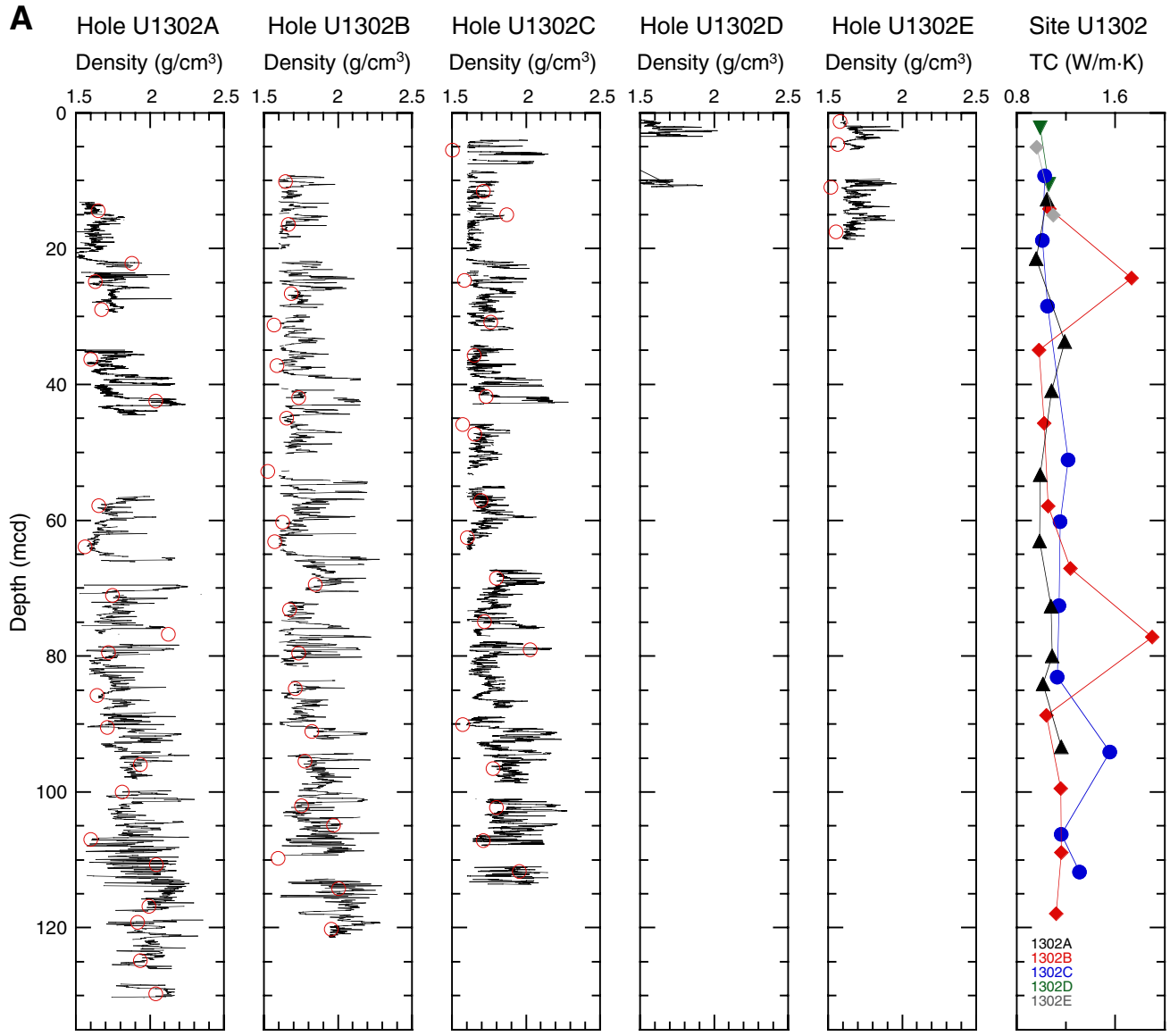

Figure F36 (continued). B. Site U1303: Combined wet bulk density measurements from the MST and bulk density from discrete measurements (red circles). Comparison with thermal conductivity (TC) measurements.

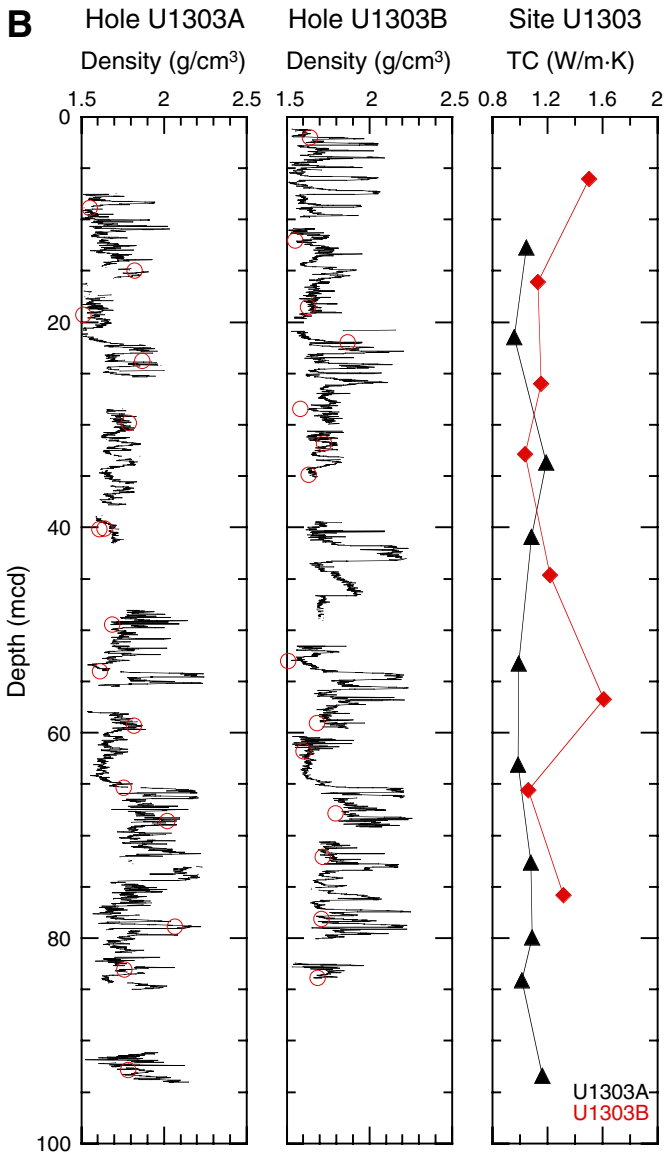

Figure F37. Natural gamma ray (NGR) counts from the MST. **A.** Site U1302. (Continued on next page.)

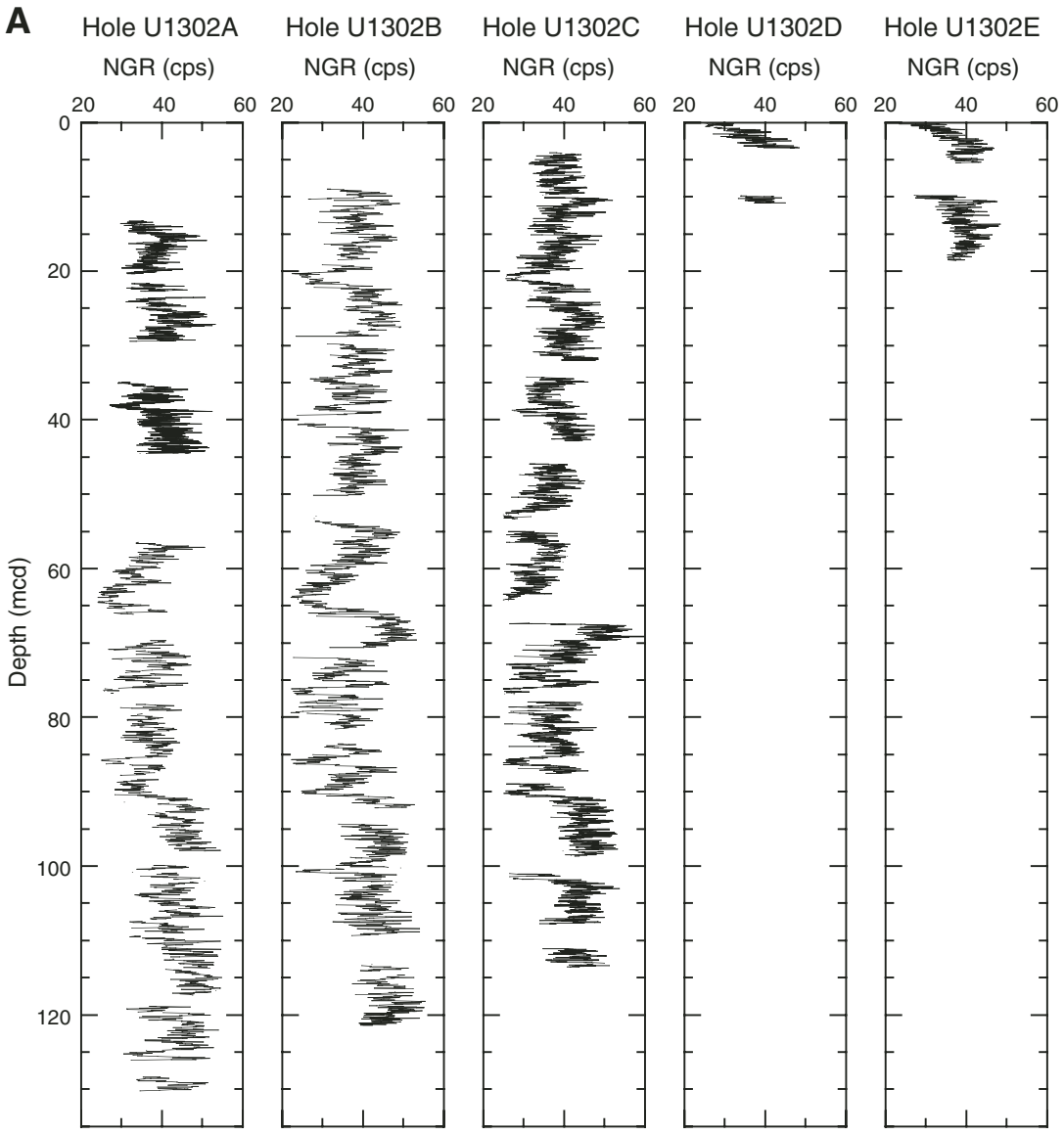

Figure F37 (continued). B. Site U1303.

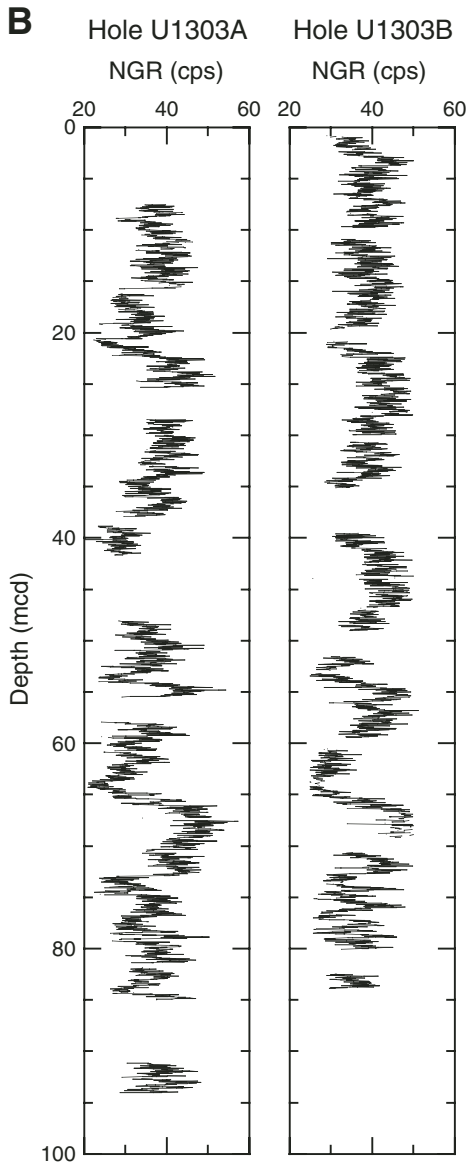

Figure F38. Downcore *P*-wave velocity records for Sites U1302 and U1303.

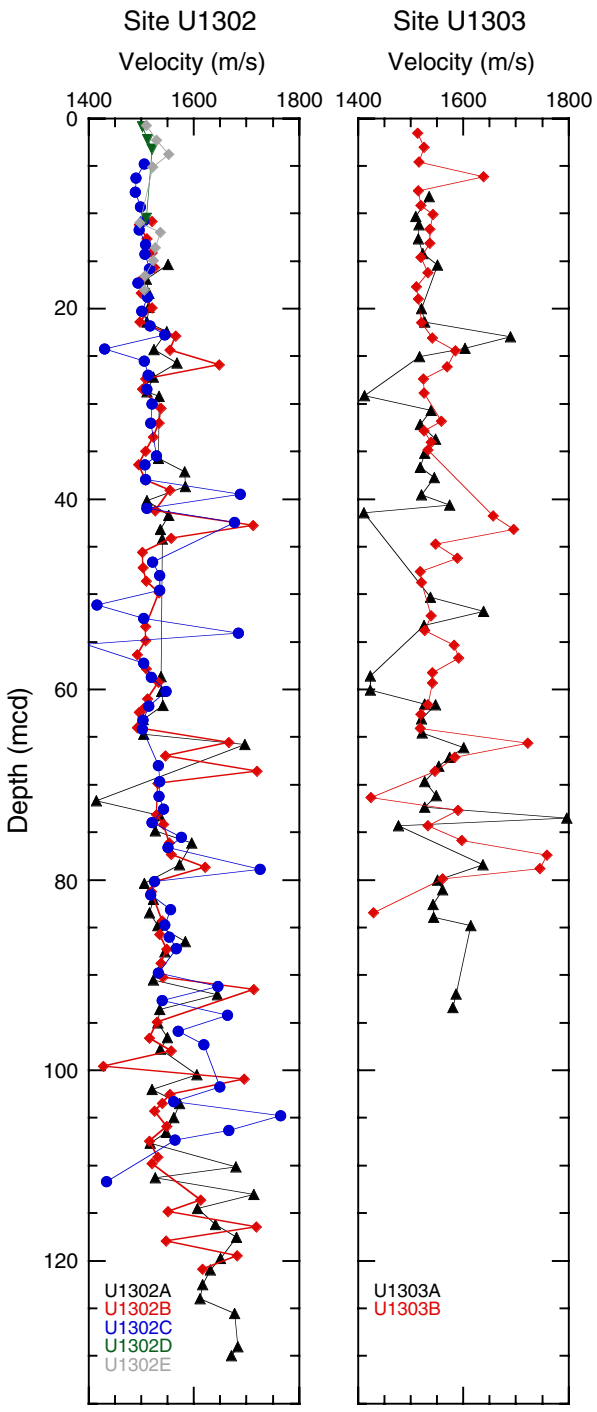

Figure F39. Downcore gamma ray attenuation–derived porosity calculations and discrete porosity measurements (red circles). **A.** Site U1302. (Continued on next page.)

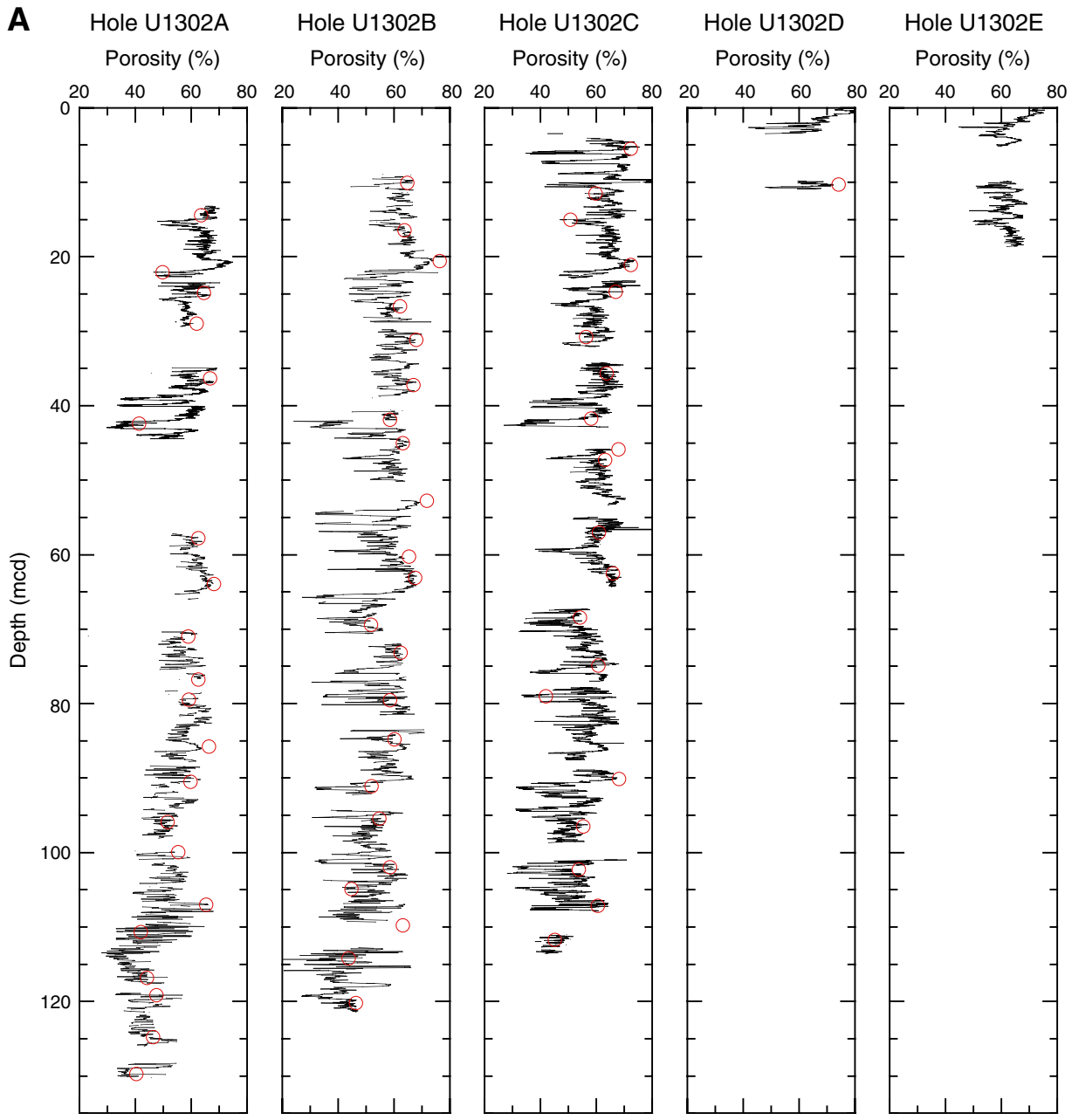

Figure F39 (continued). B. Site U1303.

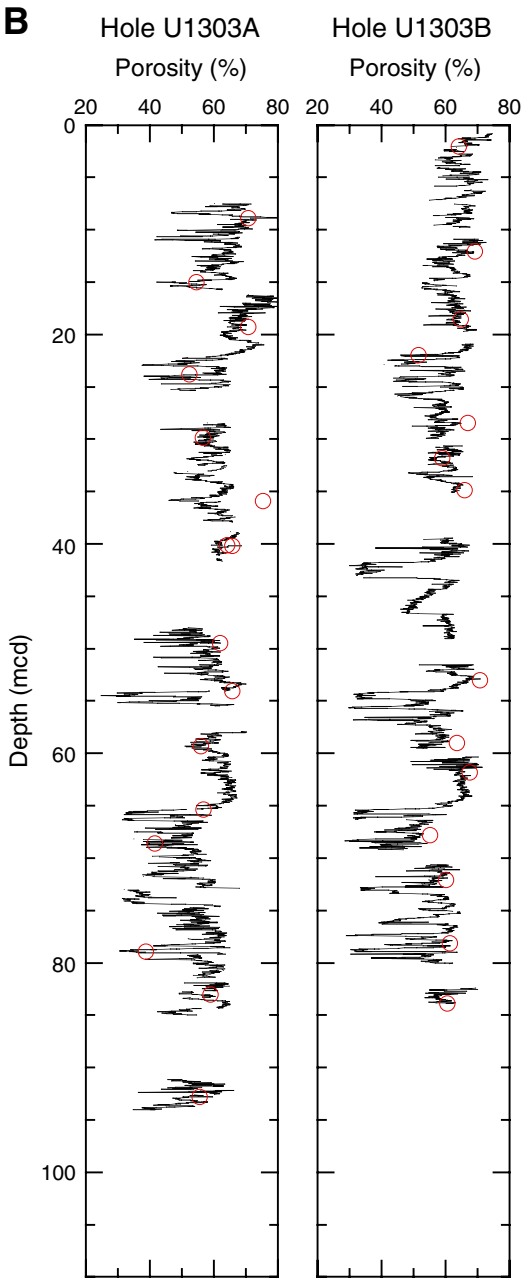

Table T1. Sites U1302 and U1303 coring summary. (Continued on next two pages.)

Hole U1302A
Latitude: 50°9.9845′N
Longitude: 45°38.2713′W
Time on site (h): 64.0 (0615 h, 2 October 2004–2215 h, 4 October 2004)
Time on hole (h): 30.5 (0615 h, 2 October 2004–1245 h, 3 October 2004)
Seafloor (drill pipe measurement from rig floor, mbrf): 3579.4
Distance between rig floor and sea level (m): 10.8
Water depth (drill pipe measurement from sea level, m): 3568.6
Total depth (drill pipe measurement from rig floor, mbrf): 3686.5
Total penetration (meters below seafloor, mbsf): 107.1
Total length of cored section (m): 107.1
Total core recovered (m): 91.7
Core recovery (%): 85.6
Total number of cores: 13

Hole U1302B
Latitude: 50°9.9952′N
Longitude: 45°38.2897′W
Time on hole (h): 13.25 (1245 h, 3 October 2004–0200 h, 4 October 2004)
Seafloor (drill pipe measurement from rig floor, mbrf): 3574.2
Distance between rig floor and sea level (m): 10.8
Water depth (drill pipe measurement from sea level, m): 3563.4
Total depth (drill pipe measurement from rig floor, mbrf): 3678.9
Total penetration (meters below seafloor, mbsf): 104.7
Total length of cored section (m): 104.7
Total core recovered (m): 102.82
Core recovery (%): 98.2
Total number of cores: 11

Hole U1302C
Latitude: 50°10.0068′N
Longitude: 45°38.3086′W
Time on hole (h): 13.67 (0200 h, 4 October 2004–1540 h, 4 October 2004)
Seafloor (drill pipe measurement from rig floor, mbrf): 3570.0
Distance between rig floor and sea level (m): 10.8
Water depth (drill pipe measurement from sea level, m): 3559.2
Total depth (drill pipe measurement from rig floor, mbrf): 3674.5
Total penetration (meters below seafloor, mbsf): 104.5
Total length of cored section (m): 104.5
Total core recovered (m): 97.06
Core recovery (%): 92.9
Total number of cores: 11

Hole U1302D
Latitude: 50°10.0194′N
Longitude: 45°38.3241′W
Time on hole (h): 2.58 (1540 h, 4 October 2004–1815 h, 4 October 2004)
Seafloor (drill pipe measurement from rig floor, mbrf): 3566.5
Distance between rig floor and sea level (m): 10.8
Water depth (drill pipe measurement from sea level, m): 3555.7
Total depth (drill pipe measurement from rig floor, mbrf): 3579.5
Total penetration (meters below seafloor, mbsf): 13.0
Total length of cored section (m): 13.0
Total core recovered (m): 4.87
Core recovery (%): 37.5
Total number of cores: 2

Hole U1302E
Latitude: 50°10.0299′N
Longitude: 45°23.1430′W
Time on hole (h): 4.0 (1815 h, 4 October 2004–2215 h, 4 October 2004)
Seafloor (drill pipe measurement from rig floor, mbrf): 3568.9
Distance between rig floor and sea level (m): 10.8
Water depth (drill pipe measurement from sea level, m): 3558.1
Total depth (drill pipe measurement from rig floor, mbrf): 3584.0
Total penetration (meters below seafloor, mbsf): 15.1
Total length of cored section (m): 15.1
Total core recovered (m): 14.59
Core recovery (%): 96.6
Total number of cores: 2

Table T1 (continued).

Hole U1303A
Latitude: 50°12.4007′N
Longitude: 45°41.2201′W
Time on site (h): 35.26 (0200 h, 5 October 2004–1315 h, 6 October 2004)
Time on hole (h): 14.83 (0200 h, 5 October 2004–1650 h, 5 October 2004)
Seafloor (drill pipe measurement from rig floor, mbrf): 3535.0
Distance between rig floor and sea level (m): 10.8
Water depth (drill pipe measurement from sea level, m): 524.2
Total depth (drill pipe measurement from rig floor, mbrf): 3628.9
Total penetration (meters below seafloor, mbsf): 93.9
Total length of cored section (m): 93.9
Total core recovered (m):
Core recovery (%): 73.6
Total number of cores: 10

Hole U1303B
Latitude: 50°9.9952′N
Longitude: 45°38.2897′W
Time on hole (h): 20.42 (1650 h, 5 October 2004–1315 h, 6 October 2004)
Seafloor (drill pipe measurement from rig floor, mbrf): 3528.7
Distance between rig floor and sea level (m): 10.8
Water depth (drill pipe measurement from sea level, m): 3517.9
Total depth (drill pipe measurement from rig floor, mbrf): 3614.4
Total penetration (meters below seafloor, mbsf): 85.7
Total length of cored section (m): 85.7
Total core recovered (m): 71.54
Core recovery (%): 83.5
Total number of cores: 9

Core	Date (Oct 2004)	Local time (h)	Depth (mbsf) Top	Depth (mbsf) Bottom	Length (m) Cored	Length (m) Recovered	Recovery (%)	Comments
303-U1302A-								
1H	2	1600	0.0	0.1	0.1	0.05	50.0	Nonmagnetic barrel
2H	2	1730	0.1	9.6	9.5	9.74	102.5	Nonmagnetic barrel
3H	2	1955	9.6	19.1	9.5	6.17	65.0	Nonmagnetic barrel
4H	2	2110	19.1	28.6	9.5	9.83	103.5	Oriented, nonmagnetic barrel
5H	2	2210	28.6	38.1	9.5	0.02	0.2	Oriented, nonmagnetic barrel
6H	2	2340	38.1	47.6	9.5	9.93	104.5	Oriented, nonmagnetic barrel
7H	3	0140	47.6	57.1	9.5	7.56	79.6	Oriented, nonmagnetic barrel
8H	3	0310	57.1	66.6	9.5	9.88	104.0	Oriented, nonmagnetic barrel
9H	3	0500	66.6	76.1	9.5	10.16	107.0	Oriented, nonmagnetic barrel, APCT
10H	3	0600	76.1	85.6	9.5	9.51	100.1	Oriented, nonmagnetic barrel
11H	3	0700	85.6	95.1	9.5	8.68	91.4	Oriented, nonmagnetic barrel
12H	3	0820	95.1	104.6	9.5	7.63	80.3	Oriented, nonmagnetic barrel, APCT
13H	3	0950	104.6	107.1	2.5	2.54	101.6	Oriented, nonmagnetic barrel
				Totals:	107.1	91.70	85.6	
303-U1302B-								
1H	3	1405	0.0	9.7	9.7	9.74	100.4	Nonmagnetic barrel
2H	3	1505	9.7	19.2	9.5	9.96	104.8	Nonmagnetic barrel
3H	3	1615	19.2	28.7	9.5	9.95	104.7	Oriented, nonmagnetic barrel
4H	3	1710	28.7	38.2	9.5	10.01	105.4	Oriented, nonmagnetic barrel
5H	3	1810	38.2	47.7	9.5	9.83	103.5	Oriented, nonmagnetic barrel
6H	3	1910	47.7	57.2	9.5	9.16	96.4	Oriented, nonmagnetic barrel
7H	3	2015	57.2	66.7	9.5	9.80	103.2	Oriented, nonmagnetic barrel
8H	3	2125	66.7	76.2	9.5	9.04	95.2	Oriented, nonmagnetic barrel
9H	3	2230	76.2	85.7	9.5	9.79	103.1	Oriented, nonmagnetic barrel
10H	3	2330	85.7	95.2	9.5	6.53	68.7	Oriented, nonmagnetic barrel
11H	4	0040	95.2	104.7	9.5	9.01	94.8	Oriented, nonmagnetic barrel
				Totals:	104.7	102.82	98.2	
303-U1302C-								
1H	4	0400	0.0	9.5	9.5	9.64	101.5	Nonmagnetic barrel
2H	4	0515	9.5	19.0	9.5	9.56	100.6	Nonmagnetic barrel
3H	4	0620	19.0	28.5	9.5	9.04	95.2	Oriented, nonmagnetic barrel
4H	4	0730	28.5	38.0	9.5	8.88	93.5	Oriented, nonmagnetic barrel
5H	4	0840	38.0	47.5	9.5	10.03	105.6	Oriented, nonmagnetic barrel
6H	4	0930	47.5	57.0	9.5	9.72	102.3	Oriented, nonmagnetic barrel
7H	4	1030	57.0	66.5	9.5	9.96	104.8	Oriented, nonmagnetic barrel
8H	4	1130	66.5	76.0	9.5	10.03	105.6	Oriented, nonmagnetic barrel

Table T1 (continued).

Core	Date (Oct 2004)	Local time (h)	Depth (mbsf) Top	Depth (mbsf) Bottom	Length (m) Cored	Length (m) Recovered	Recovery (%)	Comments
9H	4	1235	76.0	85.5	9.5	10.21	107.5	Oriented, nonmagnetic barrel
10H	4	1335	85.5	95.0	9.5	7.15	75.3	Oriented, nonmagnetic barrel
11H	4	1435	95.0	104.5	9.5	2.84	29.9	Oriented, nonmagnetic barrel
				Totals:	104.5	97.06	92.9	
303-U1302D-								
1H	4	1650	0.0	3.5	3.5	3.63	103.7	Nonmagnetic barrel
2H	4	1800	3.5	13.0	9.5	1.24	13.1	Nonmagnetic barrel
				Totals:	13.0	4.87	37.5	
303-U1302E-								
1H	4	1930	0.0	5.6	5.6	5.60	100.0	Nonmagnetic barrel
2H	4	2040	5.6	15.1	9.5	8.99	94.6	Nonmagnetic barrel
				Totals:	15.1	14.59	96.6	
303-U1303A-								
1H	5	0530	0.0	8.4	8.4	8.43	100.4	Nonmagnetic barrel
2H	5	0645	8.4	17.9	9.5	9.31	98.0	Nonmagnetic barrel
3H	5	0750	17.9	27.4	9.5	9.71	102.2	Oriented, nonmagnetic barrel
4H	5	0845	27.4	36.9	9.5	3.10	32.6	Oriented, nonmagnetic barrel
5H	5	1000	36.9	46.4	9.5	7.74	81.5	Oriented, nonmagnetic barrel
6H	5	1215	46.4	55.9	9.5	9.71	102.2	Oriented, nonmagnetic barrel
7H	5	1310	55.9	65.4	9.5	7.61	80.1	Oriented, nonmagnetic barrel
8H	5	1405	65.4	74.9	9.5	6.90	72.6	Oriented, nonmagnetic barrel
9H	5	1505	74.9	84.4	9.5	3.36	35.4	Oriented, nonmagnetic barrel
10H	5	1600	84.4	93.9	9.5	3.21	33.8	Oriented, nonmagnetic barrel
				Totals:	93.9	69.08	73.6	
303-U1303B-								
1H	5	1905	0.0	9.7	9.7	9.62	99.2	Nonmagnetic barrel
2H	5	2000	9.7	19.2	9.5	9.05	95.3	Nonmagnetic barrel
3H	5	2100	19.2	28.7	9.5	9.37	98.6	Oriented, nonmagnetic barrel
4H	5	2155	28.7	38.2	9.5	4.74	49.9	Oriented, nonmagnetic barrel
5H	5	2300	38.2	47.7	9.5	9.89	104.1	Oriented, nonmagnetic barrel
6H	6	0015	47.7	57.2	9.5	8.23	86.6	Oriented, nonmagnetic barrel
7H	6	0110	57.2	66.7	9.5	9.15	96.3	Oriented, nonmagnetic barrel
8H	6	0210	66.7	76.2	9.5	9.79	103.1	Oriented, nonmagnetic barrel
9H	6	0315	76.2	85.7	9.5	1.70	17.9	Oriented, nonmagnetic barrel
				Totals:	85.7	71.54	83.5	

Table T2. Distribution of calcareous nannofossils, Hole U1302A.

Core, section	Age (Ma)	Abundance	Preservation	*Calcidiscus leptoporus*	*Ceratolithus* spp.	*Coccolithus pelagicus*	*Cyclolithella annula*	*Discolithina japonica*	*Discolithina* spp.	*Emiliania huxleyi*	*Gephyrocapsa caribbeanica*	*Gephyrocapsa oceanica*	*Gephyrocapsa parallela*	*Gephyrocapsa* spp. (small)	*Helicosphaera carteri*	*Helicosphaera hyalina*	*Helicosphaera* cf. *wallichii*	*Pseudoemiliania lacunosa*	*Reticulofenestra asanoi*	*Reticulofenestra* spp. (small)	*Rhabdosphaera clavigera*	*Rhabdosphaera stylifera*	*Scapholithus fossilis*	*Syracosphaera pulchra*	*Umbilicosphaera sibogae*	Reworked species: *Reticulofenestra gartneri*	*Reticulofenestra pseudoumbilicus*	*Reticulofenestra umbilicus*	*Cretarhabdulus* spp.	*Cribrosphaerella ehrenbergii*	*Gartnergo* spp.	*Prediscosphaella cretacea* (s.l.)	*Watznaueria barnesae*
303-U1302A-																																
1H-CC	~0.25	C	G	R		F		+	+	A	R	R	+	C	F	R				C	+							r				r
2H-CC	~0.25	A	G	C		C			+	C	+	F	+	A	F					C				R			r			r		
3H-CC	~0.25	A	G	C		C	+			A	R	F	+	A	C		R			A	+			R	+							
4H-CC	~0.25	C	P	R	+	C						F		A						A				R	+			r		r		r
5H-CC	~0.25	C	M			R				+		F		C	R					C				+	+							
6H-CC	0.25~0.41	C	M	+		F			+	+	+	R	+	C	R	+		+		C				+								
7H-CC	0.25~0.41	A	G	R		R			+	+		R	R	A				R		R	R		+	R	R							
8H-CC	0.41~0.85	A	G	R		C		R	R			F	R	A	R			C		R	R	R		R	R							
9H-CC	0.41~0.85	R	M	R		R						R	R	C	R			R		R				R								
10H-CC	0.41~0.85	A	G	R				R	R			R	R	A	R			C		R				R	R							
11H-CC	0.85~0.95	C	M	R		R		R				R	R	C	R			R	C	C				R								
12H-CC	0.85~0.95	C	M	R		R		R	R			R	R	C	R			R	C	C					R	r		r		r		r
13H-CC	0.95~1.16	C	M	R					R						R			R	C	A				R	R			r				

Notes: Abundance: A = abundant, C = common, F = few, R = rare, + = present, r = reworked. Preservation: G = good, M = moderate, P = poor.

Table T3. Distribution of calcareous nannofossils, Hole U1302B.

Core, section, interval (cm)	Age (Ma)	Abundance	Preservation	*Calcidiscus leptoporus*	*Coccolithus pelagicus*	*Coccolithus streckerii*	*Discolithina japonica*	*Discolithina* spp.	*Emiliania huxleyi*	*Gephyrocapsa caribbeanica*	*Gephyrocapsa oceanica*	*Gepyrocapsa parallela*	*Gephyrocapsa* spp. (small)	*Helicosphaera carteri*	*Helicosphaera inversa*	*Pseudoemiliania lacunosa*	*Reticulofenestra* spp. (small)	*Rhabdosphaera clavigera*	*Rhabdosphaera stylifera*	*Scapholithus fossilis*	*Syracosphaera pulchra*	*Umbilicosphaera sibogae*
303-U1302B-																						
6H-CC	0.16~0.25	R	M	+					R		F	C	C		+		C				+	
7H-1, 0–1	0.25/0.41	A	G	R			F		R		R	R	A	R		F	C				+	
7H-2, 0–1	0.25/0.41	A	G	R	F	R	R		+		R	R	A	R		F	C				+	+
7H-3, 0–1	0.25/0.41	A	G	R	R		+	+			R	R	A	R		R	F		+		+	+
7H-4, 0–1	0.25/0.41	A	G	R	R				+		R	R	A	R		F	F				R	R
7H-5, 0–1	0.25/0.41	A	M	R				+	+		R	+	A	R		F	C				+	R
7H-6, 0–1	0.25/0.41	A	M	F	R		+		+		R	R	A	F		F	C					
7H-7, 0–1	0.25/0.41	A	G	R	F	R	R		+		R	F	A	F		F	C				R	
7H-CC	0.25/0.41	F	M	R	R			+	+		R	+	C	+		C	C	+				
8H-1, 0–1	0.25/0.41	A	M	R	R	+	+	R	+		F	R	A	R		F	C					
8H-2, 0–1	0.25/0.41	A	M	R	R				+		F	F	A	R		F	C			+	R	R
8H-3, 0–1	0.25/0.41	F	M	R	R				+		R	F	A	R		C	C				R	
8H-3, 50–51	0.41~0.85	C	M	R	F	R					R	R	A	C		C	A				R	
8H-4, 0–1	0.41~0.85	A	M	F	R						F	F	A	C		A	C				R	F
8H-5, 0–1	0.41~0.85	F	M	R	+						R	F	C	R		A	C					R
8H-6, 0–1	0.41~0.85	F	M	R	F						R	R	C	R		A	C					R
8H-CC	0.41~0.85	C	G	R	C		+	+		+	R		C	R		C	C					

Notes: Abundance: A = abundant, C = common, F = few, R = rare, + = present. Preservation: G = good, M = moderate.

Table T4. Distribution of calcareous nannofossils, Hole U1302C.

Core, section, interval (cm)	Age (Ma)	Abundance	Preservation	*Calcidiscus leptoporus*	*Coccolithus streckerii*	*Coccolithus pelagicus*	*Discolithina japonica*	*Discolithina* spp.	*Emiliania huxleyi*	*Gephyrocapsa caribbeanica*	*Gephyrocapsa oceanica*	*Gephyrocapsa parallela*	*Gephyrocapsa* spp. (large)	*Gephyrocapsa* spp. (small)	*Helicosphaera carteri*	*Helicosphaera hyalina*	*Helicosphaera inversa*	*Helicosphaera* cf. *wallichii*	*Pseudoemiliania lacunosa*	*Reticulofenestra asanoi*	*Reticulofenestra* spp. (small)	*Rhabdosphaera clavigera*	*Rhabdosphaera stylifera*	*Scapholithus fossilis*	*Syracosphaera pulchra*	*Umbilicosphaera sibogae*	Reworked species: *Isthmolithus recurvus*	Reworked species: *Sphenolithus abies*	Reworked species: *Reticulofenestra pseudoumbilicus*	Reworked species: *Reticulofenestra umbilicus*	Reworked species: *Watznaueria barnesae*
303-U1302C-																															
1H-CC	0~0.25	A	G	R	R	F	R		A		C	F		A	F						C				R	R					r
2H-CC	0~0.25	C	G	R		R			C		R	R		C	R						F										
3H-CC	0~0.25	C	G	R	R	F			C		R	R		A	F						F				R						r
4H-CC	0.16~0.25	C	M	R	R	C		R			R	R		A	F	R	R				C		R	R	R	R					
5H-CC	0.16~0.25	R	P	+										+							C										
6H-CC	0.16~0.25	A	G	R	R	F			R		R	R		A	R	R	R				F					R	R					
7H-CC	0.25/0.41	A	G	R		R			R		R	R		A	R				F		F				R	R	R		r			
8H-1, 0~1	0.25/0.41	C	G	R		R			R		R	+		A	R				C		F											
8H-2, 0~1	0.25/0.41	C	G	R		+			R		+	+		C	+				F		+											
8H-3, 0~1	0.25/0.41	A	G	R		+	+	+	R		R	F		C	R				C		R					+	+					
8H-4, 0~1	0.25/0.41	A	G	+		C			+		R	R		A	R				F		C											
8H-5, 0~1	0.25/0.41	A	G	C					F		F	F		A	R				F		C					R						
8H-6, 0~1	0.25/0.41	A	G	R			+		+		F	F		A	R	+			C		C					R	R					
8H-6, 50~51	0.41~0.85	A	G	R			+		+		F	F		A	C	R			C		C		+			R	R					
8H-6, 100~101	0.41~0.85	A	G	R			R	R			F	R		A	C				F		C	+				+	R					
8H-7, 0~1	0.41~0.85	R	M	R							R	R		C	R				C		A											
8H-CC	0.41~0.85	A	G	R		F		R			F	F		A	R				C		C				R	R						
9H-CC	0.41~0.85	A	G	R		R	R	R		+	F	F		A	F	+		+	C		C						+					
10H-CC	0.41~0.85	A	G	R		+	+			+	F	F		A	R				C		F					R	+					
11H-CC	0.85~0.95	A	G	+	+	+		+			F	R		A	R				F	R	C						+	r		r	r	

Notes: Abundance: A = abundant, C = common, F = few, R = rare, + = present, r = reworked. Preservation: G = good, M = moderate, P = poor.

Table T5. Distribution of calcareous nannofossils, Hole U1302D.

Core, section	Age (Ma)	Abundance	Preservation	*Calcidiscus leptoporus*	*Coccolithus pelagicus*	*Cyclolithella annula*	*Discolithina japonica*	*Discolithina* spp.	*Emiliania huxleyi*	*Gephyrocapsa caribbeanica*	*Gephyrocapsa oceanica*	*Gephyrocapsa parallela*	*Gephyrocapsa* spp. (small)	*Helicosphaera carteri*	*Helicosphaera hyalina*	*Reticulofenestra* spp. (small)	*Rhabdosphaera clavigera*	*Syracosphaera pulchra*	*Umbilicosphaera sibogae*
303-1302D-																			
1H-CC	0~0.25	F	G		F				C				R			+			
2H-CC	0~0.25	C	G	+	C	+	R	F	F		C	F	C	F	+	F	+	+	+

Notes: Abundance: C = common, F = few, R = rare, + = present. Preservation: G = good.

Table T6. Distribution of calcareous nannofossils, Hole U1302E.

Core, section	Age (Ma)	Abundance	Preservation	*Calcidiscus leptoporus*	*Coccolithus pelagicus*	*Cyclolithella annula*	*Discolithina japonica*	*Discolithina* spp.	*Emiliania huxleyi*	*Gephyrocapsa caribbeanica*	*Gephyrocapsa oceanica*	*Gephyrocapsa parallela*	*Gephyrocapsa* spp. (small)	*Helicosphaera carteri*	*Helicosphaera* cf. *wallichii*	*Reticulofenestra* spp. (small)	*Rhabdosphaera clavigera*	*Syracosphaera pulchra*	*Umbilicosphaera sibogae*
303-1302E-																			
1H-CC	0~0.25	A	G	+	C		+	R	F		F	F	C	R		R	+	R	+
2H-CC	0~0.25	A	G	+	C	+			F	R	F	F	C	R	+	F	+	+	+

Notes: Abundance: A = abundant, C = common, F = few, R = rare, + = present. Preservation: G = good.

Table T7. Distribution of calcareous nannofossils, Hole U1303A.

Core, section	Age (Ma)	Abundance	Preservation	*Calcidiscus leptoporus*	*Coccolithus pelagicus*	*Coccolithus streckerii*	*Cyclolithella annula*	*Discolithina japonica*	*Discolithina* spp.	*Discosphaera tubifera*	*Emiliania huxleyi*	*Gephyrocapsa oceanica*	*Gephyrocapsa parallela*	*Gephyrocapsa* spp. (small)	*Helicosphaera carteri*	*Helicosphaera hyalina*	*Helicosphaera inversa*	*Pseudoemiliania lacunosa*	*Reticulofenestra asanoi*	*Reticulofenestra* spp. (small)	*Rhabdosphaera clavigera*	*Rhabdosphaera stylifera*	*Scapholithus fossilis*	*Syracosphaera pulchra*	*Umbilicosphaera sibogae*	Reworked species: *Reticulofenestra gartneri*	*Cribrocentrum reticulatum*	*Reticulofenestra pseudoumbilicus*	*Isthmolithus recurvus*	*Reticulofenestra umbilicus*	*Cretarhabdulus* spp.	*Prediscosphaella cretacea* (s.l.)	*Watznaueria barnesae*
303-U1303A-																																	
1H-CC	0~0.25	A	G	R	F	R	R	R			A	F	F	A	R					R				R	R								
2H-CC	0~0.25	R	M	R	R						F	R		C	R					R													r
3H-CC	0~0.25	A	M	R	C	R	R				F	C	C	A	R					R				R	R								
4H-CC	0~0.25	A	G	R	A	R		R			R	F	R	A	F					R	R	R	R	R	R								r
5H-CC	0.16~0.25	A	M	R	C	R				R	R	F	R	A	F		R			R				R	R								
6H-CC	0.41~0.85	R	P	+	+		+				?	+		R	+			R		R											r		r
7H-CC	0.41~0.85	A	G	R	F	+	+		R			R	+	A	R			C		A	+				+									
8H-CC	0.41~0.85	A	G	R	C	+			+			R	+	A	R	+		C		R					R									
9H-CC	0.41~0.85	F	M		R				+			+	+	F	R			C		R				+	+	r								
10H-CC	0.85~0.95	F	M		+				+			R	+	F	+			F	+	F						r	r	r	r	r		r	r

Notes: Abundance: A = abundant, C = common, F = few, R = rare, + = present, r = reworked. Preservation: G = good, M = moderate, P = poor.

Table T8. Distribution of calcareous nannofossils, Hole U1303B.

Core, section	Age (Ma)	Abundance	Preservation	*Calcidiscus leptoporus*	*Coccolithus pelagicus*	*Coccolithus streckerii*	*Cyclolithella annula*	*Discolithina japonica*	*Discolithina* spp.	*Emiliania huxleyi*	*Gephyrocapsa caribbeanica*	*Gephyrocapsa oceanica*	*Gephyrocapsa parallela*	*Gephyrocapsa* spp. (large)	*Gephyrocapsa* spp. (small)	*Helicosphaera carteri*	*Helicosphaera hyalina*	*Helicosphaera inversa*	*Helicosphaera* cf. *wallichii*	*Pseudoemiliania lacunosa*	*Reticulofenestra* spp. (small)	*Rhabdosphaera clavigera*	*Rhabdosphaera stylifera*	*Scapholithus fossilis*	*Syracosphaera pulchra*	*Umbilicosphaera sibogae*	Reworked species: *Reticulofenestra gartneri*	Reworked species: *Reticulofenestra pseudoumbilicus*	Reworked species: *Watznaueria barnesae*
303-1303B-																													
1H-CC	0~0.25	C	M	R	F		+	+	R	R	+	F	R		C	F			+		R	+			R	+	r		r
2H-CC	0~0.25	A	G	R	C	R	+			C		C	F		A	C					F	+			R	R			
3H-CC	0~0.25	A	G		C	R		+	+	C		C	F		A	C					R	R			R	R			
4H-CC	0~0.25	A	G	R	C	+		+	R	C		C	F		A	F					R	F	+	+	R	R			
5H-CC	0~0.25	A	G	R	C	R		+	+	F	+	R	F		C	R					R	R	+		R	R			
6H-CC	0.16~0.25	A	G	R	F	+				R		R	R		A	R		+			R				R	R			
7H-CC	0.16~0.25?	A	M	R	R	R				?		R			A	R		+			C				R	R		r	r
8H-CC	0.25/0.41	A	G	F	F			R		+		F	R		A	C				F	F				R	R			
9H-CC	0.41~0.85	A	G	F	F	R		R	R			F	R		A	R	R			C					R	R			

Notes: Abundance: A = abundant, C = common, F = few, R = rare, + = present, r = reworked. Preservation: G = good, M = moderate.

Table T9. Distribution of planktonic foraminifers, Hole U1302A.

Core	Overall abundance	Preservation	*Globigerina bulloides*	*Globigerina decorata*	*Globigerina decoraperta*	*Globigerina falconensis*	*Globigerinella calida*	*Globigerinella siphonifera*	*Globigerinita glutinata*	*Globigerinita uvula*	*Globigerinoides conglobatus*	*Globigerinoides ruber*	*Globigerinoides extremus*	*Globigerinoides triloba*	*Globorotalia crassaformis*	*Globorotalia hirsuta*	*Globorotalia inflata*	*Globorotalia scitula*	*Globorotalia truncatulinoides*	*Globorotalia tumida*	*Neogloboquadrina dutertrei*	*Neogloboquadrina incompta*	*Neogloboquadrina pachyderma* (d)	*Neogloboquadrina pachyderma* (s)	*Orbulina universa*	*Pulleniatina obliquiloculata*	*Tenuitella iota*	*Turborotalita quinqueloba* (d)	*Turborotalita quinqueloba* (s)	Biozone
303-U1302A-																														
1H	R	VG	R									R					R						F	D				R	R	
2H	R	VG	A					R	R			R										R		D				F	R	
3H	A	G	R														R					P	R	D				P	P	
4H	C	G	R																P				R	D					R	
5H	C	G	A													P					P		F	D				R	R	
6H	C	VG	D					P	P			P					R	P			P		F	A						
7H	A	G	D					R	R			P				R	F		P		P		A	D				P	R	*N. pachyderma* (s)
8H	A	G	A									R					P						F	D				P	R	
9H	R	M	R																				R	D				R		
10H	A	G	A					P				R				P	R						R	D					F	
11H	A	M	A					P	R								R						R	D				R	R	
12H	C	M	F					P	R			R					R		R				F	D	P			P		
13H	A	M	A						R			P					F						F	D				R		

Notes: Abundance: D = dominant, A = abundant, F = few, C = common, R = rare, P = present. Preservation: VG = very good, G = good, M = moderate (see **"Foraminifers"** in the "Site U1302–U1308 methods" chapter). d = dextral, s = sinistral.

Table T10. Distribution of planktonic foraminifers, Hole U1302B.

Core	Overall abundance	Preservation	*Globigerina bulloides*	*Globigerina decorata*	*Globigerina decoraperta*	*Globigerina falconensis*	*Globigerinella calida*	*Globigerinella siphonifera*	*Globigerinita glutinata*	*Globigerinita uvula*	*Globigerinoides conglobatus*	*Globigerinoides ruber*	*Globigerinoides extremus*	*Globigerinoides triloba*	*Globorotalia crassaformis*	*Globorotalia hirsuta*	*Globorotalia inflata*	*Globorotalia scitula*	*Globorotalia truncatulinoides*	*Globorotalia tumida*	*Neogloboquadrina dutertrei*	*Neogloboquadrina incompta*	*Neogloboquadrina pachyderma* (d)	*Neogloboquadrina pachyderma* (s)	*Orbulina universa*	*Pulleniatina obliquiloculata*	*Tenuitella iota*	*Turborotalita quinqueloba* (d)	*Turborotalita quinqueloba* (s)	Biozone
303-U1302B-																														
1H	A	G	D				P	P	P		P	P			P		F		R	P	R	R	F	A	P					
2H	A	M	F														P						R	D						
3H	A	M	R														F		P				F	D						
4H	A	G	F															P					F	D				F	R	
5H	A	P	P														R						F	D				F	R	
6H	C	G	R																				P	D				R	R	*N. pachyderma* (s)
7H	C	M	F						P								R						R	D				R	P	
8H	C	G	R																				R	D					R	
9H	C	G	F														R						F	D				P	R	
10H	C	G	D														A	P					F	A	R				R	
11H	C	G	R														P		P				P	D					R	

Notes: Abundance: D = dominant, A = abundant, C = common, F = few, R = rare, P = present. Preservation: G = good, M = moderate, P= poor (see **"Foraminifers"** in the "Site U1302–U1308 methods" chapter). d = dextral, s = sinistral.

Table T11. Distribution of planktonic foraminifers, Hole U1302C.

Core	Overall abundance	Preservation	*Globigerina bulloides*	*Globigerina decorata*	*Globigerina decoraperta*	*Globigerina falconensis*	*Globigerinella calida*	*Globigerinella siphonifera*	*Globigerinita glutinata*	*Globigerinita uvula*	*Globigerinoides conglobatus*	*Globigerinoides ruber*	*Globigerinoides extremus*	*Globigerinoides triloba*	*Globorotalia crassaformis*	*Globorotalia hirsuta*	*Globorotalia inflata*	*Globorotalia scitula*	*Globorotalia truncatulinoides*	*Globorotalia tumida*	*Neogloboquadrina dutertrei*	*Neogloboquadrina incompta*	*Neogloboquadrina pachyderma* (d)	*Neogloboquadrina pachyderma* (s)	*Orbulina universa*	*Pulleniatina obliquiloculata*	*Tenuitella iota*	*Turborotalita quinqueloba* (d)	*Turborotalita quinqueloba* (s)	Biozone
303-U1302C-																														
1H	A	G	D						P								R						P	F						
2H	C	G	F														R						R	D					P	
3H	A	G	F														R						F	D					P	
4H	A	G																												
5H	R	G	R														R						R	R						
6H	A	G	D		R		P		R			P					A				R		F	F					A	*N. pachyderma* (s)
7H	R	G	A	P			P		F						P		P						F	A				A	A	
8H	A	VG	A		R	P			R		R	R		P			D						A	A				R	R	
9H	A	G	R						P								D						R	A	P			R	R	
10H	A	G	A	P								P	P		P		D		P				R	D		P			P	
11H	A	G	A		P				R								A				P		A	D				R		

Notes: Abundance: D = dominant, A = abundant, C = common, F = few, R = rare, P = present. Preservation: VG = very good, G = good (see **"Foraminifers"** in the "Site U1302–U1308 methods" chapter). d = dextral, s = sinistral.

Table T12. Distribution of planktonic foraminifers, Hole U1303A.

Core	Overall abundance	Preservation	*Globigerina bulloides*	*Globigerina decorata*	*Globigerina decoraperta*	*Globigerina falconensis*	*Globigerinella calida*	*Globigerinella siphonifera*	*Globigerinita glutinata*	*Globigerinita uvula*	*Globigerinoides conglobatus*	*Globigerinoides ruber*	*Globigerinoides extremus*	*Globigerinoides triloba*	*Globorotalia crassaformis*	*Globorotalia hirsuta*	*Globorotalia inflata*	*Globorotalia scitula*	*Globorotalia truncatulinoides*	*Globorotalia tumida*	*Neogloboquadrina dutertrei*	*Neogloboquadrina incompta*	*Neogloboquadrina pachyderma* (d)	*Neogloboquadrina pachyderma* (s)	*Orbulina universa*	*Pulleniatina obliquiloculata*	*Tenuitella iota*	*Turborotalita quinqueloba* (d)	*Turborotalita quinqueloba* (s)	Biozone
303-U1303A-																														
1H	C	G	F					P	R			P					R		P				F	D	P			R	R	
2H	C	VG																					P	D						
3H	A	G	F														F						R	D	P			R		*N. pachyderma* (s)
4H	A	G	D					R	P			P					R	P					R	F		P			R	
5H	A	VG			P												R	P						D				R		
6H	B																													
7H	A	G	R						R								R					P	D	A				R	R	
8H	A	G	R						P								A		P				R	D			P	R	P	*N. pachyderma* (s)
9H	R	G	P														A						R	D					P	
10H	C	G	R						R	P					P		A						R	D						

Notes: Abundance: D = dominant, A = abundant, C = common, F = few, R = rare, P = present, B = barren. Preservation: VG = very good, G = good (see "Foraminifers" in the "Site U1302–U1308 methods" chapter). d = dextral, s = sinistral.

Table T13. Distribution of planktonic foraminifers, Hole U1303B.

Core	Overall abundance	Preservation	*Globigerina bulloides*	*Globigerina decorata*	*Globigerina decoraperta*	*Globigerina falconensis*	*Globigerinella calida*	*Globigerinella siphonifera*	*Globigerinita glutinata*	*Globigerinita uvula*	*Globigerinoides conglobatus*	*Globigerinoides ruber*	*Globigerinoides extremus*	*Globigerinoides triloba*	*Globorotalia crassaformis*	*Globorotalia hirsuta*	*Globorotalia inflata*	*Globorotalia scitula*	*Globorotalia truncatulinoides*	*Globorotalia tumida*	*Neogloboquadrina dutertrei*	*Neogloboquadrina incompta*	*Neogloboquadrina pachyderma* (d)	*Neogloboquadrina pachyderma* (s)	*Orbulina universa*	*Pulleniatina obliquiloculata*	*Tenuitella iota*	*Turborotalita quinqueloba* (d)	*Turborotalita quinqueloba* (s)	Biozone
303-U1303B-																														
1H	A	G															F						F	D						
2H	A	G	A						R							P	F						A	D				R	R	
3H	A	G	A						P			P				P	A						A	D						
4H	A	VG	D														R						R	A	P			R	R	
5H	A	G	A														A		P			P	F	D	R			P	P	*N. pachyderma* (s)
6H	A	G	R														F	P					F	D				R	P	
7H	R	M	R																				R	D						
8H	A	G	A														A						F	D				R	R	
9H	A	G	R					P	P								R						A	D	P			R	R	

Notes: Abundance: D = dominant, A = abundant, F = few, R = rare, P = present. Preservation: VG = very good, G = good, M = moderate (see "Foraminifers" in the "Site U1302–U1308 methods" chapter). d = dextral, s = sinistral.

Table T14. Distribution of benthic foraminifers, Holes U1302A, U1302B, U1302C, U1303A, and U1303B.

Core	*Cassidulina crassa*	*Cassidulina minuta*	*Cibicidoides kullenbergi*	*Cibicidoides* sp.	*Cibicidoides wuellerstorfi*	*Eggerelloides bradyi*	*Elphidium* sp.	*Epistominella exigua*	*Fissurina* sp.	Lagenid sp.	*Melonis barleeanum*	Miliolid sp.	*Nonion* sp./*Astrononion* sp.	*Nuttalides* sp.	*Oridorsalis umbonatus*	*Pullenia bulloides*	*Pullenia quinqueloba*	*Pyrgo lucernula*	*Pyrgo murrhyna*	*Pyrgo* sp./*Biloculina* sp.	*Siphotextularia* sp.	*Stainforthia concava*	*Uvigerina peregrina*	*Uvigerina* sp.	*Melonis pompiloides*	*Islandiella* sp.	*Gyroidina* sp.	*Hoeglundina elegans*	*Sphaeroidina bulloides*
303-U1302A-																													
1H						P	P					P						P					P	P					
2H		P																					D	P					
3H					P											P		P						P					
4H		P		P				P		P				P	P	P	P					P	D						
13H									P							P													
303-U1302B-																													
1H								P																P					
2H	P							P		P	P					P						P	D	P					
3H						P							P			P	P												
4H								P			P																		
5H		P						D									P												
6H		P		P	P			P						D					P			P							
303-U1302C-																													
6H								P										P											
7H	P									P																			
8H						P											P	P						P					
9H								P			P					P		P											
10H			P			P																		P					
11H						P		P												P	P								
303-U1303A-																													
2H			P						P			P						P		D			D						
5H																									P				
6H													P	P												P			
7H								P															D		P		P	P	
8H			P					P			P				P														P
9H				P		P						P																	
10H								P																					
303-U1303A-																													
1H													P										P	P	P				
2H												P	P				P	P					P						
3H																							D						

Note: P = present, D = dominant.

Table T15. Distribution of diatoms, Hole U1302A.

Core, section, interval (cm)	Abundance	Preservation	*Actinocyclus* sp.	*Actinocyclus* sp.	*Actinoptychus vulgaris*	*Alveus marinus*	*Azpeitia tabularis*	*Chaetoceros lorenzianus* (setae)	RS *Chaetoceros affinis*	RS *Chaetoceros debilis*	RS *Chaetoceros* sp.	*Coscinodiscus marginatus*	*Coscinodiscus radiatus*	*Dytilum brightwellii*	*Fragilariopsis doliolus*	*Fragilariopsis fossilis*	*Fragilariopsis oceanica*	*Fragilariopsis* sp.	*Lioloma* sp.	*Nitzschia bicapitata*	*Proboscia curvirostris*	*Rhizosolenia bergonii*	*Rhizosolenia hebetata* f. *hiemalis*	*Rhizosolenia hebetata* f. *subacuta*	*Stephanopyxis turris*	*Thalassionema nitzschioides* var. *nitzschioides*	*Thalassiosira gravida*	*Thalassiosira gravida* spore	*Thalassiosira jouseae*	*Thalassiosira oestrupii*	*Thalassiosira oestrupii* var. *venrickae*	*Thalassiosira trifulta*	*Thalassiothrix longissima*
303-U1302A-																																	
1H-CC	T	P																															
2H-CC	C	P	T					T	T	T		T	T						R							T		T					
3H-CC	R	P	T									T																				T	
4H-5, 67	C	M	R											T	T				F				T					T					T
4H-5, 112	B																																
4H-10, 19	B																																
4H-CC	B																																
5H-CC	T	M								T	T																T	T		T		T	
6H-1, 90	B																																
6H-5, 100	C	P	T		T		T			T									F		T					T		T		T	T		T
6H-6, 102	B																																
6H-CC	B																																
7H-1, 120	B																																
7H-2, 120	B																																
7H-3, 125	B																																
7H-4, 105	B																																
7H-5, 7	B																																
7H-5, 128	B																																
7H-CC	T	P				*									*			T			*		T		T		*			T		*
8H-2, 70	C	M	R										T		T				F	T	T	T		T			T		T				
8H-CC	T	M	*	T		*					T				T		*				*		*						T		R	*
9H-4, 70	B																																
9H-5, 14	B																																
9H-6, 91	B																																
9H-7, 48	B																																
9H-CC	B																																
10H-1, 33	B																																
10H-1, 93	B																																
10H-5, 40	B																																
10H-5, 112	B																																
10H-CC	B																																
11H-6, 18	B																																
11H-CC	B																																
12H-3, 25	B																																
12H-4, 3	B																																
12H-CC	B																																
13H-2, 30	B																																
13H-CC	B																																

Notes: Abundance: C = common, F = few, R = rare, T = trace, B = barren. Preservation: M = moderate, P = poor. RS = resting spore.
* = fragment present.

Table T16. Distribution of diatoms and silicoflagellates, Hole U1302B. (Continued on next page.)

Core, section, interval (cm)	Abundance	Preservation	Diatoms																											
			Actinocyclus curvatulus	*Actinoptychus senarius*	*Actinoptychus vulgaris*	*Alveus marinus*	*Azpeitia neocrenulata*	*Azpeitia tabularis*	*Bacterosira fragilis*	RS *Chaetoceros affinis*	RS *Chaetoceros compresus*	RS *Chaetoceros coronatus*	RS *Chaetoceros diadema*	RS *Chaetoceros debilis*	RS *Chaetoceros* sp.	*Chaetoceros setae*	*Cocconeis* sp.	*Coscinodiscus argus*	*Coscinodiscus decrecens*	*Coscinodiscus marginatus*	*Coscinodiscus radiatus*	*Cymbella* sp. (freshwater)	*Fragilariopsis doliolus*	*Fragilariopsis* sp.	*Grammatophora marina*	*Hemidiscus cuneiformis*	*Lioloma* sp.	*Nitzschia bicapitata*	*Nitzschia oceanica*	*Nitzschia interruptestriata*	*Nitzschia* sp.	*Paralia sulcata*
303-U1302B-																														
1H-CC	A	M	R		T	T				T		T		T	T						T		R	T	T		C	T	T	T		
2H-CC	C	M	T							R	T			T	C				T							T						
3H-4, 30	C	M	T																				R	T			T				T	
3H-CC	T	P	T							T													T				T					
4H-6, 30	F	P	R			T			T																		T				T	
4H-CC	F	M	F			T							T		F	T						T	T				T					
5H-3, 70	F	P	T												R					T							R					T
5H-5, 84	T	P																														
5H-CC	A	M	T							T													T				C				T	
6H-5, 10	B																															
6H-CC	B																															
7H-3, 45	B																															
7H-4, 37	C	P	T	T						T																	T					
7H-CC	T	P	T							T										T							T				T	
8H-1, 100	T	P																														
8H-5, 25	R	P	T																				T	T								
8H-5, 80	B																															
8H-5, 103	B																															
8H-CC	F	M	F					T											T	T			T				T					T
9H-6, 34	T	P															T															
9H-CC	A	P	T				T							T	T	T		T		T	T		T	T			T		T		T	
10H-2, 100	B																															
10H-CC	B																															
11H-1, 120	B																															
11H-6, 49	B																															
10H-CC	B																															

Notes: Abundance: A = abundant, C = common, F = few, R = rare, T = trace, B = barren. Preservation: M = moderate, P = poor. RS = resting spore.

Table T16 (continued).

Core, section, interval (cm)	Abundance	Preservation	Diatoms																										Silicoflagellates	
			Porosira glacialis	*Proboscia alata*	*Proboscia curvirostris*	*Rhaphoneis surirella*	*Rhizosolenia bergonii*	*Rhizosolenia hebetata* f. *hiemalis*	*Rhizosolenia hebetata* f. *semispina*	*Rhizosolenia hebetata* f. *subacuta*	*Roperia tesselata*	*Stephanopyxis grunowii*	*Stephanopyxis turris*	*Thalassionema bacillare*	*Thalassionema nitzschioides* var. *nitzschioides*	*Thalassionema nitzschioides* var. *parva*	*Thalassiosira antiqua*	*Thalassiosira ferelineata*	*Thalassiosira gravida*	*Thalassiosira gravida* spore	*Thalassiosira grunowii*	*Thalassiosira leptopus*	*Thalassiosira lineata*	*Thalassiosira oestrupii*	*Thalassiosira oestrupii* var. *venrickae*	*Thalassiosira trifulta*	*Thalassiosira* spp.	*Thalassiothrix longissima*	*Dyctiocha fibula*	*Actiniscus pentasterias*
303-U1302B-																														
1H-CC	A	M						T						T	T		T		T	T			T	T				T	T
2H-CC	C	M								T				T						T				T					T	
3H-4, 30	C	M	T					T	T									T	T	T				T	T					
3H-CC	T	P						T																						
4H-6, 30	F	P																T		R				T						T
4H-CC	F	M		T				T			T								T	T			T		T					
5H-3, 70	F	P			T																				T					
5H-5, 84	T	P			T																									
5H-CC	A	M			R	T		T		T										R	T			F	T	T				T
6H-5, 10	B																													
6H-CC	B																													
7H-3, 45	B																													
7H-4, 37	C	P			T			T				T								T					T	T				
7H-CC	T	P						T												T				T	T					
8H-1, 100	T	P						T																						
8H-5, 25	R	P			T		T			T										T					T					
8H-5, 80	B																													
8H-5, 103	B																													
8H-CC	F	M						T								T				T					T					
9H-6, 34	T	P			*					T																				
9H-CC	A	P			T		T	R	T				T		T	T					T	T	R		T		T			
10H-2, 100	B																													
10H-CC	B																													
11H-1, 120	B																													
11H-6, 49	B																													
10H-CC	B																													

Table T17. Distribution of diatoms and silicoflagellates, Hole U1302C.

Core, section, interval (cm)	Abundance	Preservation	Diatoms																																										Silicoflagellates	
			Actinocyclus curvatulus Janish	*Actinocyclus octonarius*	*Actinoptychus senarius*	*Actinoptychus vulgaris*	*Alveus marinus*	*Azpeitia neocrenulata*	*Azpeitia tabularis*	*Bacteriastrum hyalinum*	*Bacterosira fragilis*	RS *Chaetoceros affinis*	RS *Chaetoceros diadema*	RS *Chaetoceros debilis*	RS *Chaetoceros* sp.	*Chaetoceros setae*	*Coscinodiscus asteromphalus*	*Coscinodiscus argus*	*Coscinodiscus marginatus*	*Fragilariopsis doliolus*	*Fragilariopsis fossilis*	*Fragilariopsis* sp.	*Hemidiscus cuneiformis*	*Lioloma* sp.	*Fragilariopsis oceanica*	*Nitzschia* sp.	*Paralia sulcata*	*Porosira glacialis*	*Proboscia curvirostris*	*Rhaphoneis surirella*	*Rhizosolenia hebetata* f. *hiemalis*	*Rhizosolenia hebetata* f. *subacuta*	*Roperia tesselata*	*Stephanopyxis grunowii*	*Stephanopyxis turris*	*Thalassionema frauenfeldii*	*Thalassiosira ferelineata*	*Thalassiosira gravida*	*Thalassiosira gravida* spore	*Thalassiosira lineata*	*Thalassiosira oestrupii*	*Thalassiosira oestrupii* var. *venrickae*	*Thalassiosira trifulta*	*Thalassiothrix longissima*	*Dyctiocha fibula*	*Actiniscus pentasterias*
303-U1302C-																																														
1H-CC	T	P																							T																	T		T	T		
2H-CC	B																																														
3H-5, 81	A	M	T						T	T	T	C	T		T	R			T	T			T	F								T	T						T	T		T		T	
3H-6, 3	B																																													
3H-CC	T	P																															T										*		
4H-5, 120	C	P	T	T	T													T		T				R		T					R	T				T		T	T						T	
4H-6, 59	B																																													
4H-CC	T	P					*								T				T						T						T										T			*		
5H-3, 68	C	P	T		T	T	T								T		T			T				T			T				T			T					T			T				
5H-7, 32	C	M	T										T	T	T			F						F					T															R		
5H-CC	B	P																																										*		
6H-6, 56	A	M	T				T															R		C				T	T			T		T			T	T	T		T	T		F		T
6H-CC	T	P																													T				T									T		
7H-1, 75	B																																													
7H-2, 30	B																																													
7H-5, 20	F	P	T	T									T		T					T				F		T	T		T	T							T				T	T				
7H-5, 85	T	P														T								T														T	T		T					T
7H-CC	B																														F															
8H-4, 100	F	M	F						T				T		F						T			T					T									T				T			T	T
8H-CC	C	P	T			T		T							T					T			T	F		T			T		T			T		T	T	T	T		T	T			T	T
9H-1, 148	B																																													
9H-5, 78	B																																													
9H-CC	B																																													
10H-1, 103	B																																													
10H-2, 32	B																																													
10H-8, 2	B																																													
10H-CC	B																																													
11H-CC	B																																													

Notes: Abundance: A = abundant, C = common, F = few, R = rare, T = trace, B = barren. Preservation: M = moderate, P = poor. * = fragment present. RS = resting spore.

Table T18. Distribution of diatoms, Hole U1302D.

Core, section	Abundance	Preservation	*Actinocyclus curvatulus Janish*	RS *Chaetoceros compresus*	RS *Chaetoceros* sp.	*Chaetoceros setae*	*Coscinodiscus radiatus*	*Lioloma* sp.	*Nitzschia* sp.	*Rhizosolenia hebetata* f. *hiemalis*	*Roperia tesselata*	*Stephanopyxis grunowii*	*Thalassionema nitzschioides* var. *inflata*	*Thalassionema nitzschioides* var. *parva*	*Thalassiosira convexa* var. *convexa*	*Thalassiosira ferelineata*	*Thalassiosira leptopus*	*Thalassiosira oestrupii* var. *oestrupii*	*Thalassiosira oestrupii* var. *venrickae*
303-U1302D-																			
1H-CC	T	P						T		T									
2H-CC	A	M	T	T	R	T	T	A	T	T	T	T	T	T	T	T	T	F	F

Notes: Abundance: A = abundant, F = few, R = rare, T = trace. Preservation: M = moderate, P = poor. RS = resting spore.

Table T19. Distribution of diatoms and silicoflagellates, Hole U1302E.

			Diatoms																									Silicoflagellates
Core, section	Abundance	Preservation	*Actinocyclus curvatulus*	*Actinoptychus vulgaris*	*Alveus marinus*	*Azpeitia nodulifera*	*Bacterosira fragilis*	*Chaetoceros bacteriastroides*	RS *Chaetoceros affinis*	RS *Chaetoceros cinctus*	RS *Chaetoceros compresus*	RS *Chaetoceros constrictus*	RS *Chaetoceros* aff. *debilis*	RS *Chaetoceros* sp.	*Fragilariopsis doliolus*	*Fragilariopsis reinholdii*	*Fragilariopsis* sp.	*Lioloma* sp.	*Nitzschia interruptestriata*	*Nitzschia* sp.	*Paralia sulcata*	*Rhizosolenia bergonii*	*Rhizosolenia hebetata* f. *hiemalis*	*Roperia tesselata*	*Thalassionema nitzschioides* var. *parva*	*Thalassiosira antiqua*	*Thalassiosira convexa* var. *convexa*	*Thalassiosira eccentrica*	*Thalassiosira oestrupii* var. *venrickae*	*Thalassiosira trifulta*	*Dyctiocha fibula*
303-U1302E-																															
1H-CC	R	P								T	T			T													T		T		
2H-CC	C	M	T	T	T	T	T	T	T			T	T	R	T	T	R	C	T	T	T	T	T	T	T	T	T	T	T	T	T

Notes: Abundance: C = common, R = rare, T = trace. Preservation: M = moderate, P = poor. RS = resting spore.

Table T20. Distribution of diatoms and silicoflagellates, Hole U1303A. (Continued on next page.)

Core, section, interval (cm)	Abundance	Preservation	Diatoms																																
			Actinocyclus curvatulus	*Alveus marinus*	*Asteromphalus imbricatus*	*Azpeitia africana*	*Azpeitia barronii*	*Azpeitia neocrenulata*	*Azpeitia nodulifera*	*Azpeitia tabularis*	*Bacterosira fragilis*	*Chaetoceros bacteriastroides* (one-celled)	RS *Chaetoceros compresus*	RS *Chaetoceros constrictus*	RS *Chaetoceros coronatus*	RS *Chaetoceros diadema*	RS *Chaetoceros debilis*	RS *Chaetoceros* sp.	*Chaetoceros setae*	*Coscinodiscus asteromphalus*	*Coscinodiscus marginatus*	*Coscinodiscus radiatus*	*Diploneis constricta* var. *papula*	*Fragilariopsis doliolus*	*Fragilariopsis oceanica*	*Fragilariopsis reinholdii*	*Fragilariopsis* sp.	*Hemidiscus cuneiformis*	*Lioloma* sp.	*Nitzschia bicapitata*	*Nitzschia interruptestriata*	*Nitzschia* sp.
303-U1303A-																																			
1H-3, 63	B																																		
1H-3, 63	F	M	T															R									T		T						
1H-CC	T	P	T															T												T					
2H-5, 4	B																																		
2H-5, 19	F	M	T													T		T	T												T				
2H-6, 51	B																																		
2H-CC	B																																		
3H-1, 75	T	P																											T						
3H-5, 50	C		T		T							T	T					T						T			T		F					T	
3H-CC	T	M	T	*														*						T	T						*				
4H-2, 50	R	P								T																									
3H-CC	R	M																*				*			T										
5H-4, 124	A	M	T						T	T		T					T	T					T				T		C					T	
5H-5, 10	R	P																		T															
5H-CC	T	P	*																		*														
6H-2, 5	B																																		
6H-5, 80	A	M	F							T						T	T	F									T		C						
6H-7, 127	B																																		
6H-CC	B																																		
7H-CC	C	M	T			T												T	T			T		F					F						
8H-3, 140	C	M																R			T			T		T	T	T	F						
8H-5, 30	A	M	C				T									T		F	T	T				T		T	T	T	F						
8H-CC	A	M	R					T	*	T	T		T	T	T	T	T	F	T					R	R	T	T		C		T	T			
9H-CC	B																																		
10H-CC	B																																		

Notes: Abundance: A = abundant, C = common, F = few, R = rare, T = trace, B = barren. Preservation: M = moderate, P = poor. RS = resting spore. * = fragment present.

Table T20 (continued).

Core, section, interval (cm)	Abundance	Preservation	Diatoms																								Silicoflagellates		
			Paralia sulcata	*Porosira glacialis*	*Proboscia curvirostris*	*Rhizosolenia bergonii*	*Rhizosolenia hebetata* f. *hiemalis*	*Rhizosolenia hebetata* f. *subacuta*	*Roperia tesselata*	*Stephanopyxis grunowii*	*Stephanopyxis turris*	*Thalassionema frauenfildii*	*Thalassionema nitzschioides* var. *nitzschioides*	*Thalassionema nitzschioides* var. *inflata*	*Thalassionema nitzschioides* var. *parva*	*Thalassiosira convexa* var. *aspinosa*	*Thalassiosira ferelineata*	*Thalassiosira gravida*	*Thalassiosira gravida* spore	*Thalassiosira jouseae*	*Thalassiosira leptopus*	*Thalassiosira lineata*	*Thalassiosira oestrupii var. oestrupii*	*Thalassiosira oestrupii* var. *venrickae*	*Thalassiosira trifulta*	*Thalassiosira* spp.	*Thalassiothrix longissima*	*Dyctiocha fibula*	*Distephanus speculum*	*Actiniscus pentasterias*
303-U1303A-																													
1H-3, 63	B																												
1H-3, 63	F	M						T	T					T			T	T					T						
1H-CC	T	P																							T	*			
2H-5, 4	B																												
2H-5, 19	F	M					T										T	T			T	T	T						
2H-6, 51	B																												
2H-CC	B																												
3H-1, 75	T	P	T																										
3H-5, 50	C						T									T	T				T	T			T			
3H-CC	T	M					*										*			*	*	*		*	*			
4H-2, 50	R	P					T			T							T					T						
3H-CC	R	M															T							T	T			
5H-4, 124	A	M			T					T							T	R				T		T	T	T		
5H-5, 10	R	P					T																						
5H-CC	T	P			T		T					*														*			
6H-2, 5	B																												
6H-5, 80	A	M			T	T				T								T				R	T						
6H-7, 127	B																												
6H-CC	B																												
7H-CC	C	M			T			T			T						T	T			T		T						
8H-3, 140	C	M			R		T	T									T	T	T				T						
8H-5, 30	A	M			T			T									T		T								T	T	T
8H-CC	A	M		T	T	T	T	T					T	T	T				T			R				*	T	R	T
9H-CC	B																												
10H-CC	B																												

Table T21. Distribution of diatoms and silicoflagellates, Hole U1303B. (Continued on next page.)

Core, section, interval (cm)	Abundance	Preservation	Diatoms																													
			Actinocyclus curvatulus	*Actinocyclus* sp.	*Actinoptychus vulgaris*	*Alveus marinus*	*Azpeitia barronii*	*Azpeitia neocrenulata*	*Azpeitia nodulifera*	*Azpeitia tabularis*	*Bacterosira fragilis*	*Chaetoceros bacteriastroides*	RS *Chaetoceros affinis*	RS *Chaetoceros constrictus*	RS *Chaetoceros diadema*	RS *Chaetoceros debilis*	RS *Chaetoceros* sp.	*Chaetoceros setae*	*Cocconeis costata*	*Coscinodiscus asteromphalus*	*Coscinodiscus oculus-iridis*	*Coscinodiscus radiatus*	*Ethmodiscus rex*	*Fragilariopsis doliolus*	*Fragilariopsis fossilis*	*Fragilariopsis oceanica*	*Fragilariopsis* sp.	*Lioloma* sp.	*Merosira albicans*	*Navicula distans*	*Nitzschia interruptestriata*	*Nitzschia* sp.
303-U1303B-																																
1H-1, 75	T	P								T							T											T				
1H-2, 40	B																															
1H-3, 38	T	P																										T				
1H-CC	B																															
2H-5, 100	A	M	R			T			T	T		R					F	T						T								
2H-6, 90	A	M	R		T			T	T			T				T	R	T			T			R			T	C			T	
2H-CC	C	P	T	*						T		R		T	T	T	F	T	*					T		*	T	F	*			T
3H-3, 145	B																															
3H-5, 10	T	P	*														T															
3H-5, 142	T																											T		T		
3H-6, 14	T	P																										T				
3H-CC	B																															
4H-2, 30	B																															
4H-2, 120	F	M	T			T				T						T	R						*	T				T				T
4H-CC	R	P	T			T																		T				T				T
5H-2, 52	C	M	R	T							T				T	T								T				F				
5H-2, 65	F	P	T							T		T								T		T					T	F				
5H-2, 90	B																															
5H-2, 128	B																															
5H-CC	R	M	T										T											R				T				
6H-3, 65	T	P	*																									*				
6H-CC	T	P															T							*		*						
7H-2, 70	C	M	T					T			T		T			T	T	T							T		T	C				
7H-3, 90	A	M	R		T					T	T									T				T	T			C				
7H-4, 80	B																															
7H-6, 60	B																															
7H-CC	B																															
8H-1, 10	C	M	F												T		T	T							T							
8H-3, 15	C	M	R															T						R				F				
8H-5, 100	B																															
8H-CC	F	G	T			*				*							T							T		R						
9H-1, 100	F	P	F				T						T		T		T											T				
9H-CC	T	P																														

Notes: Abundance: A = abundant, C = common, F = few, R = rare, T = trace, B = barren. Preservation: G = good, M = moderate, P = poor. RS = resting spore. * = fragment present.

Table T21 (continued).

Core, section, interval (cm)	Abundance	Preservation	Diatoms																												Silicoflagellates		
			Paralia sulcata	*Planktoniella sol*	*Porosira glacialis*	*Proboscia alata*	*Proboscia curvirostris*	*Psammodiscus panduriformis*	*Rhizosolenia bergonii*	*Rhizosolenia hebetata* f. *hiemalis*	*Rhizosolenia hebetata* f. *subacuta*	*Roperia tesselata*	*Stephanopyxis grunowii*	*Stephanopyxis turris*	*Thalassionema frauenfeldii*	*Thalassionema nitzschioides* var. *nitzschioides*	*Thalassionema nitzschioides* var. *inflata*	*Thalassionema nitzschioides* var. *parva*	*Thalassiosira antiqua*	*Thalassiosira bipora*	*Thalassiosira ferelineata*	*Thalassiosira gravida*	*Thalassiosira gravida spore*	*Thalassiosira grunowii*	*Thalassiosira jouseae*	*Thalassiosira leptopus*	*Thalassiosira lineata*	*Thalassiosira oestrupii* var. *oestrupii*	*Thalassiosira oestrupii* var. *venrickae*	*Thalassiosira trifulta*	*Thalassiosira* spp.	*Thalassiothrix longissima*	*Dyctiocha fibula*	*Distephanus speculum*	*Actiniscus pentasterias*
303-U1303B-																																	
1H-1, 75	T	P								T												T											
1H-2, 40	B																																
1H-3, 38	T	P																				T											
1H-CC	B																																
2H-5, 100	A	M				T			T	T		T									T	F				T	T	T		T			T
2H-6, 90	A	M		T					T							T	T	T				T						T	T		R	T	T	
2H-CC	C	P			T				T	*						*		T		*	T		T	*		*	T		T	T	*	T	T		T
3H-3, 145	B																																
3H-5, 10	T	P																				T											
3H-5, 142	T																																
3H-6, 14	T	P																															
3H-CC	B																																
4H-2, 30	B																																
4H-2, 120	F	M								T											T		T					T					T
4H-CC	R	P								T	T										T		T				T	T				T	
5H-2, 52	C	M	T			T			T														T										
5H-2, 65	F	P			T						T		T										R		T			T					
5H-2, 90	B																																
5H-2, 128	B																																
5H-CC	R	M									T					T					T					T	T	T	T			*		T
6H-3, 65	T	P								T																							
6H-CC	T	P					*?		T	*					*							*									*		
7H-2, 70	C	M					R			T	T		T								T		F				T	T	T				T	
7H-3, 90	A	M			T	T	T			T			T	T								T	R		T		T							
7H-4, 80	B																																
7H-6, 60	B																																
7H-CC	B																														*		
8H-1, 10	C	M	T				T	T		T					T	T												T			T	T		
8H-3, 15	C	M	T				T			T	T										T		T			T		T			T	T		T
8H-5, 100	B																																
8H-CC	F	G	*			*	*			*				*								*			T		*			*	*			
9H-1, 100	F	P	T				T			T	T										T		T				T	T					T	T
9H-CC	T	P																															

Table T22. Distribution of radiolarians, Site U1302. (**See table notes.** Continued on next page.)

Core, section	Abundance	Preservation	*Collosphaera* spp.	*Acrosphaera spinosa*	*Actinomma leptodermum*	*Actinomma* spp.	*Druppatractus* spp.	*Hexacontium enthacanthum*	*Hexacontium laevigatum*	*Saturnaris circularis*	*Stylatractus universus*	*Heliodiscus asteriscus*	*Didymocyrtis tetrathalamus*	*Hymeniastrum euclides*	*Stylochlamidium venustum*	*Stylodictya multispina*	*Spongodiscus* spp.	*Octopyle* spp.	*Pylospira octopyle*	*Larcopyle butschlii* group	*Lithelius minor*	*Lithelius nautiloides*	*Pylospira* spp.	*Ceratocyrtis* spp.	*Gondwanaria* sp.	*Peridium* spp.	*Pseudodictyophimus* spp.	*Bathropyramis* spp.	*Cycladophora davisiana davisiana*	*Cycladophora bicornis*	*Dictyophimus* spp.	*Eucecryphalus* spp.	*Eucyrtidium acuminatum*	*Eucyrtidium teucheri*	*Lithocampe punctatum*	*Pterocanium* spp.	*Lamprocyclas maritalis*	*Pterocorys zancleus*	*Theocorythium trachelium*	*Botryostrobus acquilonaris*	*Stichocorys seriata*	Radiolarian zone
303-U1302A-																																								
1H-CC	B																																							
2H-CC	R	P			R	T																							T											?
3H-CC	R	P			R						T																													
4H-CC	B																																							
5H-CC	T	M		T	T						T																	T								T				*C. d. davisiana*
6H-CC	B																																							
7H-CC	C	M	T	R	R			R				R	T	T	R		R		T	T	T	T		T					F							R		T		*C. d. davisiana*
8H-CC	T	P			T	T															T																				?
9H-CC	B																																							
10H-CC	B																																							
11H-CC	B																																							
12H-CC	B																																							
13H-CC	B																																							
303-U1302B-																																								
1H-CC	F	P			R		T	T							R	R		T			R		T				T	T	R	T	T			T			R		R		*C. d. davisiana*
2H-CC	R	P			R							T								T																					?
3H-CC	F	M			R						R				T				R	R	R								R					T							*C. d. davisiana*
4H-CC	B																																							
5H-CC	F	M			R			R			T				R	R	R		R		R	R					R	R	R							T	R				*C. d. davisiana*
6H-CC	T	P			T							T																	T								T				
7H-CC	R	P			R		T	R							R		R										T		R												
8H-CC	C	M			C	T							T		R		F		R		R								A												
9H-CC	A	M			A	R		R	T			R	T	T	R	R	C	R	R		R	T		R	T	T	R	T	A	T		R	R	R	T	T		T	R		*C. d. davisiana*
10H-CC	B																																							
11H-CC	B																																							
303-U1302C-																																								
1H-CC	B																																							
2H-CC	T	P			T					T	T										T																T				?
3H-CC	T	P									T																														
4H-CC	C	M			A	R	T							R	R	R	R		F		F			R					C			R						F			*C. d. davisiana*
5H-CC	B																																							
6H-CC	T	M					T																														T				?
7H-CC	B																																							
8H-CC	A	M			A	F	R	R			R	R	R			R	R	R	R			T								R							R	R		R	R	*C. d. davisiana*
9H-CC	B																																							
10H-CC	B																																							
11H-CC	B																																							
303-U1302D-																																								
1H-CC	B																																							

Table T22 (continued).

Core, section	Abundance	Preservation	*Collosphaera* spp.	*Acrosphaera spinosa*	*Actinomma leptodermum*	*Actinomma* spp.	*Druppatractus* spp.	*Hexacontium enthacanthum*	*Hexacontium laevigatum*	*Saturnaris circularis*	*Stylatractus universus*	*Heliodiscus asteriscus*	*Didymocyrtis tetrathalamus*	*Hymeniastrum euclides*	*Stylochlamidium venustum*	*Stylodictya multispina*	*Spongodiscus* spp.	*Octopyle* spp.	*Pylospira octopyle*	*Larcopyle bütschlii* group	*Lithelius minor*	*Lithelius nautiloides*	*Pylospira* spp.	*Ceratocyrtis* spp.	*Gondwanaria* sp.	*Peridium* spp.	*Pseudodictyophimus* spp.	*Bathropyramis* spp.	*Cycladophora davisiana davisiana*	*Cycladophora bicornis*	*Dictyophimus* spp.	*Eucecryphalus* spp.	*Eucyrtidium acuminatum*	*Eucyrtidium teucheri*	*Lithocampe punctatum*	*Pterocanium* spp.	*Lamprocyclas maritalis*	*Pterocorys zancleus*	*Theocorythium trachelium*	*Botryostrobus acquilonaris*	*Stichocorys seriata*	Radiolarian zone
303-U1302D-																																									
2H-CC	T	M			T		T																					T													*C. d. davisiana*
303-U1302E-																																									
1H-CC	T	M			T						T																	T													*C. d. davisiana*
2H-CC	R	M			R												T																					T				?

Notes: Abundance: A = abundant, C = common, F = few, R = rare, T = trace, B = barren (only in total abundance). Preservation: M = moderate, P = poor.

Table T23. Distribution of radiolarians, Holes U1303A and U1303B.

Core, section	Abundance	Preservation	*Acrosphaera spinosa*	*Actinomma medianum*	*Actinomma leptodermum*	*Actinomma* spp.	*Druppatractus* spp.	*Hexacontium enthacanthum*	*Stylatractus universus*	Other actinommids	*Heliodiscus asteriscus*	*Didymocyrtis tetrathalamus*	*Hymeniastrum euclides*	*Stylochlamidium venustum*	*Stylodictya multispina*	*Spongodiscus* spp.	*Octopyle* spp.	*Larcopyle butschlii* group	*Lithelius minor*	*Lithelius nautiloides*	*Pylospira octopyle*	*Pylospira* spp.	*Ceratocyrtis* spp.	*Lophophaena* spp.	*Pseudodictyophimus* spp.	Other plagoniids	*Cornutella* spp.	*Cycladophora davisiana davisiana*	*Cycladophora bicornis*	*Dictyophimus* spp.	*Eucecryphalus* spp.	*Eucyrtidium acuminatum*	*Eucyrtidium teucheri*	*Litharachnium* spp.	*Carpocanistrum* spp.	*Anthocyrtidium* spp.	*Lamprocyclas maritalis*	*Pterocorys zancleus*	*Theocorythium trachelium*	*Botryostrobus acquilonaris*	*Stichocorys seriata*	Radiolarian zone
303-U1303A-																																									
1H-CC	T	P									T																												T		?
2H-CC	B																																								
3H-CC	R	P			R		T	T						R	T	R			T		T				T		R					T						R		*C. d. davisiana*
4H-CC	T	P			T		T		T								T				T																				?
5H-CC	F	P			R		R	R						R	T	T					T		T				R									T				T	*C. d. davisiana*
6H-CC	B																																								
7H-CC	A	M	R		A	R	R			F		R	F	R	R	F		F	A		F	F	R			R		A	T	R	R			R		T	R		R	*C. d. davisiana*
8H-CC	F	M			R					R				R		R	R	R	R		R	R						R								T	R			R	
9H-CC	B																																								
10H-CC	B																																								
303-U1303B-																																									
1H-CC	B																																								
2H-CC	T	P			T					T																											T				?
3H-CC	T	P			T				T	T																															
4H-CC	T	P			T		T			T							T				T							T													*C. d. davisiana*
5H-CC	T	P			T														T									T													*C. d. davisiana*
6H-CC	F	M	T		R		T		T	T	T					T																					T				?
7H-CC	B																																								
8H-CC	A	G	R	R	A		R			R			R	A	R	R		R	C	R	C	C	T	F	C	R	R	A	R			R	R		R	T		R	R	*C. d. davisiana*
9H-CC	A	G			A		R	R		F	R	R	R	C	F	C	F		C		F	C			R			A								R	R	R			

Notes: Abundance: A = abundant, C = common, F = few, R = rare, T = trace, B = barren (only in total abundance). Preservation: G = good, M = moderate, P = poor.

Table T24. Distribution of palynomorphs, Hole U1302A.

	Marine			Terrestrial				Reworked					Dinocyst assemblages											
Core	Preservation	Dinocysts	Foraminifer organic linings	Preservation	Pollen	Spores of Pteridophytes	Spores of *Sphagnum*	Acritarchs	Dinocysts	Angiosperm pollen	Bisaccate pollen	Trilete spores	*Brigantedinium* spp.	*Brigantedinium simplex*	*Impagidinium patulum*	*Impagidinium sphaericum*	*Impagidinium aculeatum*	*Impagidinium paradoxum*	*Impagidinium plicatum*	*Bitectatodinium tepikeiense*	*Operculodinium centrocarpum*	*Operculodinium centrocarpum* (short process form)	*Nematosphaeropsis labyrinthus*	*Spiniferites* sp.
303-U1302A-																								
1H	G	XX		G	XX				x	r	x	x	P	o	o									
3H	G	XX		G	XXX	x	x		XX		x	x	P		P	o				o	P	P	o	o
4H	G	x		G	x						x	x			o					P				
6H	G	x	r	G	x	r				x	XX	XX	P											
8H	G	XX	r	G	x	x				r	x	x	P	o			o			P	P			
10H	G	x	r	G	x			x	x	x	x	x	P	P				o		o	P			
12H	G	x	x	G	x				x		x	x	o		P					P	o		P	

Notes: Absolute abundances: XXX = abundant, XX = common, x = few, r = rare. Relative abundance of dinocyst taxa: P = present, o = single occurrence.

Table T25. Distribution of palynomorphs, Hole U1302B.

Core	Marine			Terrestrial					Reworked					Dinocyst assemblages																										
	Preservation	Dinocysts	Foraminifer organic linings	Preservation	Pollen	Spores of Pteridophytes	Spores of *Sphagnum*	*Pediastrum*	Acritarchs	Mesozoic–Paleogene dinocysts	Angiosperm pollen	Bisaccate pollen	Trilete spores	*Brigantedinium* spp.	*Brigantedinium simplex*	*Quinquecuspis concreta*	*Selenopemphix nephroides*	*Impagidinium aculeatum*	*Impagidinium paradoxum*	*Impagidinium patulum*	*Impagidinium plicatum*	*Impagidinium sphaericum*	*Impagidinium pallidum*	*Impagidinium japonicum*	*Bitectatodinium tepikiense*	*Operculodinium centrocarpum*	*Operculodinium centrocarpum* (short process form)	*Operculodinium* cf. *israelianum*	*Nematosphaeropsis labyrinthus*	*Pyxidinopsis reticulata*	*Achomosphaera andalousiense*	*Spiniferites bentorii*	*Spiniferites bulloideus*	*Spiniferites delicatus*	*Spiniferites elongatus*	*Spiniferites hyperhacantus-mirabilis* type	*Spiniferites membranaceus*	*Spiniferites ramosus*	*Spiniferites* sp.	*Lingulodinium machaerophorum*
303-U1302B-																																								
1H	G	XX	x	G	XX				r	x	r	x	x	XX	F					F					XXX	F			F											
2H	G	XX	x	G	XX						r	r	r	P	P					P	o	o			o	o			o										o	
3H	G	x	r	G	x	r				x	r	x	x		o			o		P		P			P		o				o	P						o		
4H	G	XX		G	x	x		r							P				o				o		o	P			P							P			o	
5H	G	XXX	x	G	XX	x						x	x	XX	XX	x	x			x			r		x				XXX											r
6H	G	XX		G	XX	r			r	r		x	x	XXX	XX	r				x					r	x			r				r						r	r
7H	G	x	r	G	XX		r				x	XX	x	P	P					o		o			o	o	P	o												
8H	G	XXX	x	G	XX	r						x	x	XXX	x		x			r					x	r	r	r								r				
9H	G	XX	XX	G	XX	x						r		XXX	x	r		r		r		x				r			r							XX				
10H	G	XX	x	G	x	r				x	r	r						o				o	o		P	P	o			o	o			o		o			P	
11H	G	x	x	G	XX	x			r		r	x	x							P				o											o	P	o		P	

Notes: Absolute abundances: XXX = abundant, XX = common, x = few, r = rare. Relative abundance of dinocyst taxa: XXX = dominant, XX = common, x = few, r = rare, P = present, o = single occurrence.

Table T26. Distribution of palynomorphs, Hole U1303A.

	Marine				Terrestrial			Reworked					Dinocyst assemblages																				
Core	Preservation	Dinocysts	Foraminifers organic linings	Prasinophytes	Preservation	Pollen	Spores of Pteridophytes	Acritarchs	Mesozoic–Paleogene dinocysts	Angiosperm pollen	Bisaccate pollen	Trilete spores	*Brigantedinium* spp.	*Brigantedinium simplex*	*Brigantedinium cariacoense*	*Selenopemphix nephroides*	*Impagidinium aculeatum*	*Impagidinium paradoxum*	*Impagidinium patulum*	*Impagidinium sphaericum*	*Impagidinium pallidum*	*Impagidinium japonicum*	*Bitectatodinium tepikiense*	*Operculodinium centrocarpum*	*Operculodinium centrocarpum* (short process form)	*Operculodinium janduchenei*	*Nematosphaeropsis labyrinthus*	*Spiniferites ramosus*	*Spinirites* cf. *granosus*	*Lingulodinium machaerophorum*	*Filisphaera filifera*	*Cymatiosphaera invaginata*
303-U1303A-																																	
1H	G	XX	x		G	XX					r	r	P	P									P	P	o							
2H	G	x	r		G	x	x				x	r	P	P					o													
3H	G	XX	x		G	XX		r				x	XX	x	r					x	x		XXX	x			x	r				
4H	G	XX	XX		G	XX	XX	r			x	x	P						P	o			P	o		P	o					
5H	M	x	r		G	r					x		P				o	o	o			o							o		P	
6H	G				G	x	x	x	r	x	x	r																				
7H	G	XXX	x		G	XX						r	XXX	XX		x		r		r			x	x								
8H	G	XX	XX	x	G	XX	x				x	x	XXX	XX		r		r	x				x	x			x			r		x
9H	G				G	x			XX		XX	XX																				
10H	G	x			G	XX			x		x	x							o				P									

Notes: Absolute abundances: XXX = abundant, XX = common, x = few, r = rare. Relative abundance of dinocyst taxa: XXX = dominant, XX = common, x = few, r = rare, P = present, o = single occurrence.

Table T27. Shipboard composite and corrected composite depths, Holes U1302A, U1302B, U1302C, U1302D, U1302E, U1303A, and U1303B.

Core	Top depth (mbsf)	Offset (m)	Top depth (mcd)	Top depth (cmcd)
303-U1302A-				
2H	0.10	13.05	13.15	11.64
3H	9.60	13.85	23.45	20.75
4H	19.10	15.83	34.93	30.91
5H	28.60	15.83	44.43	
6H	38.10	18.32	56.42	49.93
7H	47.60	21.92	69.52	61.52
8H	57.10	21.10	78.20	69.20
9H	66.60	21.71	88.31	78.15
10H	76.10	23.68	99.78	88.30
11H	85.60	23.68	109.28	96.71
12H	95.10	23.68	118.78	105.12
13H	104.60	23.68	128.28	113.52
303-U1302B-				
1H	0.00	8.90	8.90	7.88
2H	9.70	9.44	19.14	16.94
3H	19.20	10.55	29.75	26.33
4H	28.70	11.77	40.47	35.81
5H	38.20	14.48	52.68	46.62
6H	47.70	14.14	61.84	54.73
7H	57.20	14.73	71.93	63.65
8H	66.70	16.79	83.49	73.88
9H	76.20	18.08	94.28	83.43
10H	85.70	17.99	103.69	91.76
11H	95.20	17.53	112.73	99.76
303-U1302C-				
1H	0.00	4.02	4.02	3.56
2H	9.50	4.06	13.56	12.00
3H	19.00	4.24	23.24	20.52
4H	28.50	5.72	34.22	30.24
5H	38.00	7.50	45.50	40.53
6H	47.50	7.45	54.95	48.58
7H	57.00	10.29	67.29	59.50
8H	66.50	11.35	77.85	68.85
9H	76.00	12.89	88.89	78.83
10H	85.50	15.47	100.97	89.52
11H	95.00	16.02	111.02	98.42
303-U1302D-				
1H	0.00	0.00	0.00	0.00
2H	3.50	6.34	9.84	8.71
303-U1302E-				
1H	0.00	0.11	0.11	0.1
2H	5.60	4.21	9.81	8.68
303-U1303A-				
1H	0.00	7.46	7.46	6.6
2H	8.40	7.81	16.21	14.35
3H	17.90	10.53	28.43	25.16
4H	27.40	11.44	38.84	34.37
5H	36.90	11.13	48.03	42.50
6H	46.40	11.49	57.89	51.23
7H	55.90	11.51	67.41	59.65
8H	65.40	9.32	74.72	66.12
9H	74.90	6.94	81.84	72.42
10H	84.40	6.73	91.13	80.65
303-U1303B-				
1H	0.00	0.82	0.82	0.73
2H	9.70	1.16	10.86	9.61
3H	19.20	1.59	20.79	18.40
4H	28.70	1.90	30.60	27.08
5H	38.20	1.24	39.44	34.90
6H	47.70	3.83	51.53	45.60
7H	57.20	3.14	60.34	53.40
8H	66.70	3.90	70.60	62.48
9H	76.20	6.22	82.42	72.94

Table T28. Sampling composite and corrected composite depths, Holes U1302A, U1302B, U1302C, U1302D, U1302E, U1303A, and U1303B.

Core	Top depth (mbsf)	Offset (m)	Top depth (mcd)	Top depth (cmcd)
303-U1302A-				
2H	0.1	13.05	13.15	12.26
3H	9.6	13.85	23.45	21.85
4H	19.1	14.23	33.33	31.06
6H	38.1	13.85	51.95	48.42
7H	47.6	17.46	65.06	60.63
8H	57.1	16.65	73.75	68.73
9H	66.6	16.99	83.59	77.90
10H	76.1	19.15	95.25	88.77
11H	85.6	19.15	104.75	97.62
12H	95.1	19.15	114.25	106.48
13H	104.6	19.15	123.75	115.33
303-U1302B-				
1H	0	8.9	8.9	8.29
2H	9.7	9.44	19.14	17.84
3H	19.2	8.89	28.09	26.18
4H	28.7	10.12	38.82	36.18
5H	38.2	9.96	48.16	44.88
6H	47.7	9.7	57.4	53.49
7H	57.2	10.28	67.48	62.89
8H	66.7	12.35	79.05	73.67
9H	76.2	13.47	89.67	83.57
10H	85.7	13.38	99.08	92.34
11H	95.2	12.82	108.02	100.67
303-U1302C-				
1H	0	4.02	4.02	3.75
2H	9.5	4.06	13.56	12.64
3H	19	4.19	23.19	21.61
4H	28.5	4.15	32.65	30.43
5H	38	6.19	44.19	41.18
6H	47.5	5.92	53.42	49.79
7H	57	5.82	62.82	58.55
8H	66.5	6.94	73.44	68.44
9H	76	8.41	84.41	78.67
10H	85.5	11.05	96.55	89.98
11H	95	11.48	106.48	99.24
303-U1302D-				
1H	0	0	0	0
2H	3.5	6.34	9.84	9.17
303-U1302E-				
1H	0	0.11	0.11	0.10
2H	5.6	4.21	9.81	9.14
303-U1303A-				
1H	0	7.46	7.46	6.95
2H	8.4	7.81	16.21	15.11
3H	17.9	8.99	26.89	25.06
4H	27.4	10.16	37.56	35.00
5H	36.9	6.69	43.59	40.62
6H	46.4	6.71	53.11	49.50
7H	55.9	7.47	63.37	59.06
8H	65.4	5.28	70.68	65.87
9H	74.9	2.95	77.85	72.55
10H	84.4	2.92	87.32	81.38
303-U1303B-				
1H	0	0.82	0.82	0.76
2H	9.7	1.16	10.86	10.12
3H	19.2	1.59	20.79	19.38
4H	28.7	0.29	28.99	27.02
5H	38.2	–0.23	37.97	35.39
6H	47.7	–0.66	47.04	43.84
7H	57.2	–1.39	55.81	52.01
8H	66.7	–0.95	65.75	61.28
9H	76.2	1.15	77.35	72.09

Table T29. Shipboard splice tie points, Sites U1302 and U1303.

Hole, core, section, interval (cm)	Depth (mbsf)	Depth (mcd)		Hole, core, section, interval (cm)	Depth (mbsf)	Depth (mcd)
303-				303-		
U1302D-1H-2, 142.50	2.92	2.92	Tie to	U1303B-1H-2, 60.00	2.10	2.92
U1303B-1H-5, 117.50	7.18	8.01	Tie to	U1302C-1H-3, 97.50	3.98	8.00
U1302C-1H-5, 122.50	7.23	11.25	Tie to	U1302B-1H-2, 85.00	2.35	11.25
U1302B-1H-5, 120.00	7.20	16.10	Tie to	U1302C-2H-2, 103.50	12.04	16.10
U1302C-2H-6, 67.50	17.68	21.74	Tie to	U1302B-2H-2, 110.00	12.30	21.74
U1302B-2H-5, 5.00	15.75	25.19	Tie to	U1302C-3H-2, 45.00	20.95	25.19
U1302C-3H-5, 1.10	26.11	30.35	Tie to	U1302B-3H-1, 0.60	19.80	30.35
U1302B-3H-5, 40.00	25.60	36.15	Tie to	U1302A-4H-1, 121.80	20.32	36.15
U1302A-4H-5, 102.50	26.12	41.96	Tie to	U1302B-4H-1, 147.80	30.19	41.96
U1302B-4H-5, 75.00	35.45	47.22	Tie to	U1302C-5H-1, 136.00	39.37	47.22
U1302C-5H-5, 150.00	45.50	53.35	Tie to	U1302B-5H-1, 65.50	38.87	53.35
U1302B-5H-5, 45.00	44.65	59.13	Tie to	U1302A-6H-2, 119.00	40.81	59.13
U1302A-6H-6, 115.00	46.75	65.07	Tie to	U1302B-6H-3, 22.00	50.93	65.07
U1302B-6H-5, 65.00	54.35	68.49	Tie to	U1302C-7H-1, 120.00	58.20	68.49
U1302C-7H-6, 140.00	65.90	76.19	Tie to	U1302B-7H-3, 124.00	61.46	76.19
U1302B-7H-5, 115.00	64.35	79.08	Tie to	U1302C-8H-1, 122.50	67.73	79.08
U1302C-8H-6, 12.50	74.13	85.48	Tie to	U1302B-8H-2, 48.50	68.69	85.48
U1302B-8H-5, 140.00	74.10	90.89	Tie to	U1302C-9H-2, 50.00	78.00	90.89
U1302C-9H-5, 67.50	82.68	95.57	Tie to	U1302B-9H-1, 128.50	77.49	95.57
U1302B-9H-5, 25.00	82.45	100.53	Tie to	U1302A-10H-1, 75.00	76.85	100.53
U1302A-10H-7, 75.00	85.35	109.03	Append to	U1302A-11H-1, 0.00	85.60	109.28
U1302A-11H-6, 0.80	93.91	117.59				

Table T30. Sampling splice tie points, Sites U1302 and U1303.

Hole, core, section, interval (cm)	Depth (mbsf)	Depth (mcd)		Hole, core, section, interval (cm)	Depth (mbsf)	Depth (mcd)
303-				303-		
U1302D-1H-2, 0.70	2.21	2.21	Tie to	U1303B-1H-1, 138.00	1.39	2.21
U1303B-1H-6, 87.50	8.38	9.19	Tie to	U1302C-1H-4, 66.70	5.17	9.19
U1302C-1H-6, 130.00	8.80	12.82	Tie to	U1302B-1H-3, 90.50	3.92	12.82
U1302B-1H-5, 120.00	7.20	16.10	Tie to	U1302C-2H-2, 103.50	12.04	16.10
U1302C-2H-6, 92.50	17.93	21.99	Tie to	U1302B-2H-2, 135.00	12.55	21.99
U1302B-2H-5, 5.00	15.75	25.19	Tie to	U1302C-3H-2, 50.00	21.00	25.19
U1302C-3H-5, 82.50	25.83	30.02	Tie to	U1302B-3H-2, 42.00	21.13	30.02
U1302B-3H-6, 110.00	27.80	36.69	Tie to	U1302A-4H-3, 35.20	22.46	36.69
U1302A-4H-5, 95.00	26.05	40.28	Tie to	U1302B-4H-1, 144.00	30.16	40.28
U1302B-4H-5, 0.60	35.33	45.45	Tie to	U1303A-5H-2, 0.40	38.76	45.45
U1303A-5H-5, 5.00	42.95	49.64	Tie to	U1303B-6H-2, 110.00	50.30	49.64
U1303B-6H-4, 117.50	53.38	52.71	Tie to	U1302B-5H-4, 5.00	42.75	52.71
U1302B-5H-6, 20.00	45.90	55.86	Tie to	U1302A-6H-3, 89.80	42.02	55.86
U1302A-6H-6, 135.00	46.95	60.80	Tie to	U1302B-6H-3, 40.00	51.10	60.80
U1302B-6H-5, 10.00	53.80	63.50	Tie to	U1302C-7H-1, 67.50	57.68	63.50
U1302C-7H-6, 0.80	65.25	71.07	Tie to	U1302B-7H-3, 0.60	60.79	71.07
U1302B-7H-5, 1.40	64.60	74.88	Tie to	U1302C-8H-1, 1.40	67.94	74.88
U1302C-8H-6, 7.50	74.08	81.02	Tie to	U1302B-8H-2, 45.10	68.67	81.02
U1302B-8H-6, 10.00	74.30	86.65	Tie to	U1302C-9H-2, 73.50	78.24	86.65
U1302C-9H-6, 35.00	83.88	92.29	Tie to	U1302B-9H-2, 111.60	78.83	92.29
U1302B-9H-5, 130.00	83.50	96.97	Tie to	U1302A-10H-2, 20.50	77.82	96.97
U1302A-10H-7, 75.00	85.35	104.50	Append to	U1302A-11H-1, 0.00	85.60	104.75
U1302A-11H-6, 0.80	93.91	113.05	Append to	U1302A-12H-1, 0.00	95.10	114.25
U1302A-12H-5, 130.00	102.40	121.55	Append to	U1302A-13H-1, 0.00	104.60	123.75
U1302A-13H-2, 55.00	106.65	125.80				

Table T31. Headspace hydrocarbon gases, Holes U1302A and U1303A.

Core, section, interval (cm)	Depth (mbsf)	Depth (mcd)*	C_1 (ppmv)
303-U1302A-			
2H-2, 0.0–5.0	1.60	14.65	3.8
3H-2, 0.0–5.0	11.10	24.95	2.6
4H-2, 0.0–5.0	20.60	36.43	3.9
6H-2, 0.0–5.0	39.60	57.92	2.2
7H-2, 0.0–5.0	49.10	71.02	2.2
8H-2, 0.0–5.0	58.60	79.70	2.1
9H-3, 0.0–5.0	69.60	91.31	2.5
10H-2, 0.0–5.0	77.60	101.28	2.4
11H-2, 0.0–5.0	87.10	110.78	2.8
12H-2, 0.0–5.0	96.60	120.28	2.4
303-U1303A-			
1H-2, 0.0–5.0	1.50	8.96	2.4
2H-3, 0.0–5.0	11.40	19.21	2.9
3H-2, 0.0–5.0	19.40	29.93	3.7
4H-2, 0.0–5.0	28.71	40.15	3.1
5H-3, 0.0–5.0	39.90	51.03	3.6
6H-3, 0.0–5.0	49.35	60.84	3.8
7H-2, 0.0–5.0	57.40	68.91	3.8
8H-2, 0.0–5.0	66.90	76.22	3.1
9H-2, 0.0–5.0	76.40	83.34	3.0
10H-2, 0.0–5.0	85.90	92.63	3.3

Note: * refers to the shipboard mcd (see **"Composite section"**).

Table T32. Bulk sedimentary carbon, nitrogen, and hydrogen, Sites U1302 and U1303. (See **table notes.** Continued on next page.)

Core, section, interval (cm)	Depth (mbsf)	Depth (mcd)*	Carbon (wt%) Inorganic	$CaCO_3$	Total	Organic	Nitrogen (wt%)	Organic C/N
303-U1302A-								
2H-1, 129.0–130.0	1.39	14.44	2.99	24.87	3.29	0.30	0.06	5.19
2H-6, 144.5–145.5	9.05	22.10	5.15	42.93	5.80	0.65	0.05	14.49
3H-1, 141.0–142.0	11.01	24.86	1.65	13.71	2.08	0.43	0.06	7.01
3H-5, 5.0–6.0	15.15	29.00	2.87	23.92	3.42	0.55	0.06	9.87
4H-1, 140.0–141.0	20.50	36.33	1.88	15.67	2.13	0.25	0.05	4.78
4H-6, 4.0–5.0	26.64	42.47	4.21	35.06	4.86	0.65	0.03	21.10
6H-1, 143.0–144.0	39.53	57.85	2.83	23.54	3.40	0.57	0.07	8.17
6H-6, 3.0–4.0	45.63	63.95	5.56	46.31	6.37	0.81	0.05	16.05
7H-2, 3.0–4.0	49.13	71.05	1.17	9.71	1.44	0.27	0.05	5.40
7H-5, 128.0–129.0	54.88	76.80	3.76	31.32	4.02	0.26	0.03	9.14
8H-1, 128.0–129.0	58.38	79.48	4.14	34.49	4.79	0.65	0.04	17.70
8H-6, 3.0–4.0	64.63	85.73	3.95	32.94	4.47	0.52	0.05	10.93
9H-2, 68.0–69.0	68.78	90.49	3.73	31.03	4.21	0.48	0.05	9.27
9H-6, 15.0–16.0	74.25	95.96	0.74	6.18	1.39	0.65	0.09	7.37
10H-1, 18.0–19.0	76.28	99.96	4.05	33.71	5.16	1.11	0.06	19.97
10H-5, 123.0–124.0	83.33	107.01	0.16	1.36			0.07	
11H-1, 140.0–141.0	87.00	110.68	1.73	14.38	1.86	0.13	0.03	4.09
11H-6, 10.0–11.0	93.20	116.88	2.54	21.17	3.14	0.60	0.05	12.89
12H-1, 37.0–38.0	95.47	119.15	4.07	33.90	4.16	0.09	0.06	1.61
12H-5, 4.0–5.0	101.14	124.82	2.36	19.68	3.13	0.77	0.04	18.24
13H-1, 148.0–150.0	106.08	129.76	5.54	46.12	6.58	1.04	0.05	22.50
303-U1302B-								
1H-1, 125.0–126.0	1.25	10.15	1.92	15.96	2.26	0.34	0.04	7.95
1H-6, 2.0–3.0	7.52	16.42	2.67	22.25	3.15	0.48	0.06	8.19
2H-1, 146.0–147.0	11.16	20.60	5.50	45.78	6.29	0.79	0.06	12.70
2H-6, 2.0–3.0	17.22	26.66	1.08	9.01	1.77	0.69	0.08	8.37
3H-1, 145.0–146.0	20.65	31.20	1.39	11.59				
3H-6, 3.0–4.0	26.73	37.28	2.60	21.69	3.08	0.48	0.07	7.33
4H-1, 147.0–148.0	30.17	41.94	3.38	28.19	3.74	0.36	0.05	7.36
4H-6, 2.0–3.0	36.22	47.99	2.18	18.15	2.41	0.23	0.05	4.83
5H-1, 8.0–9.0	38.28	52.76	4.63	38.58				
5H-6, 8.0–9.0	45.78	60.26	5.83	48.55	6.87	1.04	0.05	19.77

Table T32 (continued).

Core, section, interval (cm)	Depth (mbsf)	Depth (mcd)*	Carbon (wt%) Inorganic	Carbon (wt%) $CaCO_3$	Carbon (wt%) Total	Carbon (wt%) Organic	Nitrogen (wt%)	Organic C/N
6H-1, 128.0–129.0	48.98	63.12	5.00	41.64				
6H-6, 8.0–9.0	55.28	69.42	0.48	4.00	1.07	0.59	0.09	6.65
7H-1, 123.0–124.0	58.43	73.16	3.76	31.33				
7H-6, 8.0–9.0	64.78	79.51	4.44	37.01				
8H-1, 128.0–129.0	67.98	84.77	3.64	30.28	4.15	0.51	0.06	8.50
8H-6, 8.0–9.0	74.28	91.07	0.96	7.99	1.55	0.59	0.09	6.69
9H-1, 118.0–118.0	77.38	95.46	0.80	6.62	1.15	0.35	0.07	4.94
9H-6, 18.0–19.0	83.91	101.99	0.29	2.46	0.64	0.35	0.08	4.36
10H-1, 119.0–120.0	86.89	104.88	4.00	33.32				
303-U1302C-								
1H-1, 147.0–148.0	1.47	5.49	1.31	10.88	1.54	0.23	0.06	3.98
2H-1, 149.0–150.0	10.99	15.05	3.87	32.22				
2H-6, 1.0–2.0	17.01	21.07	5.10	42.51				
3H-1, 149.0–150.0	20.49	24.73	1.41	11.74				
4H-1, 149.0–150.0	29.99	35.71	3.18	26.50				
4H-6, 1.0–2.0	36.01	41.73	1.86	15.49				
5H-6, 1.0–2.0	45.51	53.36	3.63	30.21				
6H-2, 58.0–59.0	49.58	57.03	2.66	22.19				
6H-6, 8.0–9.0	55.08	62.53	4.52	37.68				
7H-1, 118.0–119.0	58.18	68.47	1.43	11.90				
8H-1, 118.0–119.0	67.68	79.03	4.02	33.47				
8H-6, 8.0–9.0	74.08	85.43	4.52	37.64				
10H-1, 128.0–129.0	86.78	102.25	4.36	36.34				
303-U1302D-								
2H-1, 53.0–54.0	4.03	10.37	1.07	8.89				
303-U1302E-								
1H-1, 118.0–119.0	1.18	1.29	3.97	33.09	4.46	0.49	0.05	9.39
1H-4, 8.0–9.0	4.58	4.69	2.58	21.50				
2H-1, 118.0–119.0	6.78	10.99	2.84	23.65				
303-U1302E-								
2H-3, 8.0–9.0	8.68	12.89	3.31	27.57				
2H-6, 18.0–19.0	13.28	17.49	2.58	21.53				
303-U1303A-								
1H-1, 143.0–144.0	1.43	8.89	1.20	10.03	1.64	0.44	0.09	4.83
1H-6, 0.0–1.0	7.50	14.96	2.94	24.48	3.41	0.47	0.05	10.23
2H-6, 8.0–9.0	15.98	23.79	2.41	20.04	2.51	0.10	0.05	1.90
3H-1, 143.0–144.0	19.33	29.86	2.47	20.61	2.79	0.32	0.05	6.26
3H-6, 1.0–2.0	25.41	35.94	4.71	39.27	5.01	0.30	0.05	6.53
4H-1, 120.0–130.0	28.60	40.04	5.08	42.32	5.57	0.49	0.05	10.21
4H-2, 1.0–2.0	28.72	40.16	5.08	42.28	5.47	0.39	0.05	7.91
5H-1, 147.0–148.0	38.37	49.50	5.07	42.24	5.32	0.25	0.05	4.97
5H-5, 1.0–2.0	42.91	54.04	4.02	33.50	4.47	0.45	0.05	10.04
6H-1, 143.0–144.0	47.83	59.32	3.24	26.96	3.40	0.16		
6H-6, 1.0–2.0	53.86	65.35	5.17	43.11	5.61	0.44	0.04	10.30
7H-1, 118.0–119.0	57.08	68.59	0.44	3.67	0.50	0.06	0.05	1.29
8H-3, 118.0–119.0	69.58	78.90	4.32	35.95	4.88	0.56	0.03	17.80
9H-1, 116.0–117.0	76.06	83.00	4.54	37.80	5.49	0.95	0.03	35.98
10H-2, 18.0–19.0	86.08	92.81	2.20	18.29	2.32	0.12	0.04	2.86
303-U1303B-								
1H-1, 18.0–19.0	0.18	1.00	3.22	26.79	4.01	0.79	0.07	11.36
1H-1, 118.0–119.0	1.18	2.00	2.75	22.94	3.39	0.64	0.04	16.13
2H-1, 118.0–119.0	10.88	12.04	2.06	17.13	2.41	0.35	0.05	6.84
2H-6, 18.0–19.0	17.38	18.54	4.15	34.61	4.73	0.58	0.05	11.30
3H-1, 117.0–118.0	20.37	21.96	4.80	39.96	5.31	0.51	0.04	12.85
3H-6, 18.0–19.0	26.88	28.47	4.08	34.00	4.77	0.69	0.07	10.51
4H-1, 118.0–119.0	29.88	31.78	2.47	20.62	2.75	0.28	0.05	5.75
4H-4, 23.0–24.0	32.93	34.83	3.41	28.38	3.87	0.46	0.05	8.72
5H-2, 18.0–19.0	39.88	41.12	1.41	11.72	2.24	0.83	0.11	7.91
6H-1, 149.0–150.0	49.19	53.02	4.38	36.48	5.06	0.68	0.07	10.59
6H-6, 1.0–2.0	55.21	59.04	5.62	46.82	6.03	0.41	0.05	8.36
7H-1, 149.0–150.0	58.69	61.83	3.87	32.21	4.39	0.52	0.05	10.13
7H-6, 1.0–2.0	64.71	67.85	1.44	11.96	2.00	0.56	0.07	7.56
8H-1, 149.0–150.0	68.19	72.09			2.60		0.05	
8H-6, 1.0–2.0	74.21	78.11	5.53	46.10	5.99	0.46	0.04	11.19
9H-1, 149.0–150.0	77.69	83.91	3.52	29.29	4.12	0.60	0.05	12.15

Note: * refers to the shipboard mcd (see **"Composite sections"**).

Table T33. Interstitial water geochemistry, Holes U1302A, U1303A, and U1303B.

Core, section, interval (cm)	Depth (mbsf)	Depth (mcd)*	Anions (mM) SO_4^{2-}	Anions (mM) Cl^-	pH	Alkalinity (mM)	Salinity (g/kg)	Major cations (mM) Na^+	K^+	Mg^{2+}	Ca^{2+}	Minor and trace constituents (μM) NH_4^+	B	Ba^{2+}	Fe^{2+}	Li^+	Mn^{2+}	H_4SiO_4	Sr^{2+}	Sr/Ca (μM/mM)
303-U1302A-																				
2H-1, 145.0–150.0	1.55	14.60	19.67	560	7.4	8.26	34	480	11.56	50.30	7.53	583	548	0.41	9.8	20.4	19.9	718	80.8	10.73
3H-1, 145.0–150.0	11.05	24.90	16.72	565	7.4	9.08	34	484	11.57	49.48	6.66	718	595	0.47	7.8	19.8	14.8	751	76.2	11.45
4H-1, 145.0–150.0	20.55	36.38	13.90	566	7.5	9.73	34	485	11.38	47.94	6.04	877	542	0.38	3.2	18.6	9.3	772	75.4	12.50
6H-1, 145.0–150.0	39.55	57.87	10.53	565	7.4	9.48	34	483	10.50	46.01	5.38	932	559	0.64	2.8	18.5	6.0	830	72.5	13.46
7H-1, 145.0–150.0	49.05	70.97	9.76	563	7.6	9.44	34	482	10.34	44.93	5.28	915	558	0.74	2.4	19.9	9.2	717	69.1	13.07
8H-1, 145.0–150.0	58.55	79.65	8.55	562	7.4	9.11	34	479	9.57	44.70	5.27	963	499	0.61	3.1	18.3	4.7	880	69.1	13.11
11H-1, 145.0–150.0	87.05	110.73	5.76	558	7.7	8.69	33	468	7.76	44.60	6.24	811	547	0.96	2.0	20.7	8.5	327	73.1	11.71
303-U1303A-																				
1H-1, 145.0–150.0	1.45	8.91	22.45	559	7.5	7.19	36	483	11.17	49.89	8.08	443	496	0.31	12.6	20.9	17.0	682	81.7	10.10
2H-2, 145.0–150.0	11.35	19.16	17.39	561	7.4	9.94	35	484	11.04	49.53	6.16	710	545	0.67	6.6	19.5	14.1	751	76.6	12.44
3H-1, 145.0–150.0	19.35	29.88	15.11	563	7.4	10.40	36	485	10.82	48.75	5.51	832	552	0.43	3.8	17.9	11.1	790	73.3	13.30
5H-2, 145.0–150.0	39.85	50.98	11.35	567	7.3	10.44	35	486	10.24	47.20	4.65	964	551	0.50	7.0	18.8	6.4	847	72.7	15.61
6H-2, 145.0–150.0	49.30	60.79	10.53	563	7.3	10.56	34	484	10.08	45.91	4.55	890	541	0.52	4.3	18.8	6.5	838	72.6	15.96
7H-1, 145.0–150.0	57.35	68.86	9.32	563	7.5	10.50	34	484	10.07	44.81	4.61	978	623	0.62	1.4	19.4	11.4	692	72.6	15.74
10H-1, 145.0–150.0	85.85	92.58	14.88	556	7.6	6.46	34	478	9.49	46.31	6.11	809	459	0.65	1.6	20.6	8.4	567	78.2	12.80
303-U1303B-																				
1H-1, 145.0–150.0	1.45	2.27	26.70	555	7.5	4.54	36	478	12.21	51.24	9.75	165	500	0.24	18.3	23.0	52.2	579	84.6	8.68
2H-1, 145.0–150.0	11.15	12.31	20.10	563	7.3	8.68	36	486	11.44	50.55	7.07	602	530	0.31	17.0	20.4	17.9	669	80.2	11.34

Note: * refers to the shipboard mcd (see **"Composite section"**).

Table T34. Thermal conductivity, Holes U1302A, U1302B, U1302C, U1302D, and U1302E.

Core, section, interval (cm)	Depth (mbsf)	Depth (mcd)	Thermal conductivity (W/m·K)
303-U1302A-			
2H-4, 74	5.34	18.39	0.9880
3H-4, 74	14.84	28.69	1.1443
4H-4, 74	24.34	40.17	1.0010
6H-4, 74	43.34	61.66	1.1813
7H-4, 74	52.84	74.76	1.2673
8H-4, 74	62.34	83.44	1.1347
9H-4, 74	71.84	93.55	1.1493
10H-4, 74	81.34	105.02	1.3267
11H-4, 74	90.84	114.52	1.6800
12H-4, 74	100.34	124.02	1.2907
13H-1, 70	105.30	128.98	1.4647
303-U1302B-			
1H-4, 75	5.25	5.25	1.0643
2H-4, 75	14.95	14.95	1.7347
3H-4, 75	24.45	24.45	0.9827
4H-4, 75	33.95	33.95	1.0237
5H-4, 75	43.45	43.45	1.0590
6H-4, 75	52.95	52.95	1.2363
7H-4, 75	62.45	62.45	1.8993
8H-4, 75	71.95	71.95	1.0413
9H-4, 75	81.45	81.45	1.1603
10H-4, 75	90.95	90.95	1.1653
11H-4, 75	100.43	100.43	1.1237
303-U1302C-			
1H-4, 75	5.25	9.27	1.0280
2H-4, 75	14.75	18.81	1.0123
3H-4, 75	24.25	28.49	1.0543
4H-4, 75	33.75	39.47	2.0027
5H-4, 75	43.25	51.10	1.2200
6H-4, 75	52.75	60.20	1.1543
7H-4, 75	62.25	72.54	1.1460
8H-4, 75	71.75	83.10	1.1307
9H-4, 75	81.25	94.14	1.5550
10H-4, 75	90.75	106.22	1.1623
11H-1, 75	95.75	111.77	1.3130
303-U1302D-			
1H-2, 75	2.25	2.25	0.9940
2H-1, 75	4.25	10.59	1.0610
303-U1302E-			
1H-4, 50	5.00	5.11	0.9623
2H-4, 75	10.85	15.06	1.0987

Table T35. Thermal conductivity, Holes U1303A and U1303B.

Core, section, interval (cm)	Depth (mbsf)	Depth (mcd)	Thermal conductivity (W/m·K)
303-U1303A-			
1H-4, 75	5.25	12.71	1.0467
2H-4, 75	13.65	21.46	0.9587
3H-4, 75	23.15	33.68	1.1915
4H-2, 75	29.46	40.9	1.0830
5H-4, 75	42.15	53.28	0.9947
6H-4, 75	51.60	63.09	0.9863
7H-4, 75	61.15	72.66	1.0810
8H-4, 75	70.65	79.97	1.0900
9H-2, 75	77.15	84.09	1.0153
10H-2, 75	86.65	93.38	1.1643
303-U1303B-			
1H-4, 75	5.25	6.07	1.5050
2H-4, 75	14.95	16.11	1.1300
3H-4, 75	24.45	26.04	1.1567
4H-2, 75	30.95	32.85	1.0390
5H-4, 75	43.45	44.69	1.2193
6H-4, 75	52.95	56.78	1.6103
7H-4, 75	62.45	65.59	1.0640
8H-4, 75	71.95	75.85	1.3177